Trente ans d'évolutions technologiques et industrielles des cellules solaires à base de silicium cristallin

16/02/2022

Etienne Drahi

TotalEnergies/IPVF/E4C

Etienne.drahi@totalenergies.com

Chaire Innovation technologique Liliane Bettencourt 2021-2022
Daniel Lincot - Énergie solaire photovoltaïque et transition énergétique
(chaire annuelle 2021-2022)

TotalEnergies History in PV

In PV Since 1972 & A Growing Ambition Over Last 6 Years

TotalEnergies

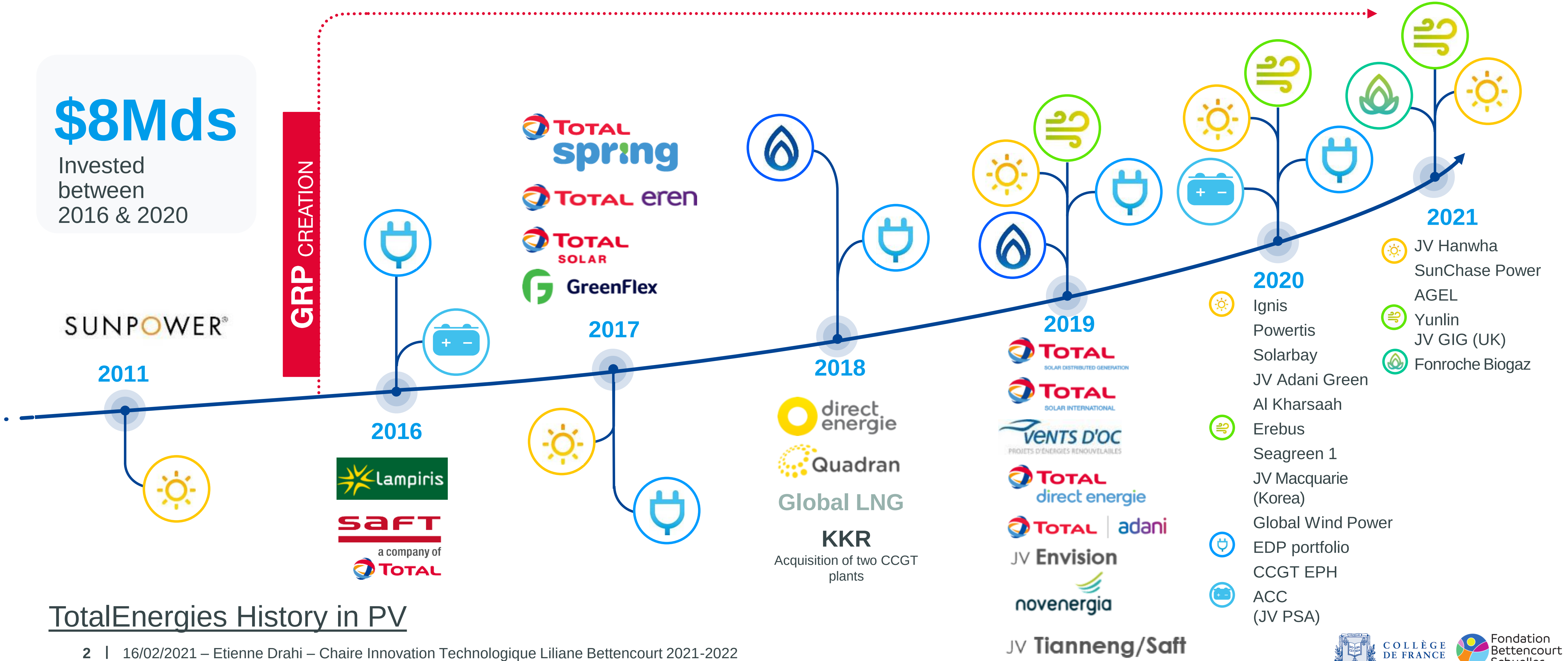

TotalEnergies History in PV

COLLÈGE DE FRANCE 1530

Fondation Bettencourt Schueller

TotalEnergies History in PV
Integrate Renewables Energies Top 5 Players

TotalEnergies

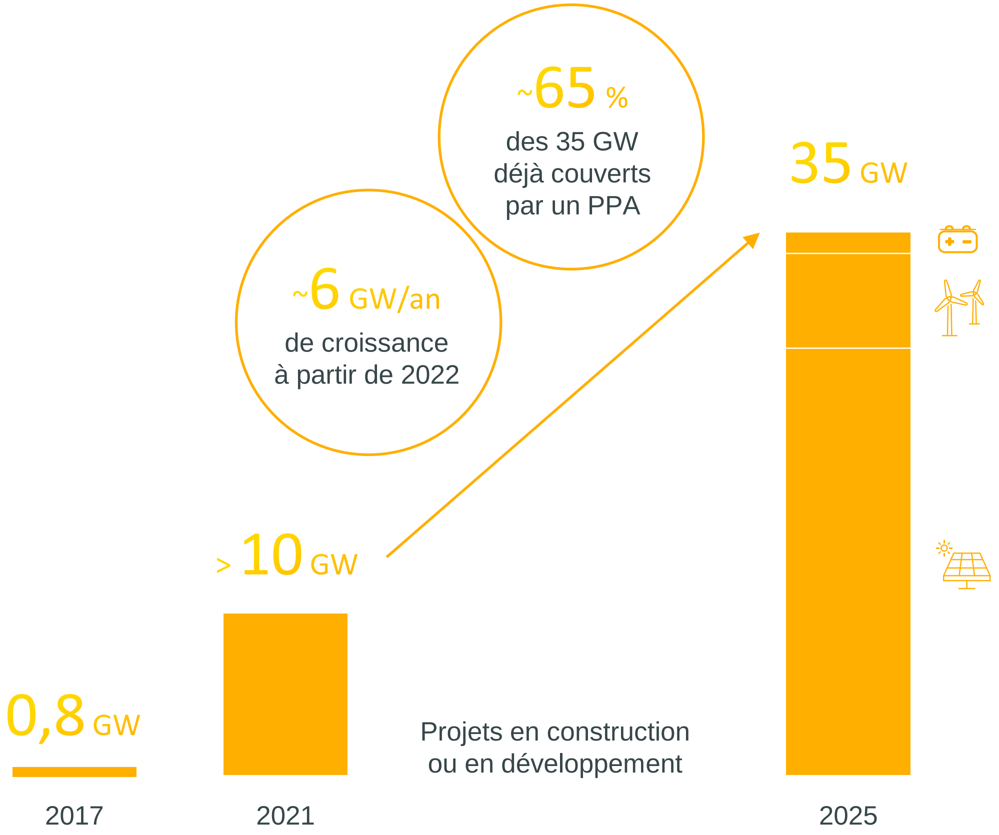

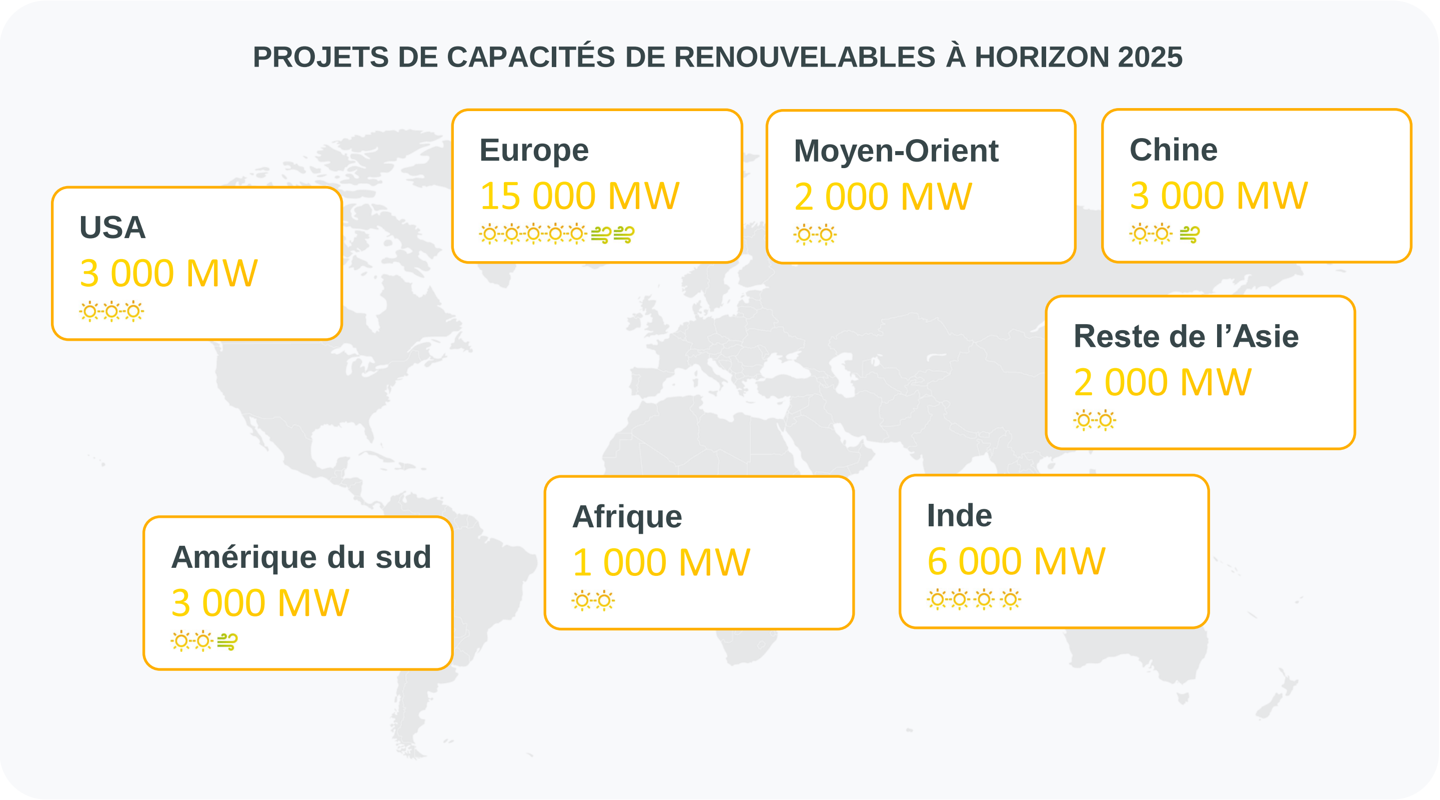

TotalEnergies History in PV
R&D Challenges

Develop solutions to accelerate solar energy deployment, improve assets and cost efficiency

Better estimate resources

- Predict variability
- Identify sites
- Estimate Yield

Select the best components

- Explore new technologies
- Estimate long term degradation

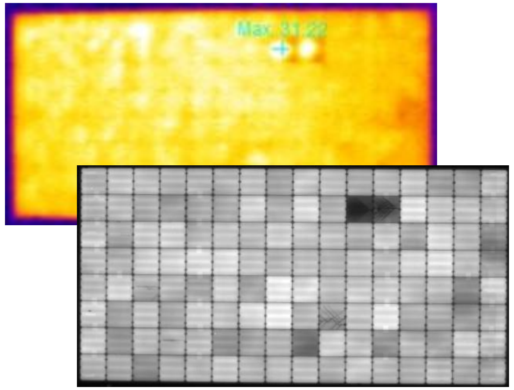

Ensure high systems performances

- Build demonstrators
- Explore new construction schemes
- Reduce O&M costs

Construct a sustainable activity

- Explore new markets
- Manage End of life
- Reduce HSE risks and environmental footprint

Introduction

PV Industry Overview

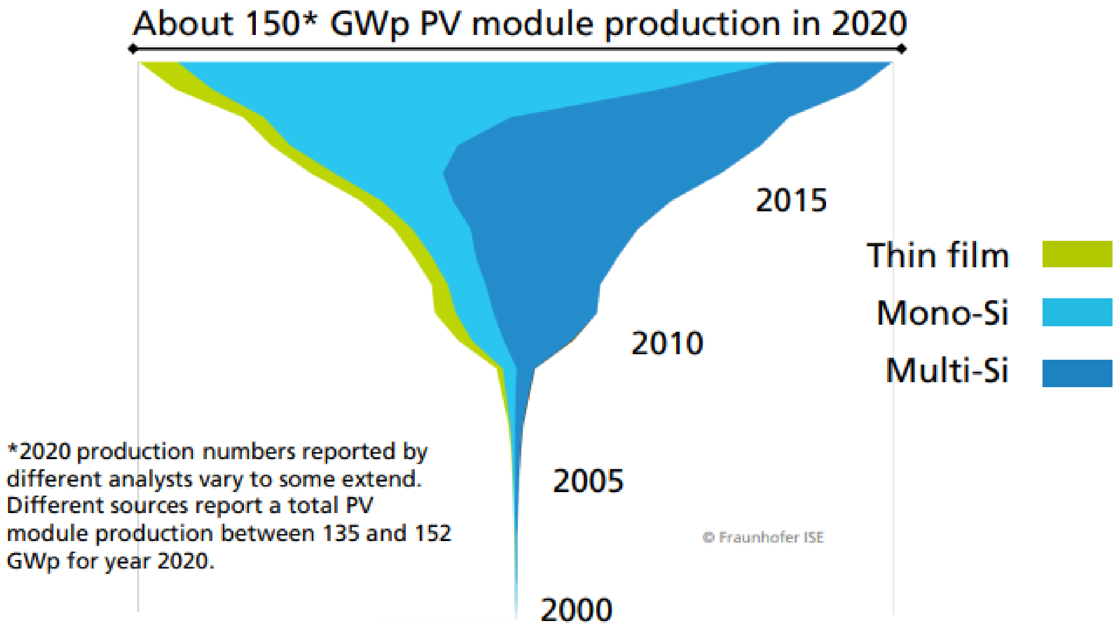

New build forecast to 2030, mid scenario

Source: BloombergNEF

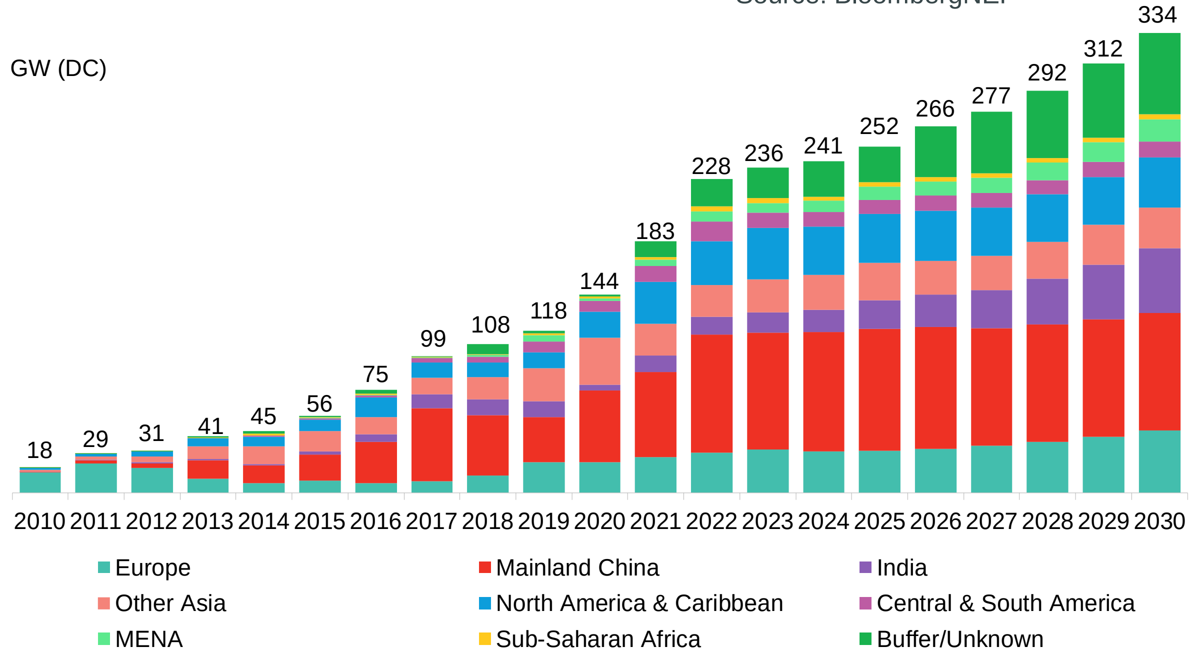

- Annual PV Production in 2020: **Monocrystalline Si 120.6 GW + Multicrystalline Si 23.3 GW + Thin Films 7.7 GW = 151.6 GW**
- PV Installation strong growth mostly supported by **'c-Si technology' ~95% market share**
- **China, India & Rest of Asia are the drivers** of both production and PV installation

Introduction

Al-BSF & PERC: Kings of Crystalline Silicon PV

Crystalline Silicon (c-Si) industrial workhorses:

Al-BSF (~20%)

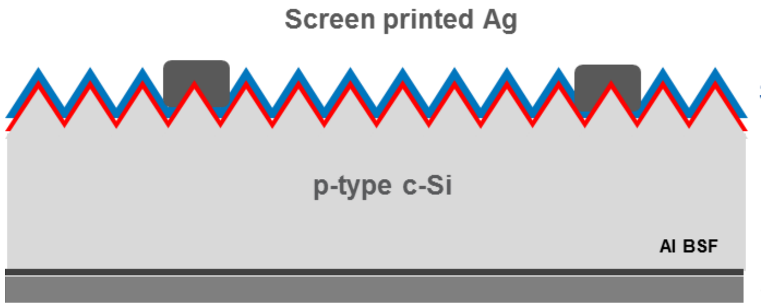

Monofacial PERC (~22.5%)

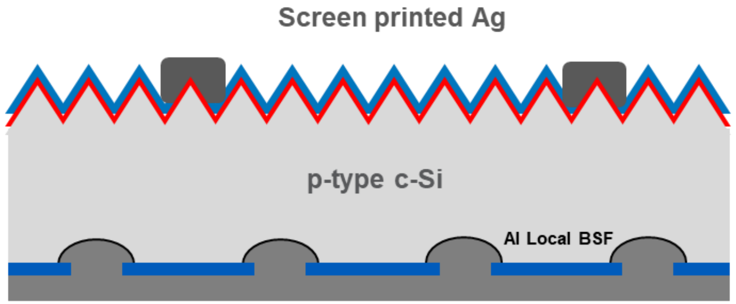

20% efficiency silicon solar cells

A. W. Blakers and M. A. Green
Solar Photovoltaic Laboratory, Joint Microelectronics Research Centre, University of New South Wales, Kensington 2033, Australia

(Received 19 September 1985; accepted for publication 20 November 1985)

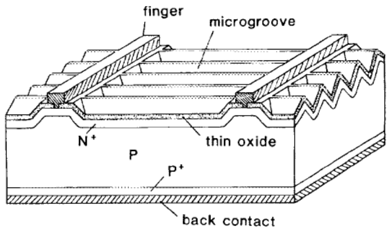

FIG. 1. Schematic diagram of a microgrooved passivated emitter solar cell (PESC). The cell double layer antireflection coating is not shown (not to scale).

Further improvements in crystalline silicon solar cell performance have been obtained by combining the high levels of surface recombination control demonstrated in earlier passivated emitter solar cells with an improved optical approach. This approach involves the use of microgrooved surfaces which retain the advantages of pyramidally textured surfaces while avoiding some disadvantages of the latter. The approach results in a 5–6% improvement in cell short-circuit current density for cells fabricated on 0.1 and 0.2 Ω cm (*p* type) substrates. This results in an energy conversion efficiency for these devices above 20% under standard terrestrial test conditions (AM1.5, 100 mW/cm^2) for the first time.

24% EFFICIENT SILICON SOLAR CELLS

Jianhua Zhao, Aihua Wang, Pietro P. Altermatt, Stuart R. Wenham and Martin A. Green
Centre for Photovoltaic Devices and Systems
University of New South Wales, Sydney 2052, Australia

ABSTRACT

This paper reports significant progress in silicon solar cell performance, taking confirmed efficiency beyond 24% for the first time. This progress has been achieved by a combination of several mechanisms. One is the reduction of recombination at the cell front surface by improved passivation of the silicon/silicon dioxide interface. Resistive losses in the cell have been reduced by a double-plating process which increases the thickness for the coarse cell metallization features. Finally, reflective losses have been reduced by the application of a double layer anti-reflection (DLAR) coating. Another advantage of DLAR coating is that it will give further 3% higher current density than the SiO_2 single layer anti-reflection (SLAR) coated cells when encapsulated into modules. The cells display a monochromatic light energy conversion efficiency of 46.3% for 1.04 μm wavelength light, also the highest ever for a silicon device.

cell immediately demonstrated an improved efficiency of 23.5% [3].

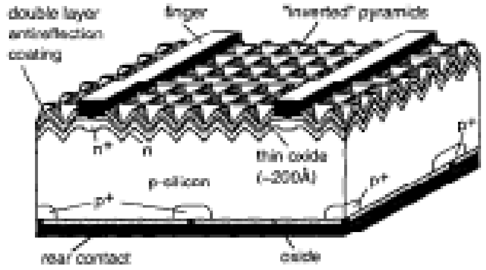

Figure 1: Passivated emitter, rear locally-diffused (PERL) cell with a double layer anti-reflection coating.

Introduction
One Material, Several Technologies

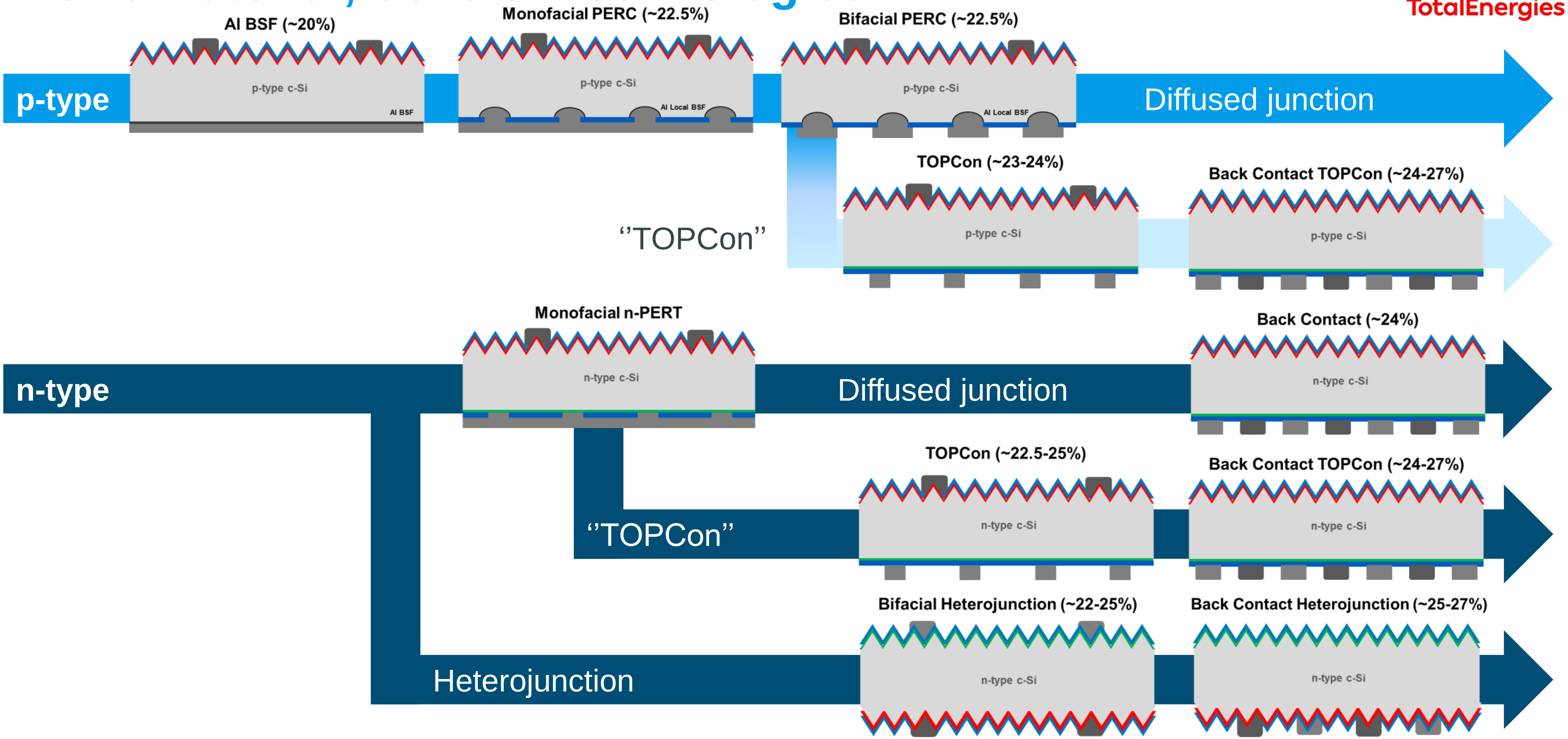

Introduction
One Material, Several Technologies

TotalEnergies

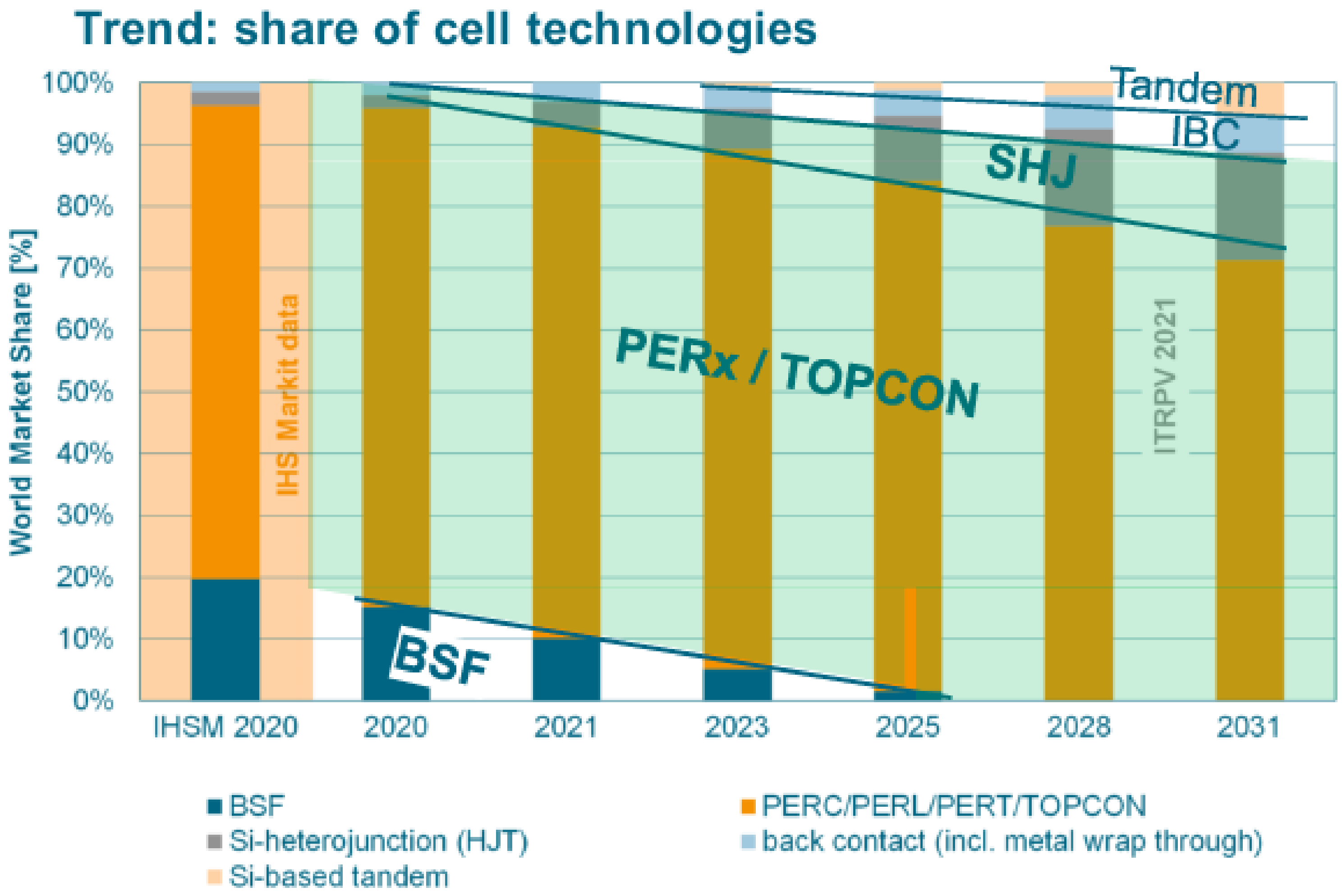

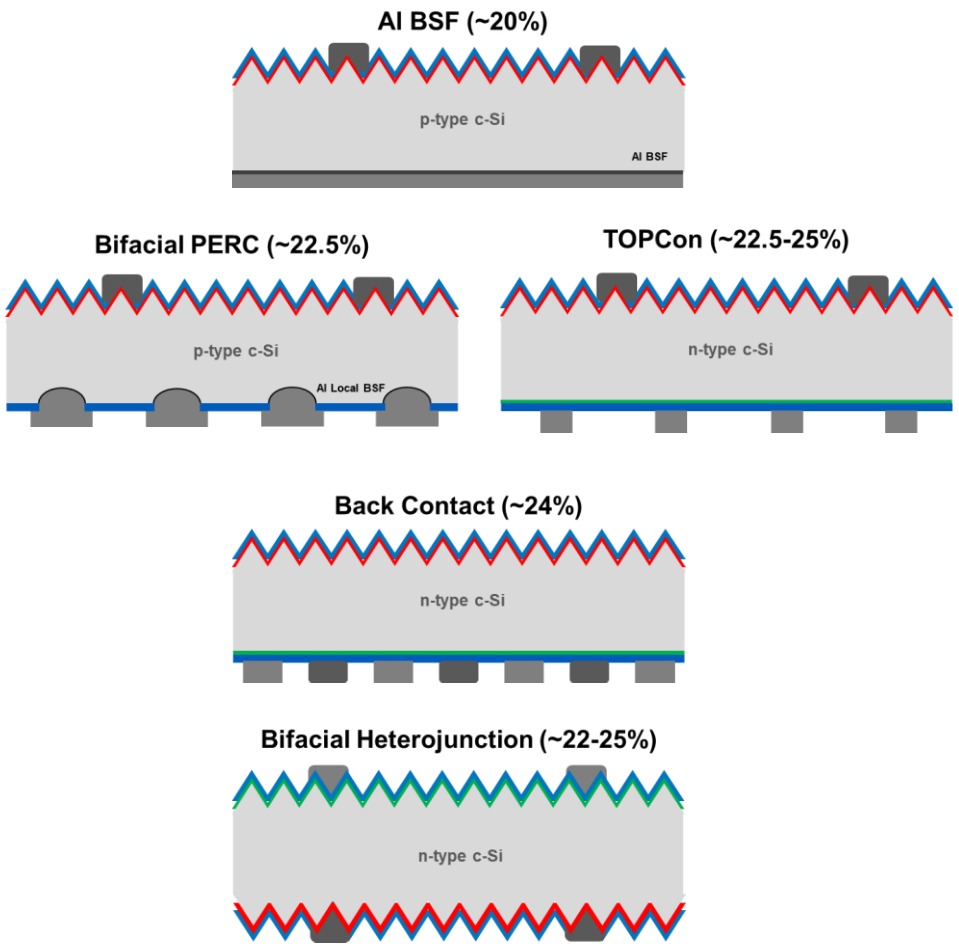

COLLÈGE DE FRANCE 1530

Fondation Bettencourt Schueller

Introduction

From Al-BSF era to PERC era & New Architectures: Reducing Lab-to-Fab Technology Transfer Time

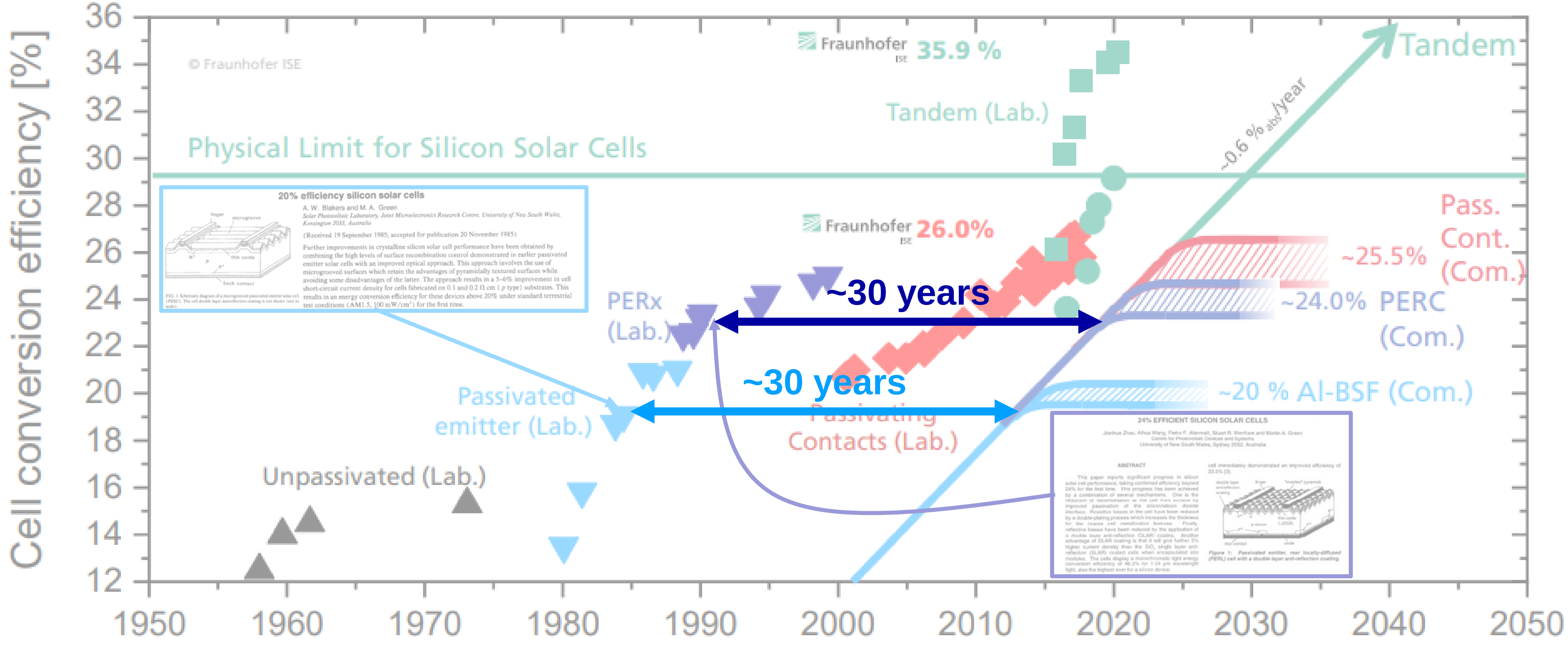

Graph: Fraunhofer ISE 2021

Introduction

Crystalline Silicon Solar Cells Efficiencies & Limits

- **Basic principles of a solar cells consists of three steps to be optimized:**
  1. Incident light absorption & conversion in photocarriers
  2. Photocarriers separation and transport towards contacts
  3. Photocarriers collection and extraction

- **Theoretical efficiency limit:**
  - **29.43% for ~110 µm** undoped c-Si solar cell
  - **29.1% for ~100 µm 1 Ohm.cm** doped wafer

- **World record with back contact SHJ:**
  - **26.63%** for wafer of 200 µm & 7 Ohm.cm n-type
  - **Practical limit identified: 27.1%**
  - **But more realistically: 26.8%**

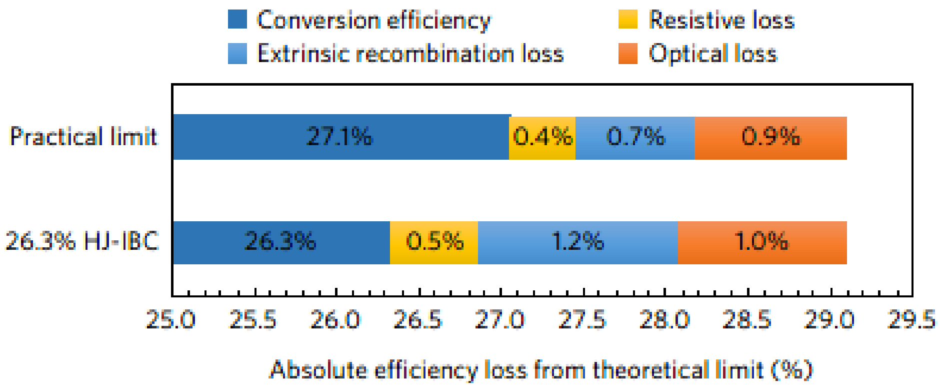

Yoshikawa *et al. Nat Energy* **2,** 17032 (2017)

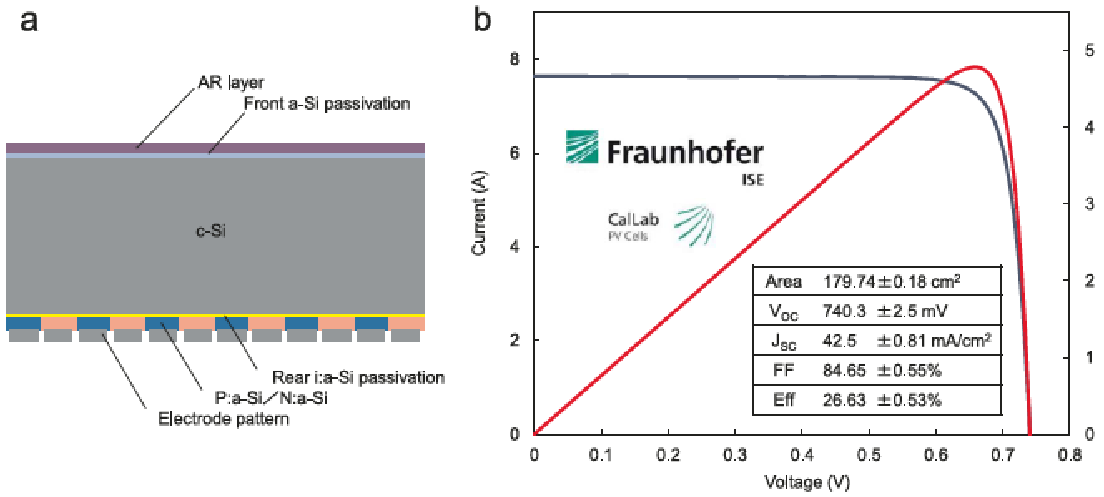

K. Yoshikawa et al. Solar Energy Materials and Solar Cells 173 (2017) 37–4238

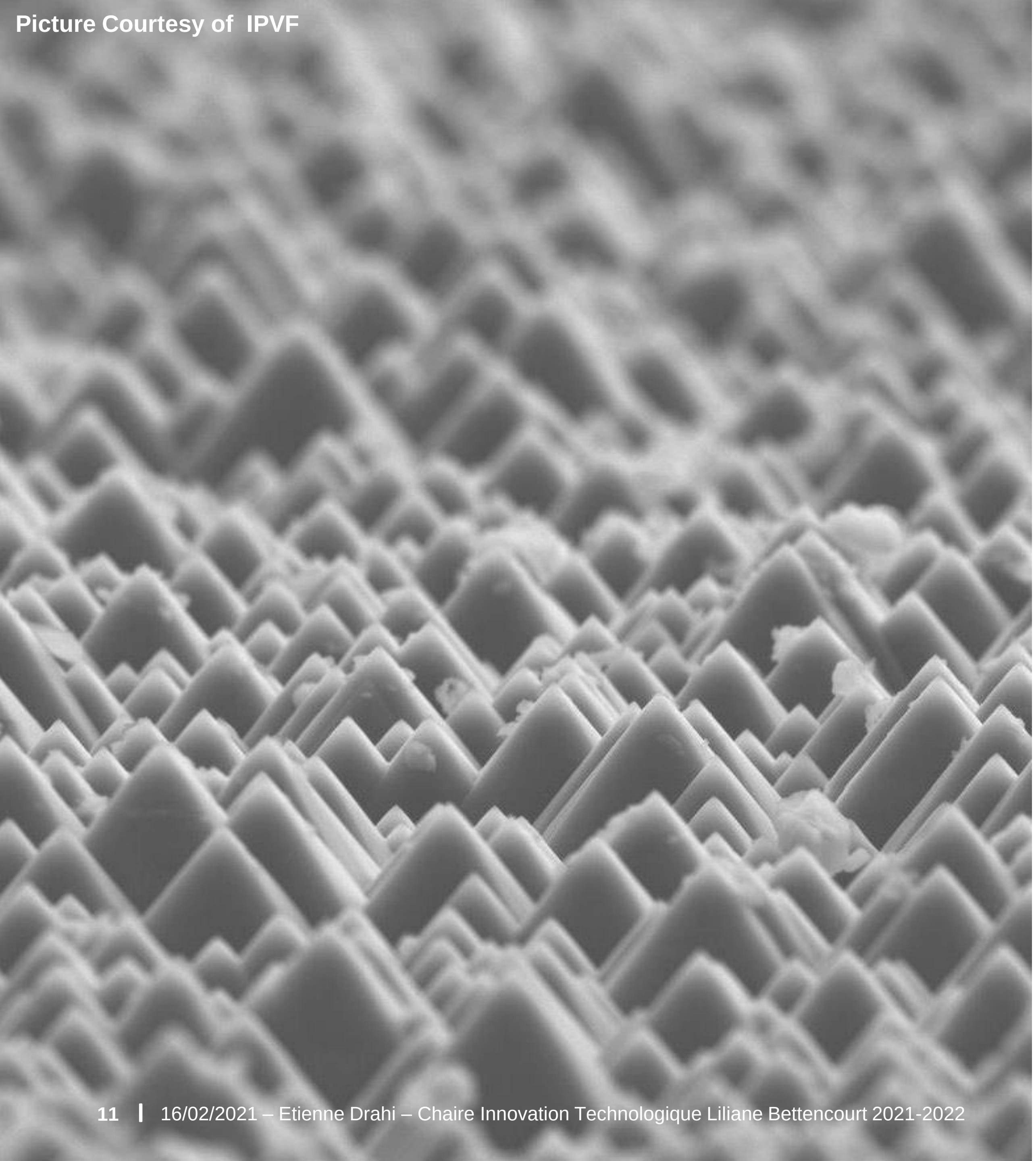
Picture Courtesy of IPVF

Agenda

- Introduction
- **Improved Photon Conversion**
  - From Simple Absorption to Light Trapping
  - Bifaciality: The Future of PV Has Two Sides
- Photocarriers Separation & Transport
  - Bulk Material Quality Improvement
  - Wafer Thickness Reduction
- Photocarriers Collection & Extraction
  - From Passivated Contacts to Passivating Contacts
  - Advanced Metallization & Interconnexion Processes
- Conclusions

Improved Photons Conversion
From Simple Absorption to Light Trapping

- **c-Si is a 'weak' absorber** compared to thin film materials → **'thick' wafers** (<200 µm) vs thin film (~µm)

- Theoretical max J_{sc}**~43.7 mA/cm^{-2} (for 165 µm wafer = Kaneka record device)**

- **Need to increase number of times the photons 'rebound' within the wafer = F**, the optical path enhancement factor
  - F=1 for single pass
  - F=2 for double pass
  - F=4n^2~50 for Lambertian scattering model in c-Si

How to do that practically and industrially?

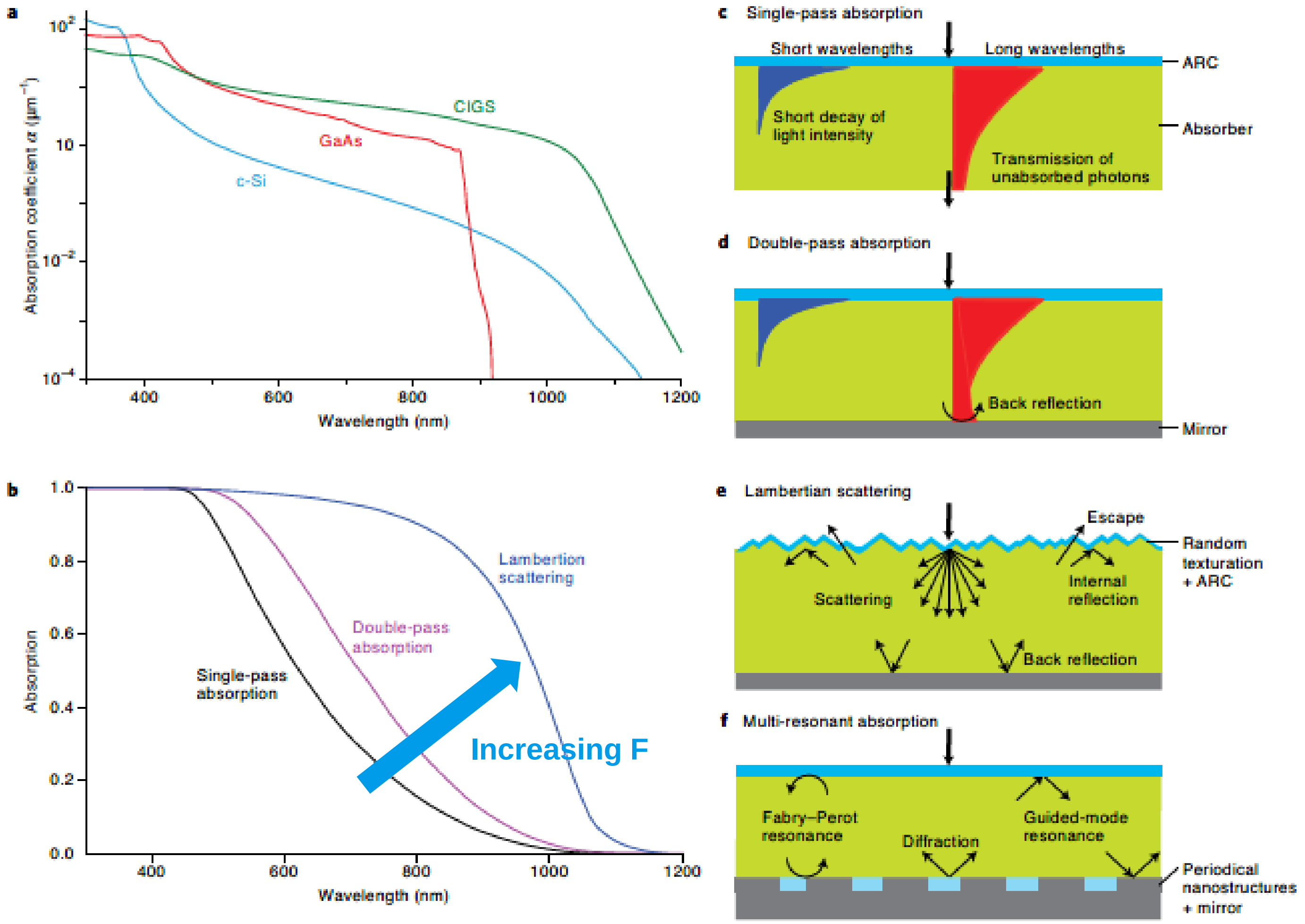

Massiot, I., Cattoni, A. & Collin, S. Progress and prospects for ultrathin solar cells. *Nat Energy* **5,** 959–972 (2020). https://doi.org/10.1038/s41560-020-00714-4

Improved Photons Conversion
From Simple Absorption to Light Trapping

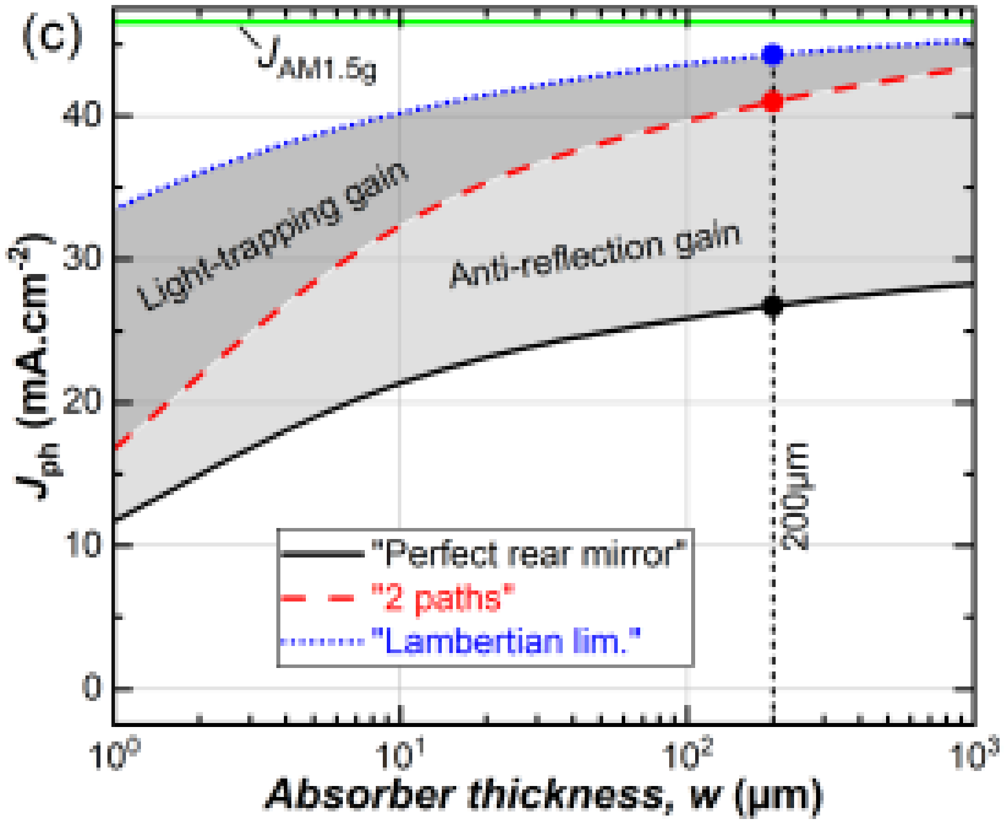

Fischer, G. PhD Thesis 2018 Plasma Nanotexturing of Silicon for Photovoltaic Applications: Tailoring Plasma-Surface Interactions for Improved Light Management.

- **Photogenerated current depends on:**
  - **Absorber bandgap & thickness,**
  - **Light Trapping scheme,**
  - **Anti-Reflection gains →** Antireflective coating (ARC)

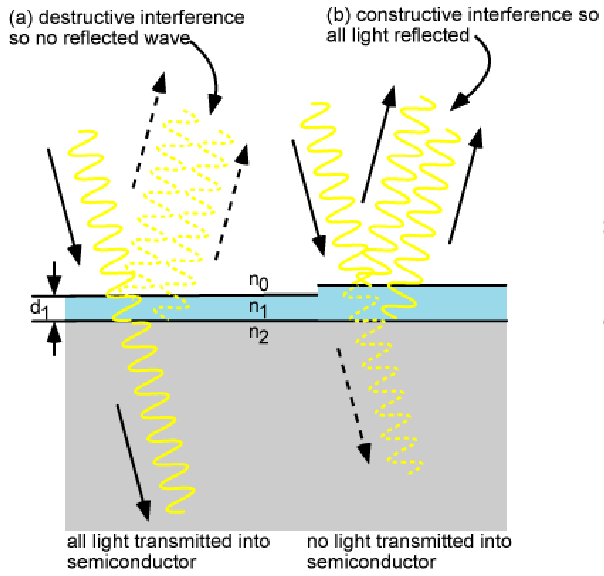

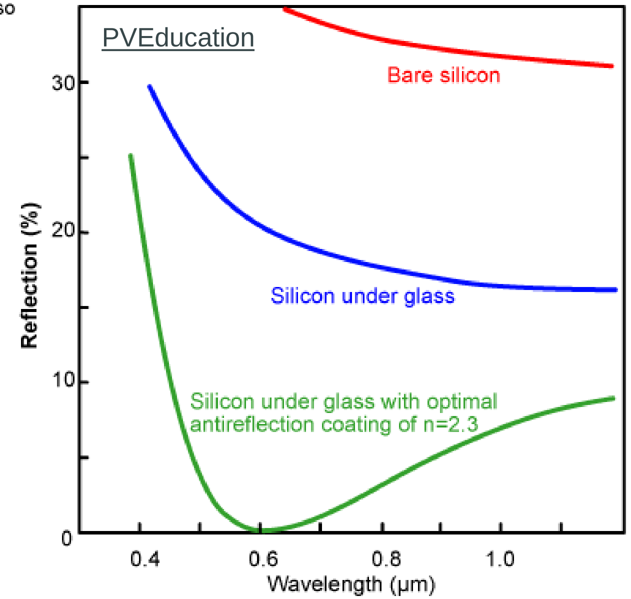

Improved Photons Conversion
From Simple Absorption to Light Trapping

Crystalline Si is FCC based crystal
wafers are usually 100 oriented

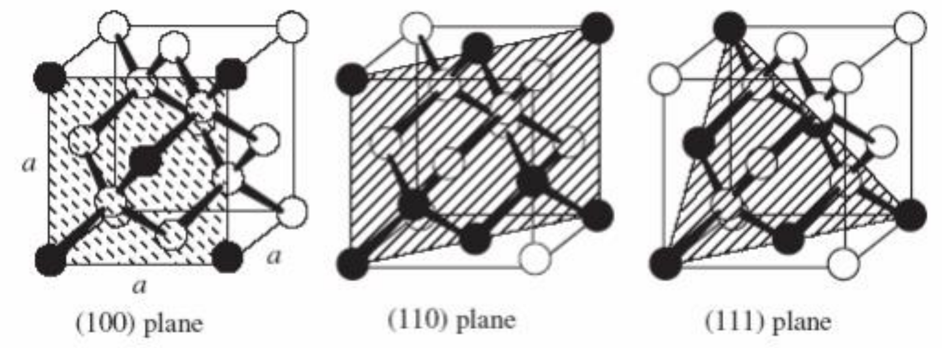

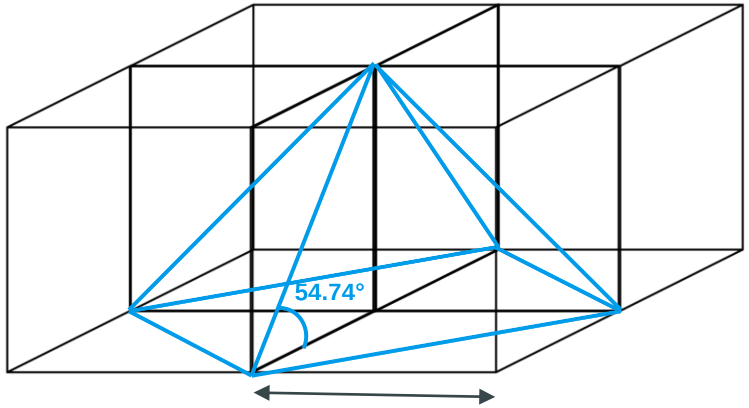

Texturing for improved light trapping using c-Si crystallographic structure

- Using **alkaline-based solution**, etch rate of 111 planes much slower than 100 planes (74x for KOH) → promotes **pyramids growth using H_2 bubbles as a 'mask'**

K. Tokoro, et al , *MHA'98.*

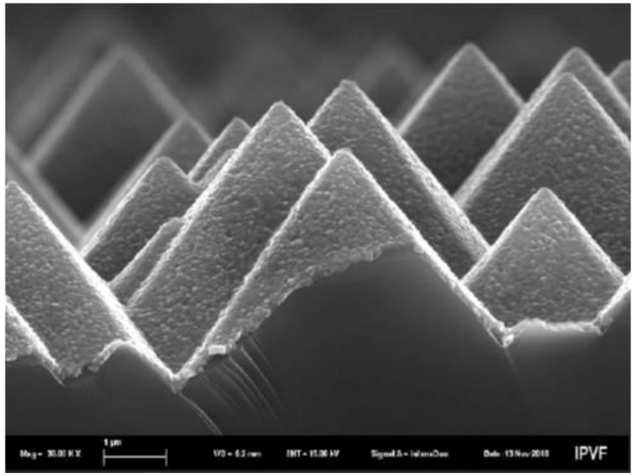

K. Saliou et al., 2019 IEEE 46th Photovoltaic Specialists Conference (PVSC), 2019

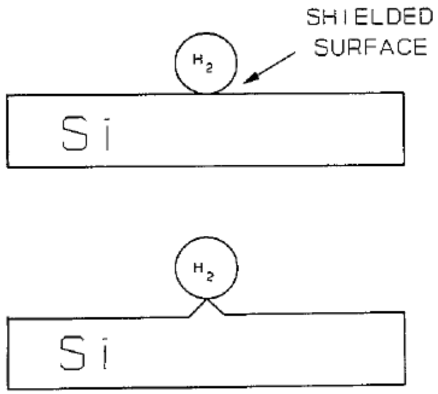

Figure 1. Schematic diagram to show the initiation of pyramid formation as a result of the surface attachment of hydrogen bubbles produced during the dissolution reaction.

S A Campbell *et al* 1995 *J. Micromech. Microeng.* **5** 209

- Use of an **additive such as IPA** or other to **change the wettability** behavior of the surface and detachment of H_2 bubbles

L. Bailey, Coleman, M. G., Harris, C. B., and Lesk, I. A., "United States Patent: 4137123 - Texture etching of silicon: method". 1979.

Improved Photons Conversion
Bifaciality: The Future of PV Has Two Sides

A quite 'old' idea…

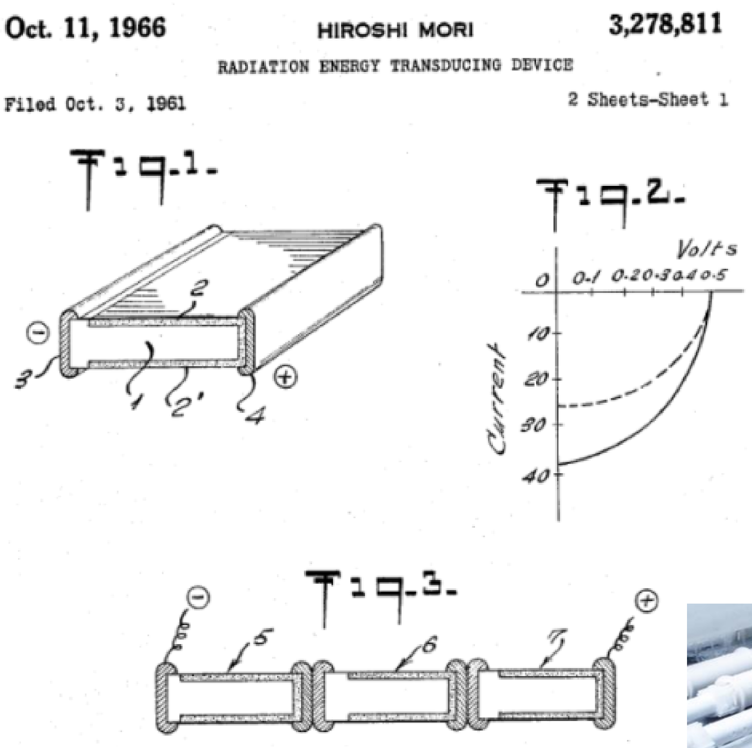

Made possible by deployment of new PV cell architectures…

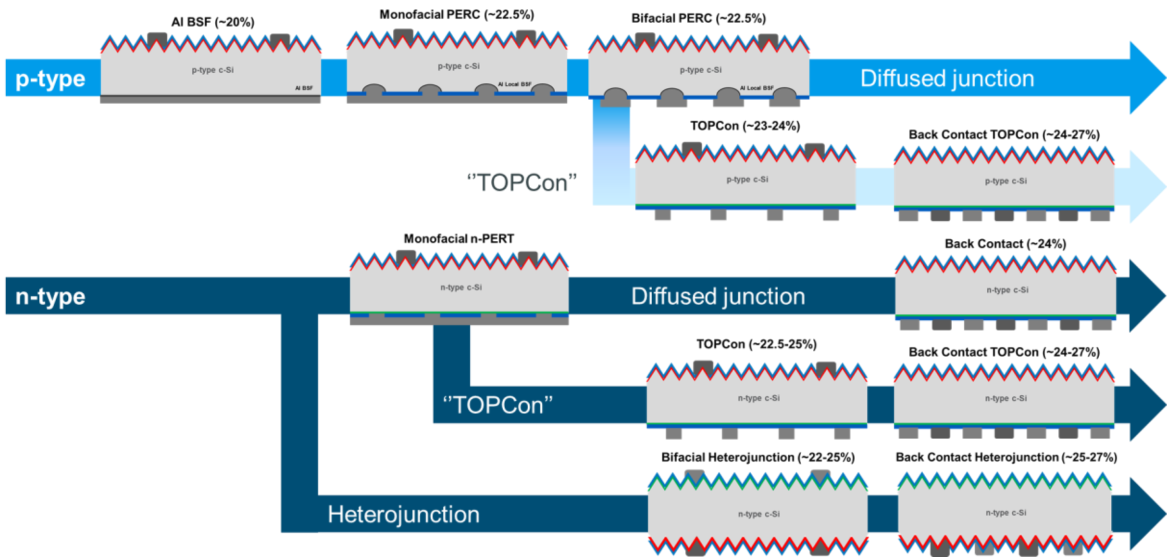

And new fabrication processes

Inline wetbenches

RENA

Laser contact opening

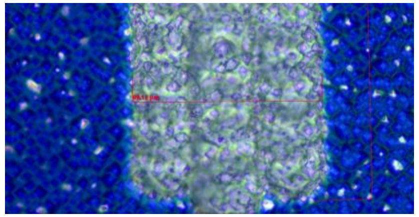

IPVF

Advanced Screen Printing

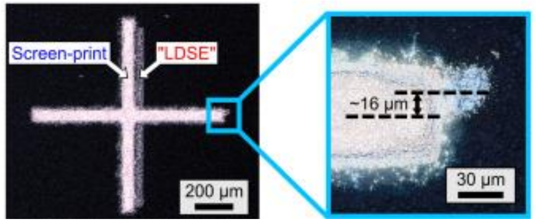

IEEE JOURNAL OF PHOTOVOLTAICS, VOL. 10, NO. 2, MARCH 2020

Improved Photons Conversion
Bifaciality: The Future of PV Has Two Sides

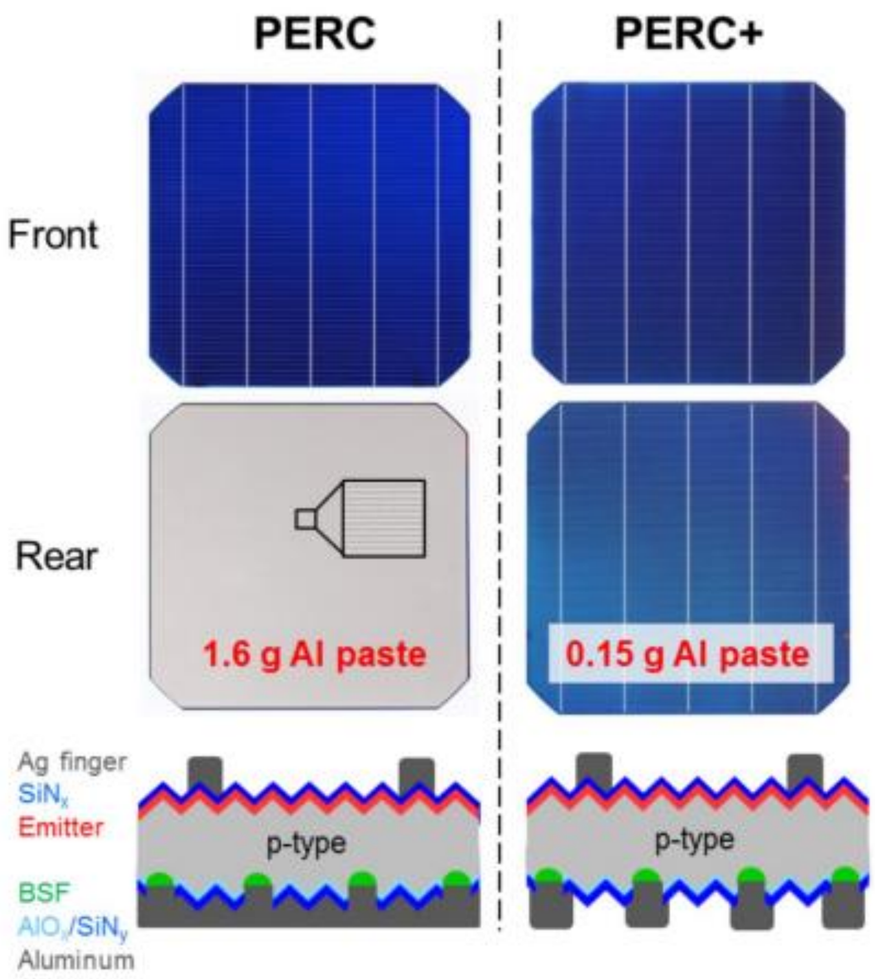

Dullweber nPV workshop 2017

- **Advantages:**
  - Light collection from the rear side. Bifaciality ~70-80% PERC or TOPCon, ~90% SHJ
  - Metal savings

- **Disadvantages:**
  - More complex alignment between laser openings & Screen-printing
  - Need for new screen-printing pastes
  - Need for certification/norm in bifaciality measurement and

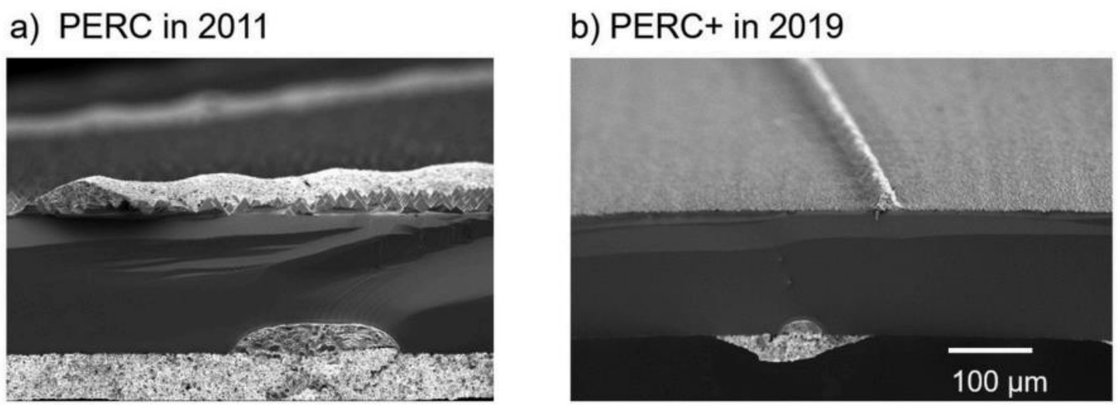

Solar Energy Materials and Solar Cells 212 (2020) 110586

Improved Photons Conversion
Bifaciality: The Future of PV Has Two Sides

- **Imec and Jolywood achieve a record of 23.2 percent with bifacial n-PERT solar cells**

APRIL 8, 2019

A batch of 12 new M2-sized cells (244.3 cm^2) measured at ISFH CalTec showed an average conversion efficiency of 23.0 percent, with the best cell topping 23.2 percent, and our own measurements revealed a bifaciality above 80 percent. Moreover, used under standard front illumination conditions in conjunction with an additional 0.15 sun rear illumination, the cells can achieve an effective conversion efficiency of almost 26 percent. In addition, ISFH Caltec measured an average reverse current of -0.4A (at -12V) indicating excellent breakdown characteristics.

Bifacial n-PERT (~23%)

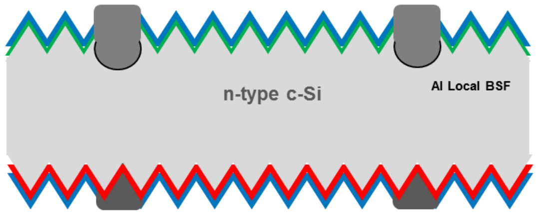

Picture Courtesy of Air Liquide

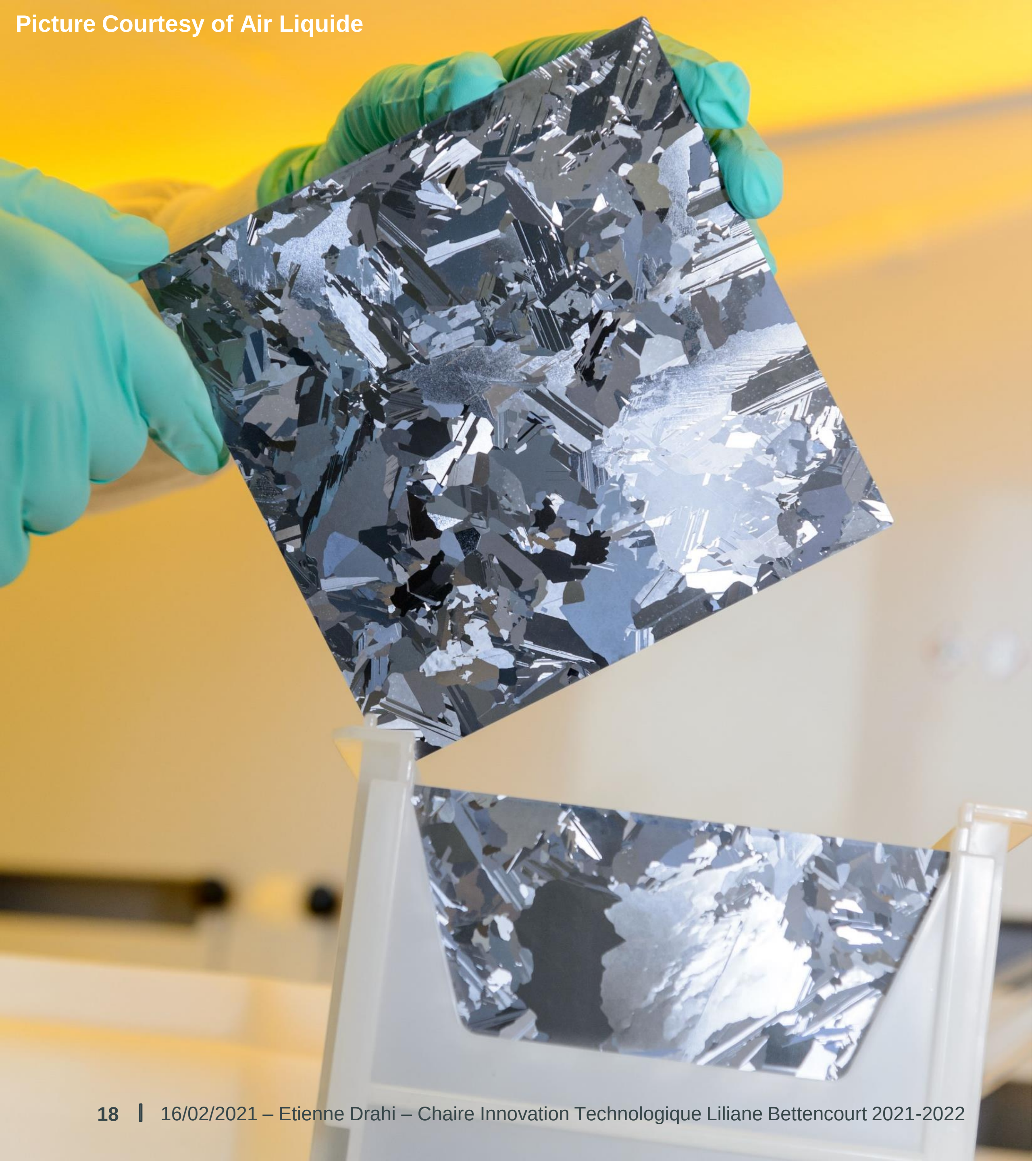

Agenda

- Introduction
- Improved Photon Conversion
  - From Simple Absorption to Light Trapping
  - Bifaciality: The Future of PV Has Two Sides
- **Photocarriers Separation & Transport**
  - Bulk Material Quality Improvement
  - Wafer Thickness Reduction
- Photocarriers Collection & Extraction
  - From Passivated Contacts to Passivating Contacts
  - Advanced Metallization & Interconnexion Processes
- Conclusions

Photocarriers Separation & Transport
Bulk Material Quality Improvement

c-Si is our bucket to harvest photons but naturally it is a leaking bucket → PV technologist are putting patches – the art is to know which one to cover first, then to find the new leaking hole

Solar Energy Materials and Solar Cells 185 (2018) 260–269261

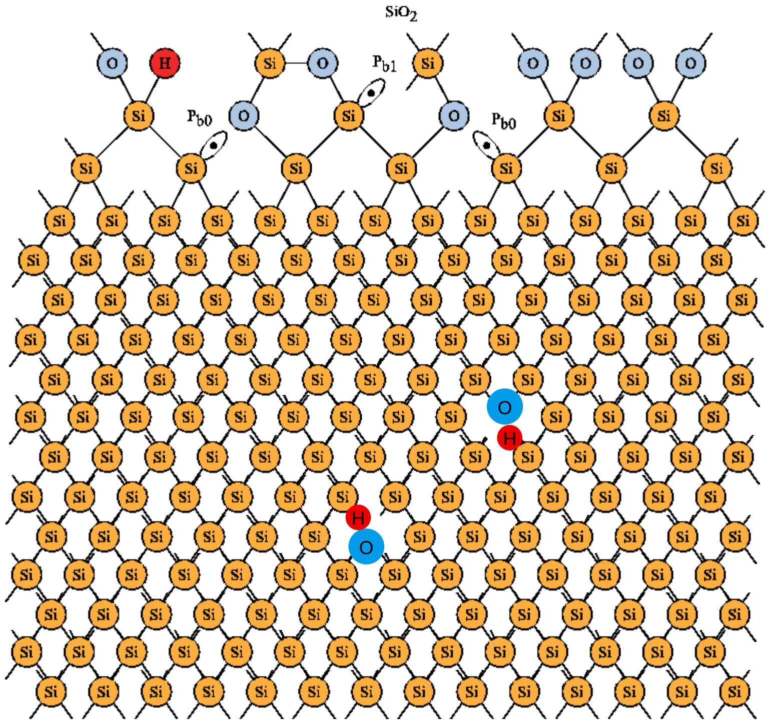

A. Richter et al. / Energy Procedia 27 (2012) 88 – 94

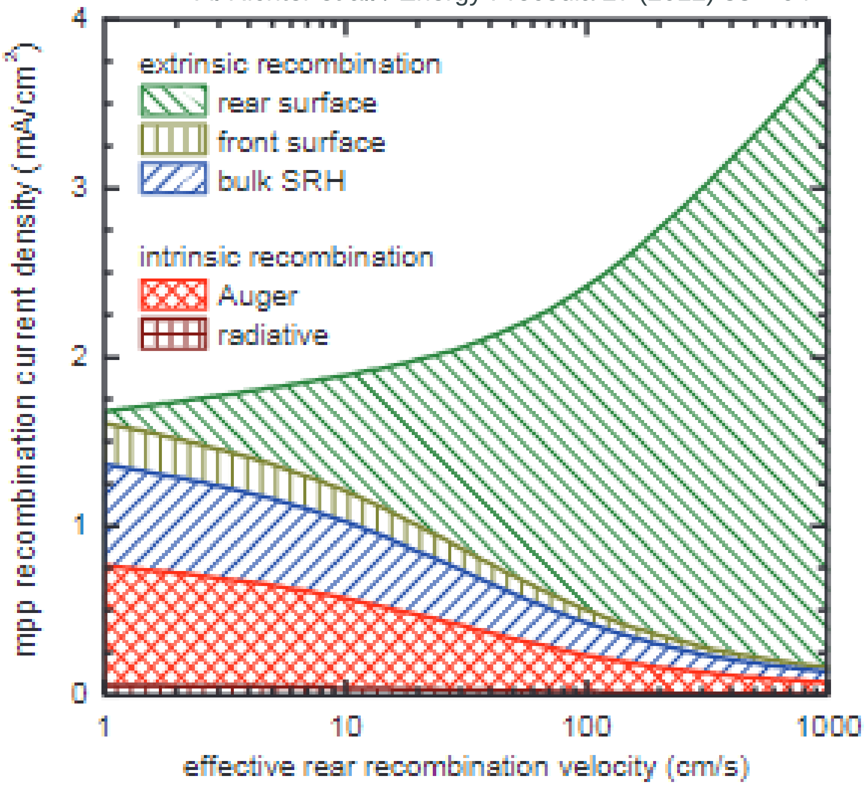

Photocarriers Separation & Transport
Bulk Material Quality Improvement

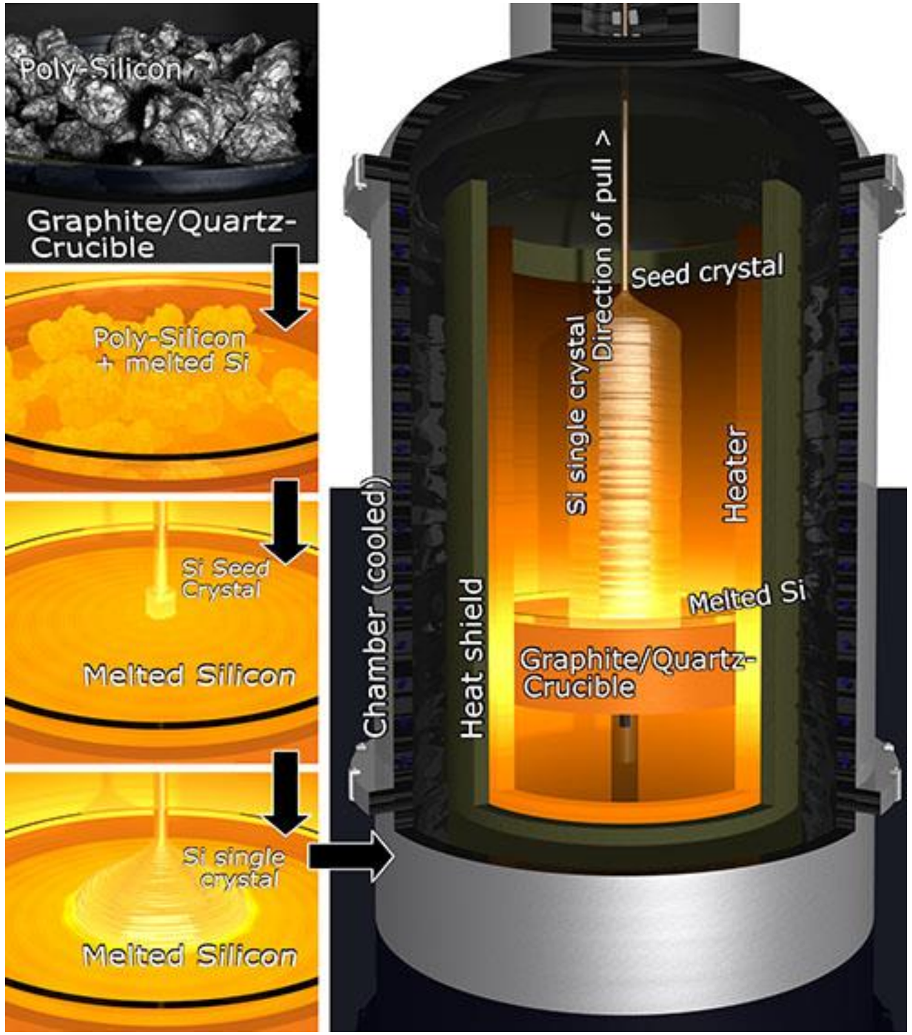

Date of market introduction in white for information from ITRPV 2021

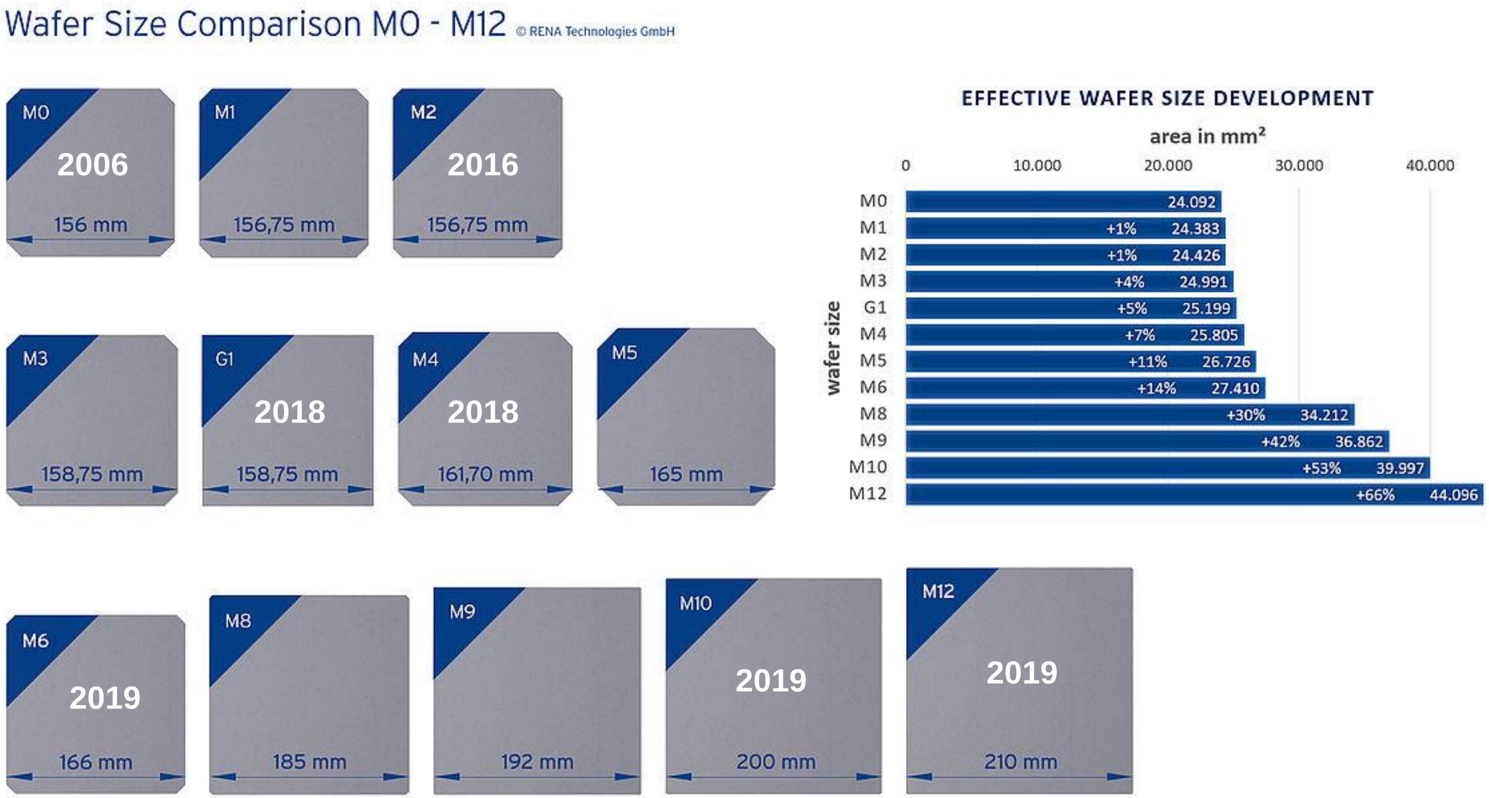

https://www.rena.com/en/products/large-wafer-wet-processing/

https://www.microchemicals.com/products/wafers/silicon_ingot_production.html

Photocarriers Separation & Transport
Bulk Material Quality Improvement

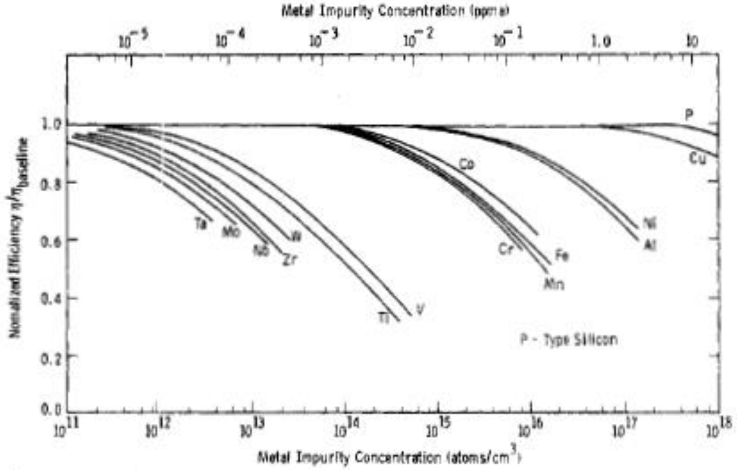

Fig. 4. Solar-cell efficiency versus impurity concentration for 4-Ω · cm p-base devices.

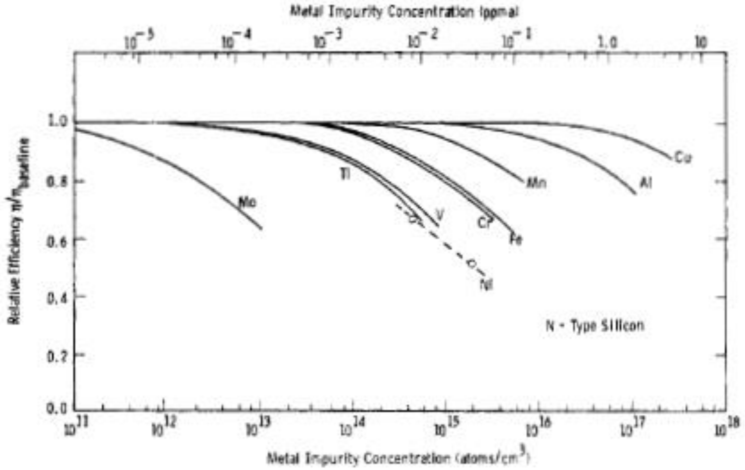

Fig. 5. Solar-cell efficiency versus impurity concentration for 1.5-Ω · cm n-base devices.

***Table 1.1** Crystallisation methods and contamination source*

Method	Crystallinity	Product	Contamination source	Contamination type
Czochralski	Monocrystalline	Ingots	Polysilicon Crucible Hot-zone parts	C, O, Al, transition metals
Float zone	Monocrystalline	Ingots	Feeding rod RF coil	Cu
Directional solidification	Multicrystalline	Ingots	Silicon feedstock Crucible Crucible coating layer Hot-zone parts	C, O, N, Al, transition metals

Gianluca Coletti PhD Thesis

- **Metalic impurities** comes from Polysilicon + ingot + wafering processes
- Cu, Fe… are lifetime killers in c-Si → creation of bulk SRH defects

→ **Device efficiency can be strongly reduced** with increasing impurities concentration

→ n-type silicon less sensitive than p-type to Fe

→ **Gettering strategy** deployed on c-Si cells processes to mitigate this

J. R. Davis *et al*. *IEEE Transactions on Electron Devices*, vol. 27, no. 4, pp. 677-687, April 1980

Photocarriers Separation & Transport
Bulk Material Quality Improvement

- As early as 1973 **degradation of p-type c-Si solar cell under illumination (strong J_{sc} loss)** has been observed by Fischer and Pschunder. They observed that **J_{sc} was recovered after annealing @200°C in the dark**. This phenomenon has later been called **LID – Light Induced Degradation**

- Later this phenomenon has been intensively studied by several authors:
  - It was quite early attributed to the **creation of B-O pairs reducing the bulk lifetime**.
  - By **replacing B by Ga**, this bulk lifetime reduction can be strongly mitigated.
  - **PERC are more sensitive than Al-BSF to LID** due to their better nIR absorption

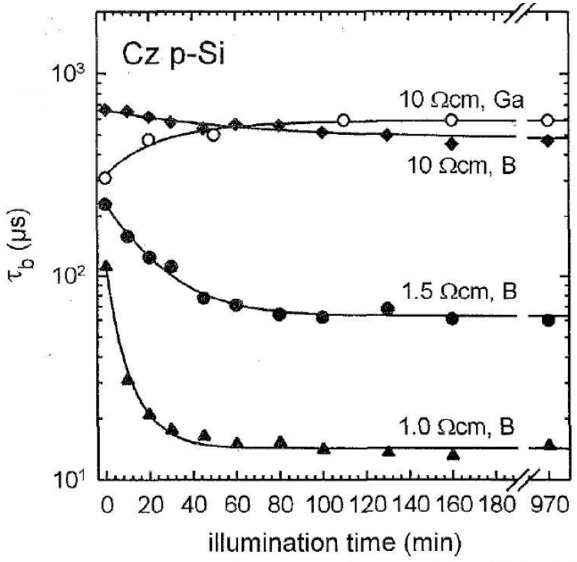

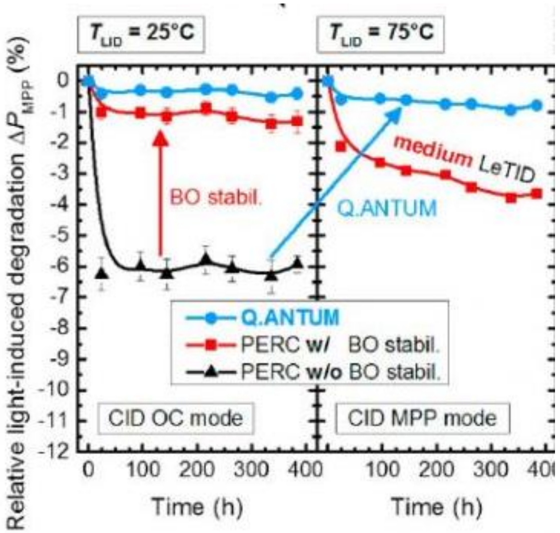

Meng Xiajie 2019, PV-Tech

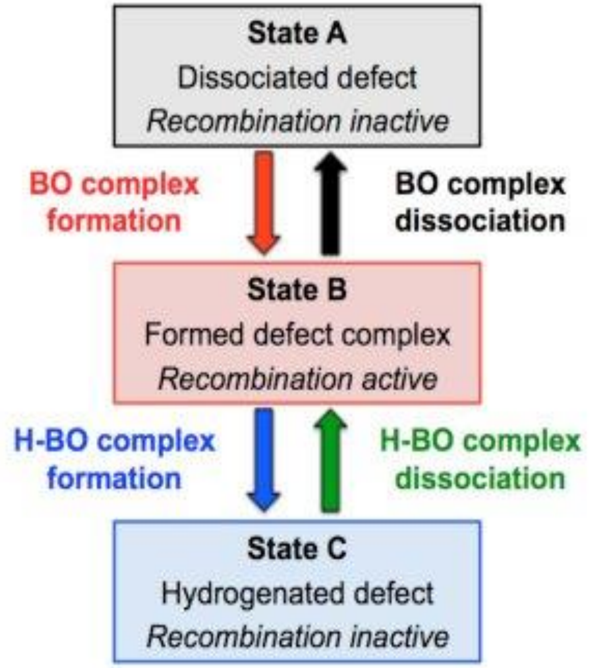

Hallam et al. EUPVSEC 2015

Photocarriers Separation & Transport
Wafer Thickness Reduction

- **Theoretical limit efficiency of c-Si solar cells achievable for wafer thickness ~100 µm.**

- **Advantages of lower wafer thickness=**
  - Lower material usage per W_p
  - Higher V_{oc} → higher output voltage of cell & module
  - Reduced resistive losses → higher P_{mpp} + lower heating
  - Flexible cells

- **Disadvantages of lower wafer thickness=**
  - Need to improved light trapping scheme
  - Surfaces & Edges impacts are more and more important
  - Mechanical handling more difficult → more breakage
  - <100 µm standard wet processes might have to be replaced

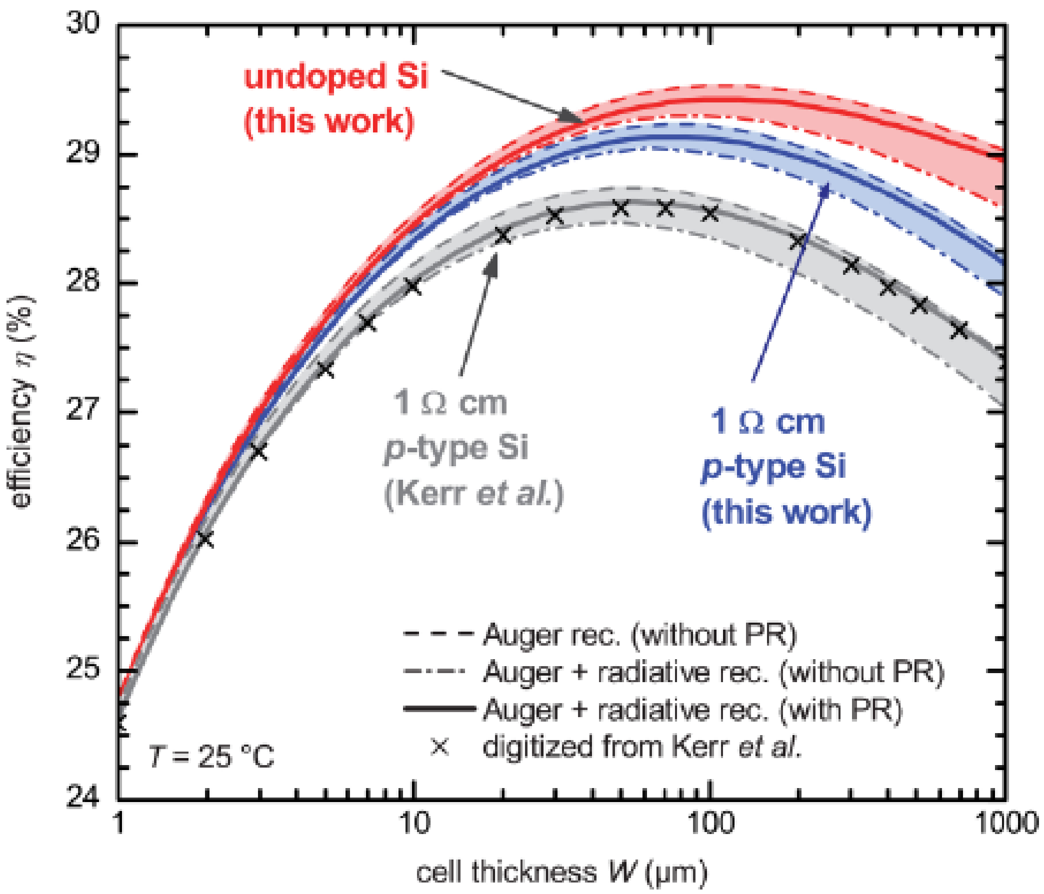

A. Richter et al. IEEE Journal of Photovoltaics, vol. 3, no. 4, pp. 1184-1191,. 2013

Photocarriers Separation & Transport
Wafer Thickness Reduction

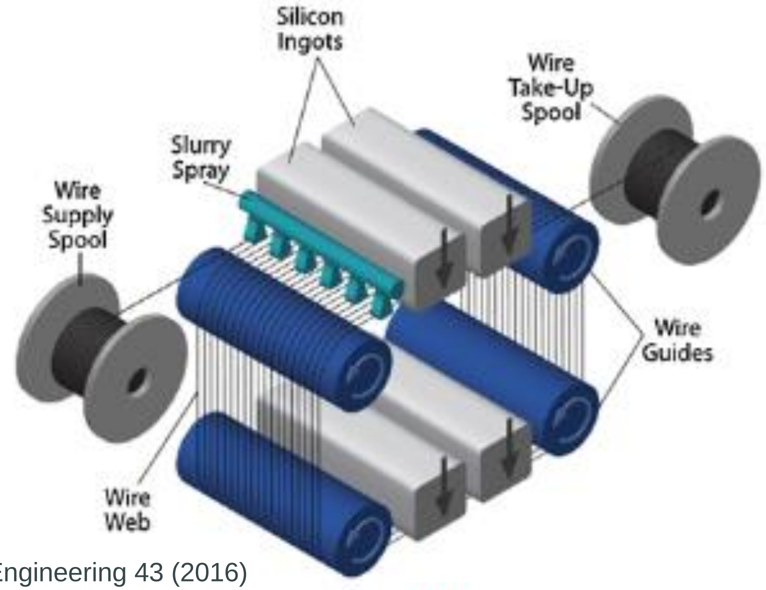

H. Wu / Precision Engineering 43 (2016)

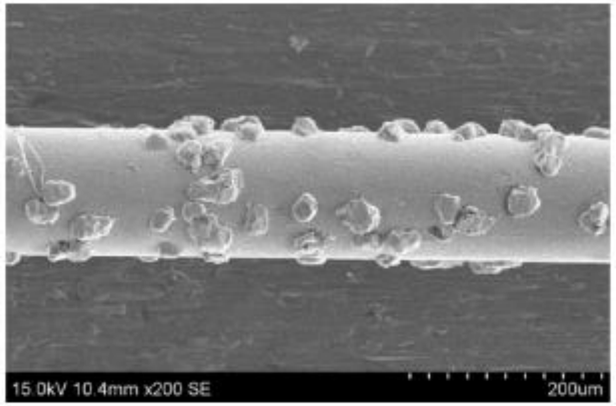

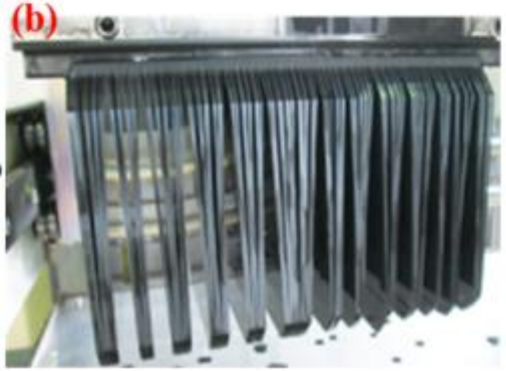

AIP Conference Proceedings 2147, 150001 (2019); https://doi.org/10.1063/1.5123902

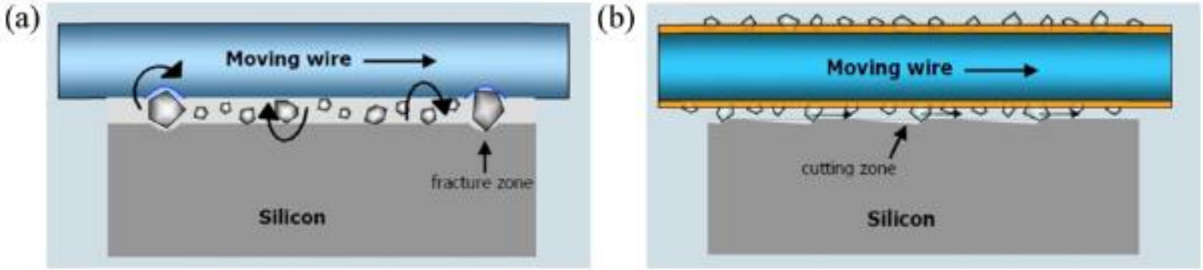

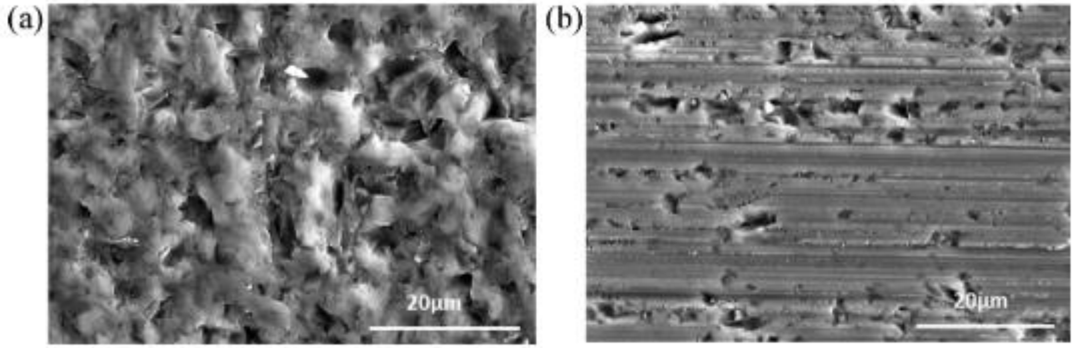

Fig. 6. SEM of wafer surface morphology: slurry sawn wafer (a), diamond wire sawn wafer (b).

Table 1. Comparison of typical wire slicing production conditions for LAS and DWS [25].

Feature	LAS	DWS
Feed rate	0.42 mm/min	1.1 mm/min
Cutting time 156mm X 156 mm	6.8 hours	2.8 hours
Cutting time 125mm X 125 mm	5.6 hours	2.2 hours
Wafer production capacity (156 mm square)	6500 wafers/day	13800 wafers/day
Wafer production capacity (125 mm square)	7800 wafers/day	16100 wafers/day
Temperature rise	40-60° C	< 20° C

Arkadeep Kumar et al. / Procedia Manufacturing 21 (2018) 549–566

Photocarriers Separation & Transport
Wafer Thickness Reduction

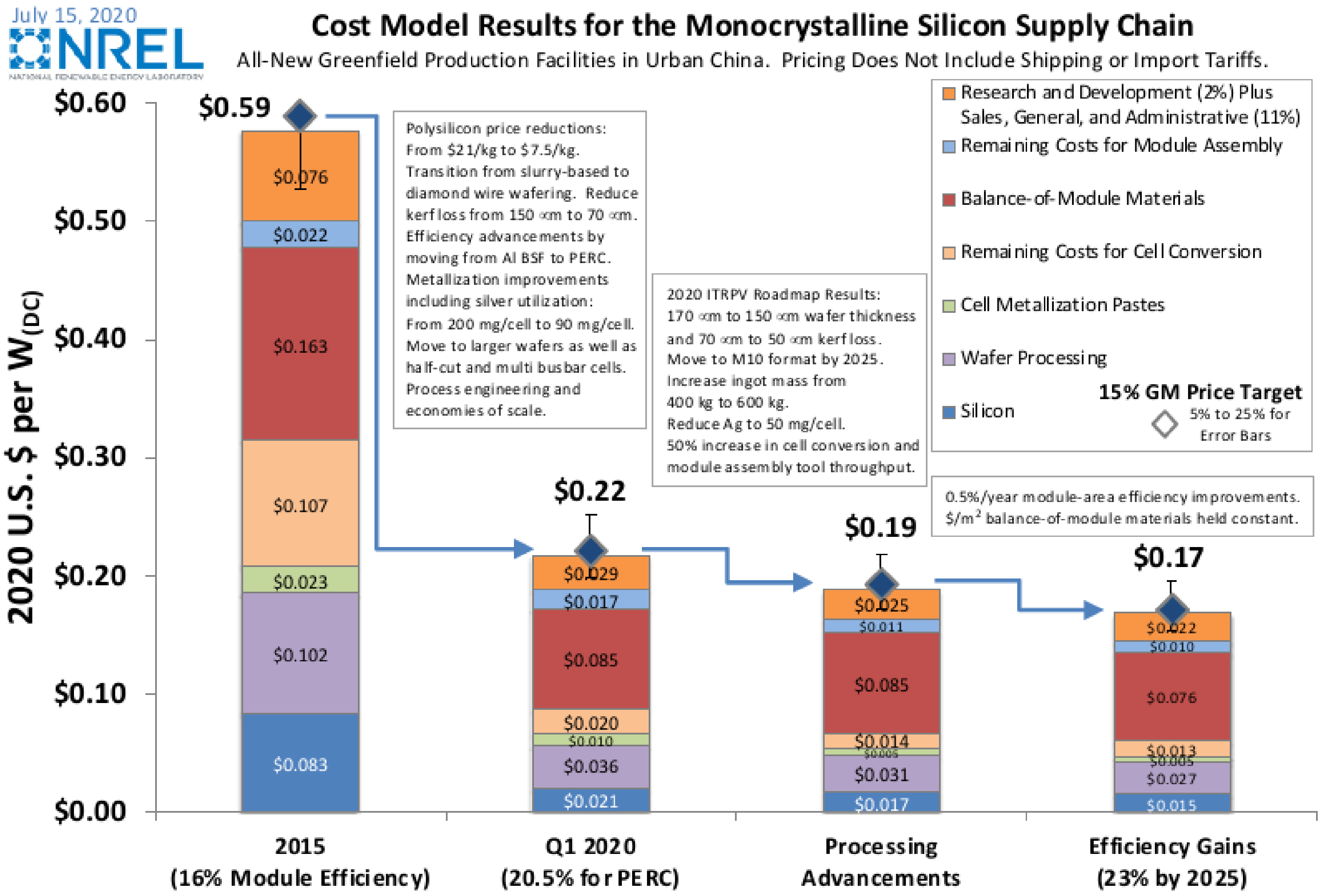

- **Wafer Thickness:**
  - 2015→2020: 180 µm→170 µm
  - 2020→2025:
    - For p-type: 170 µm→~165 µm
    - For n-type: 160 µm→~<150 µm
    - HJT using thinner wafers!
- **Kerf Loss:**
  - 2015→2020: 150 µm→70 µm
  - 2020→<2025: 70 µm→50 µm
- **Silicon and Wafering Cost:**
  - 2015→2020: 18.5c$→5.7c$
  - 2020→2025: 5.7c$→4.2c$

Applied Physics Letters 104, 113902 (2014)

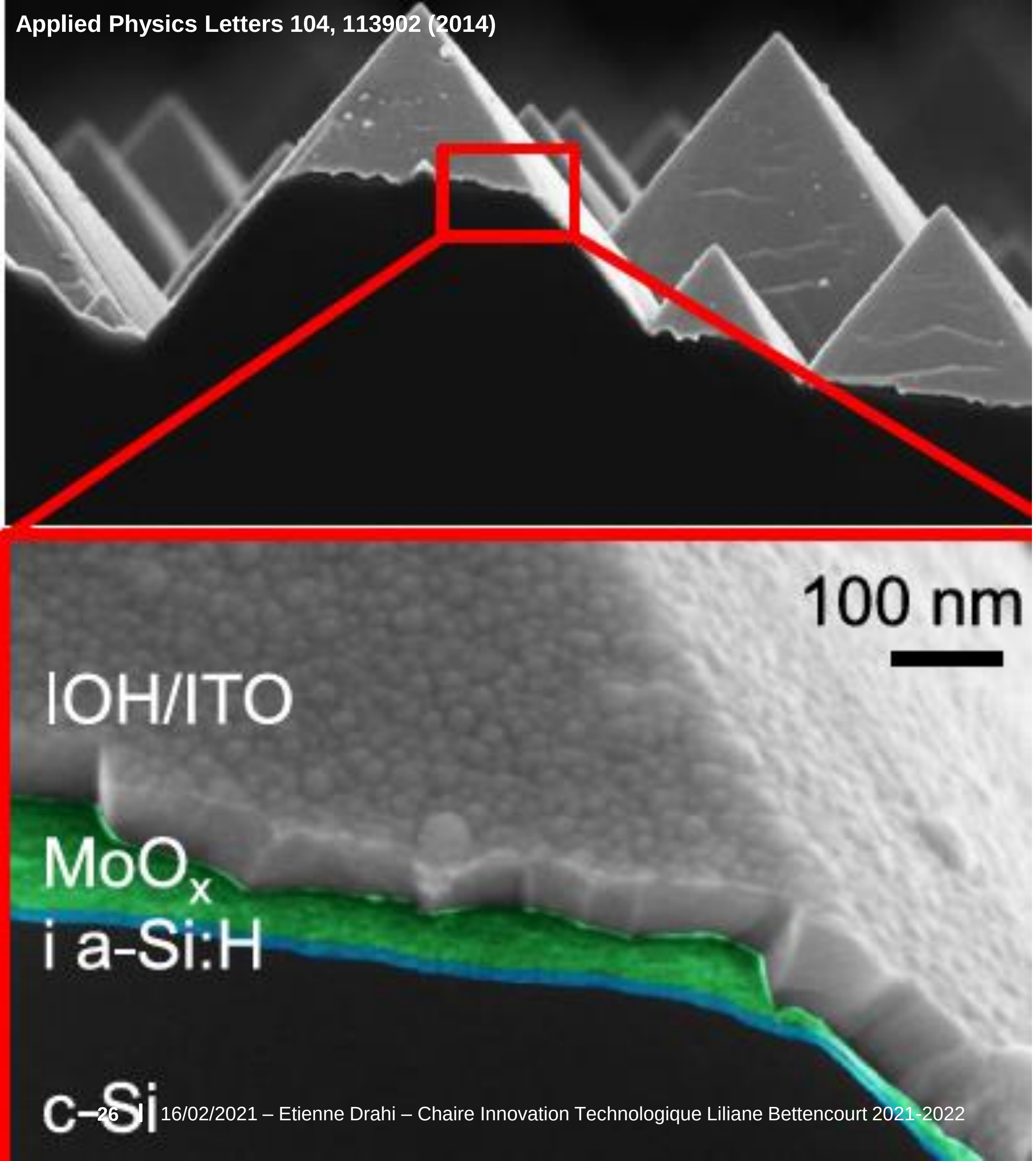

Agenda

TotalEnergies

- **Introduction**
- **Improved Photon Conversion**
  - From Simple Absorption to Light Trapping
  - Bifaciality: The Future of PV Has Two Sides
- **Photocarriers Separation & Transport**
  - Bulk Material Quality Improvement
  - Wafer Thickness Reduction
- **Photocarriers Collection & Extraction**
  - From Passivated Contacts to Passivating Contacts
  - Advanced Metallization & Interconnexion Processes
- **Conclusions**

COLLÈGE DE FRANCE 1530

Fondation Bettencourt Schueller

Photocarriers Collection & Extraction
From Passivated Contacts to Passivating Contacts

From PESC solar cells to Al-BSF: Aluminum Back Scattering Field

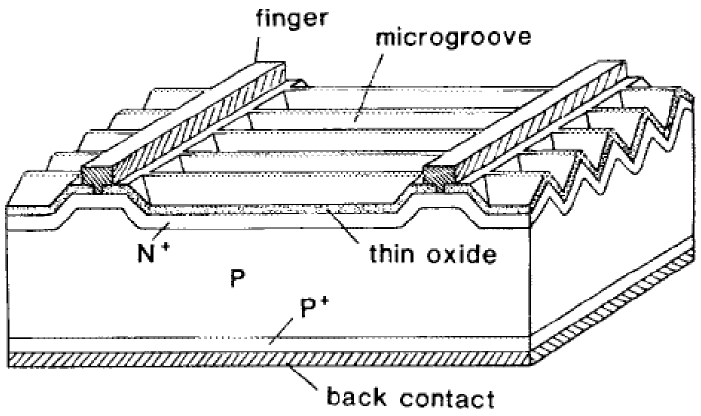

A. W. Blakers and M. A. Green Appl. Phys. Lett. 48, 215 (1986)

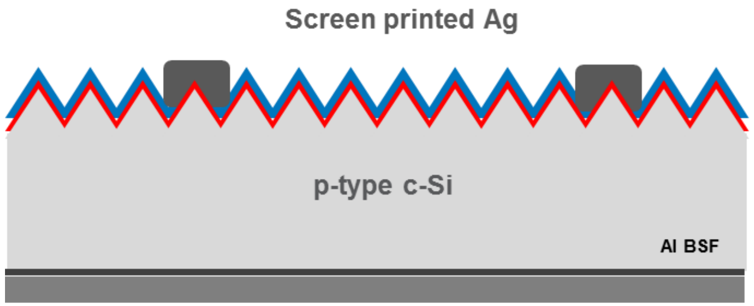

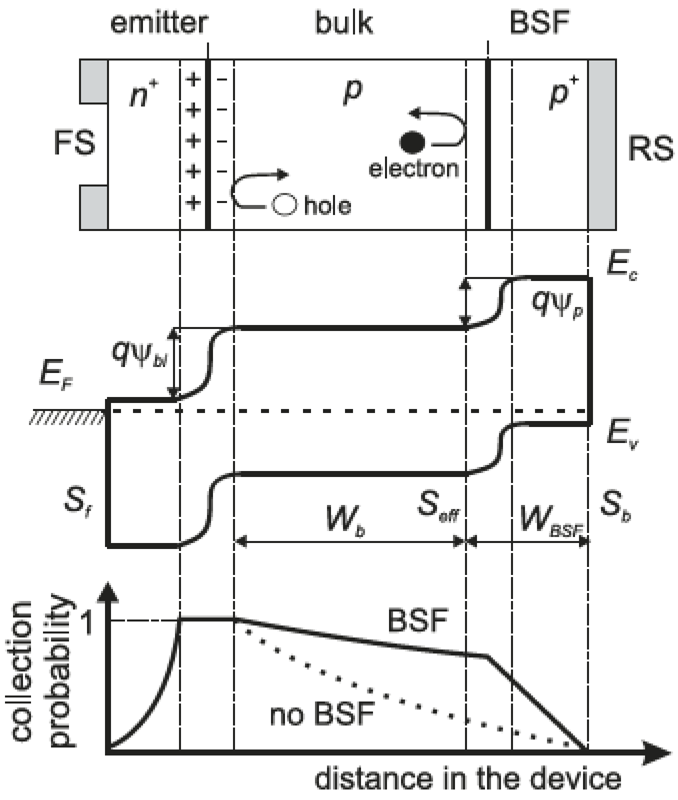

The heavily doped BSF region is formed by the alloying of an Al layer evaporated onto the rear surface. After removal of excess Al remaining after this step, a second Al layer is deposited which is sintered at lower temperatures. This sequence is believed to be consistent with obtaining BSF action while maintaining good infrared reflection from the rear surface [14].

Back surface fields are capable of improving both the short-circuit current and open-circuit voltage of cells when the minority-carrier diffusion length is comparable to the cell thickness [11]. The requirements upon the BSF properties to obtain the full voltage improvement are more severe than those to obtain the full current improvement. These requirements also become more severe as the substrate resistivity is decreased.

M. A. Green et al IEEE Transactions on Electron Devices, vol. 31, no. 5, pp. 679-683, May 1984

Photocarriers Collection & Extraction
From Passivated Contacts to Passivating Contacts

From PESC solar cells to Al-BSF: Aluminum Back Scattering Field

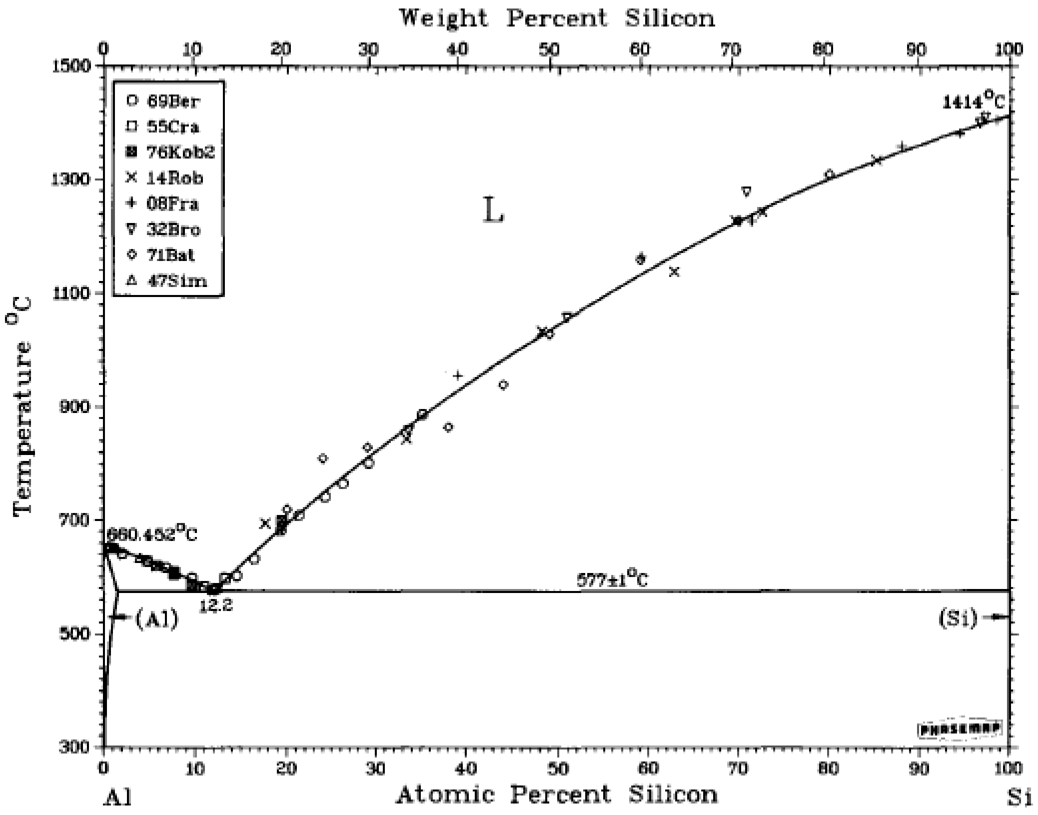

Murray, J.L., McAlister, A.J. The Al-Si (Aluminum-Silicon) system. *Bulletin of Alloy Phase Diagrams* **5,** 74 (1984).

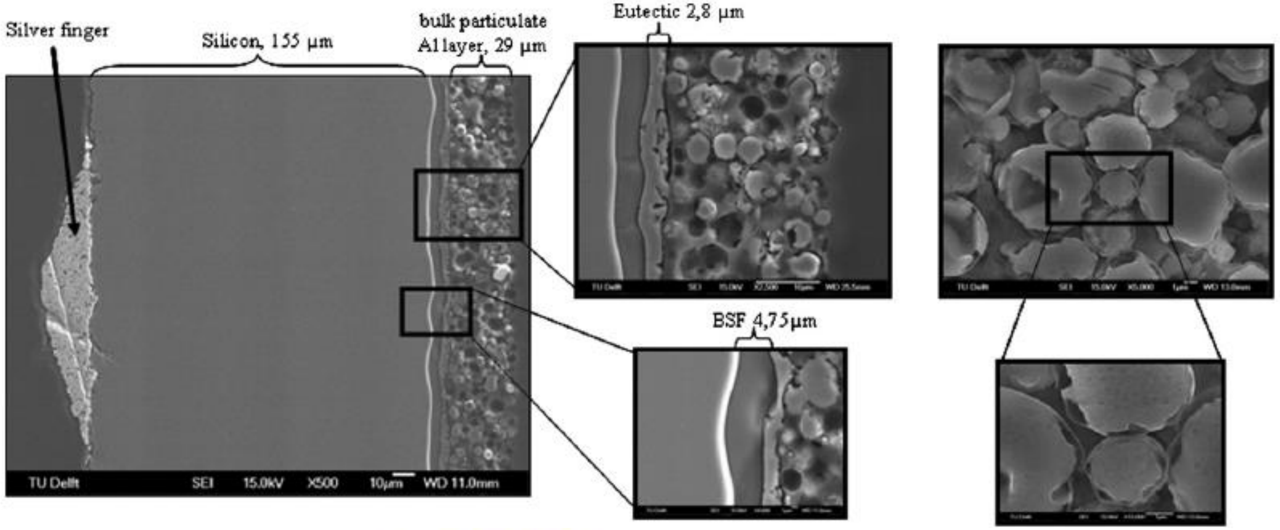

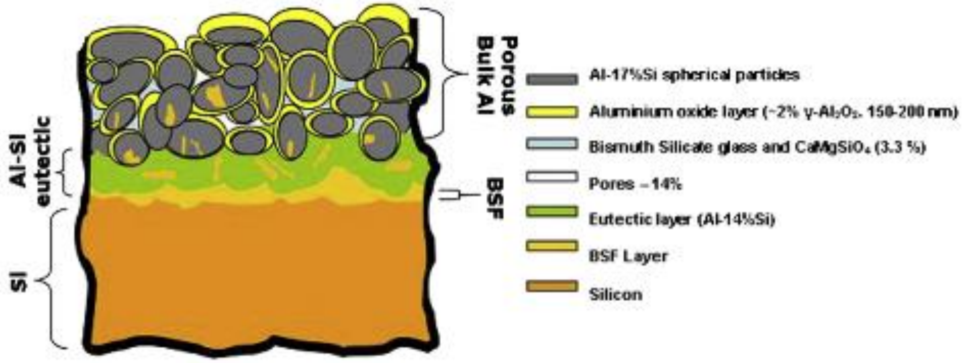

V.A. Popovich et al. / Solar Energy Materials & Solar Cells 95 (2011) 93–9696

Photocarriers Collection & Extraction
From Passivated Contacts to Passivating Contacts

From Al-BSF solar cells to PERC

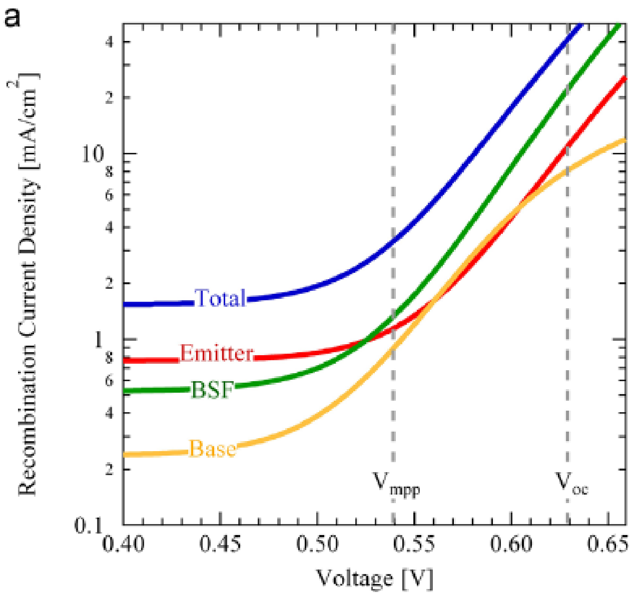

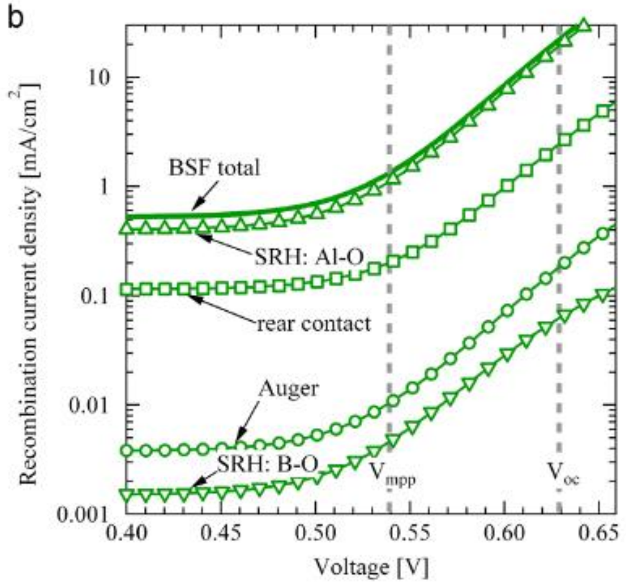

Y. Chen et al. / Solar Energy Materials & Solar Cells 120 (2014) 356–362

Status:

- Efficiency up to 20% efficiency
- High yield >95%
- Throughput >3600 wfr/hr (probably around 6000 today)
- Simple & lean process flow
- Low cost ~0.2 $\$/W_p$

Device limits:

- Reduced performance in nIR due to parasitic absorption of rear BSF + metal
- Strong recombination at the c-Si/metal interface: $J_{0,met}$~200-600 fA/cm²
- Not bifacial
- High consumption of Al paste
- Degradation rate

→ **Performant field effect but need for 'chemical passivation'**

Photocarriers Collection & Extraction
From Passivated Contacts to Passivating Contacts

From Al-BSF solar cells to PERC

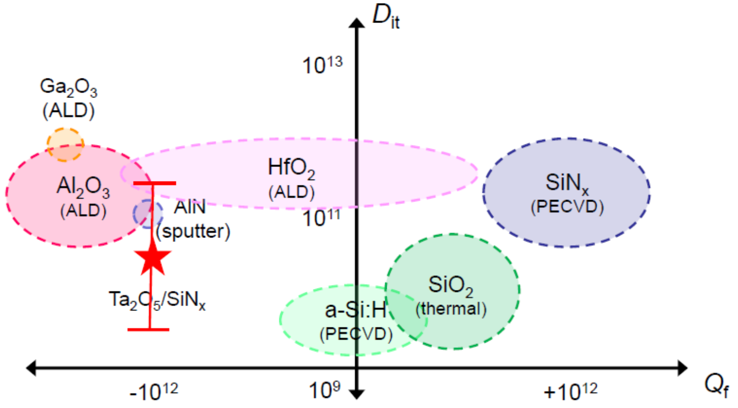

Wan et al. 5th SiliconPV 2015

- **Need for both low defect density (D_{it}) and high concentration of negative fixed charges ($-Q_f$).**
  - A lot of materials and stacks tested → Al_2O_3 dielectric layer + SiN_x capping layer
  - In 1989 Hezel & Jaeger first demonstrated Al_2O_3 dielectric layer in a solar cell.
  - Roughly two decades later Agostinelli et al. reached SRV <10 cm/s on p-type c-Si
  - Al_2O_3 can be deposited by various techniques: PECVD, (spatial) ALD…

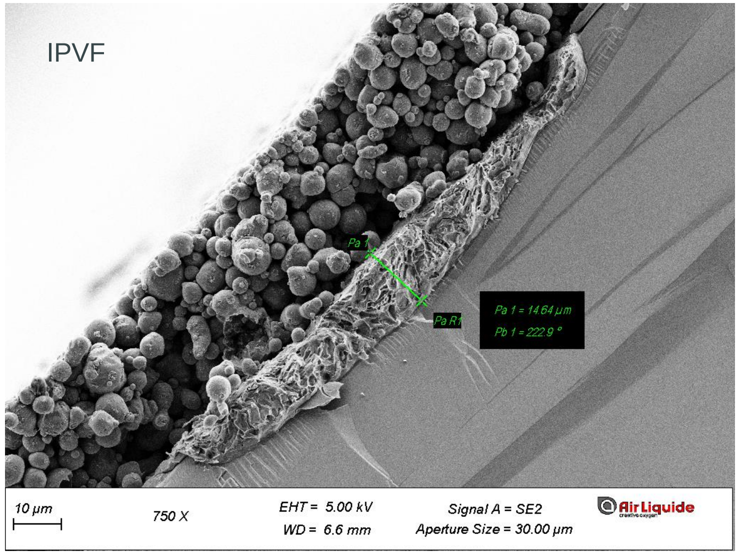

- **Need to open locally dielectric stack** (6-20 nm AlO_x + ~100 nm SiN_x) → laser process + local Al-BSF process

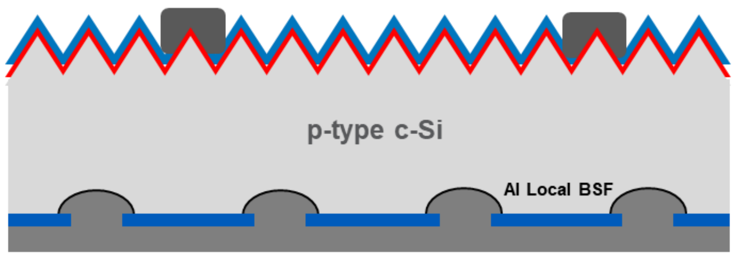

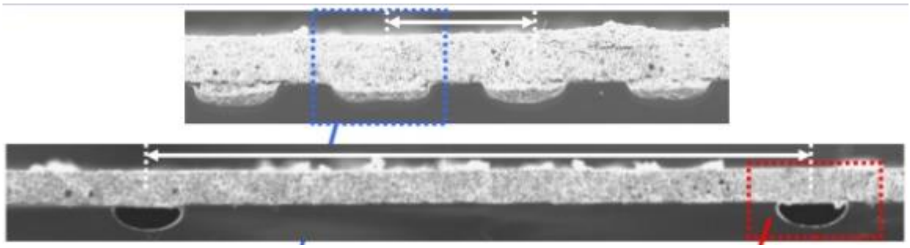

Elías Urrejola Metallization Workshop 2011

Photocarriers Collection & Extraction
From Passivated Contacts to Passivating Contacts

From PERC to TOPCon & Heterojunction

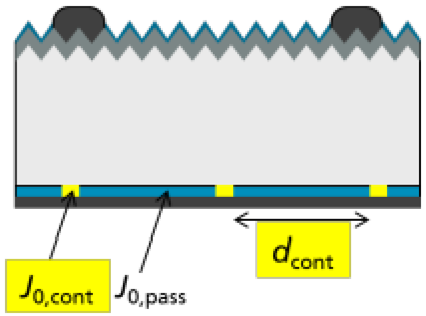

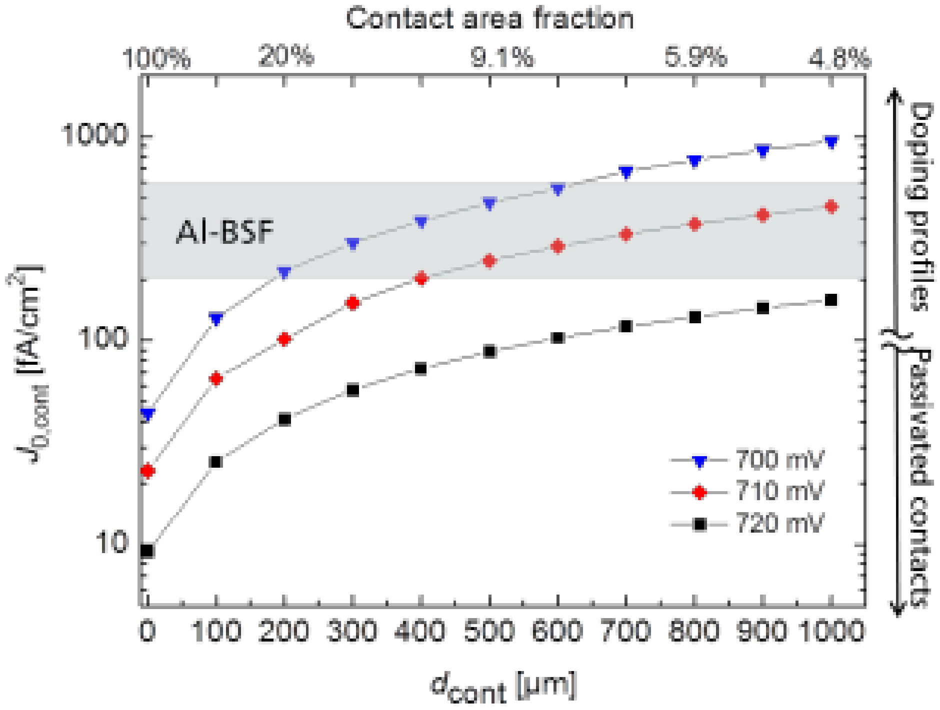

Fig. 3: $J_{0,cont}$ values necessary to achieve certain open-circuit voltages for different rear contact distances.

Glunz et al EUPVSEC 2015

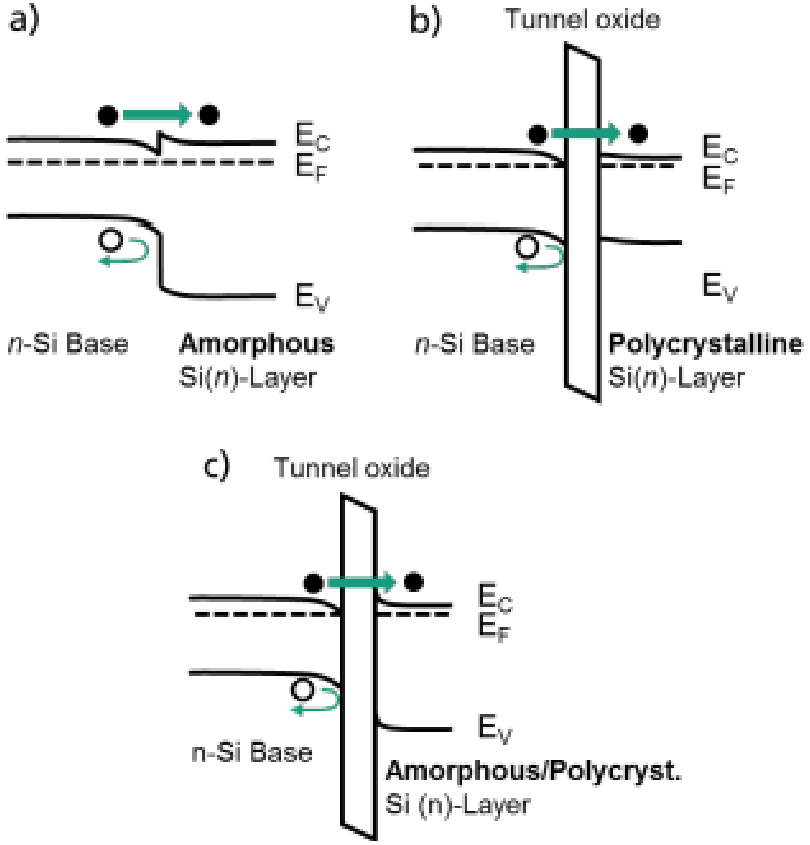

Fig. 6: Schematic concepts of different passivated contact technologies. a) a-Si/c-Si heterojunction, b) poly-Si with tunnel oxide, c) TOPCon.

Photocarriers Collection & Extraction
From Passivated Contacts to Passivating Contacts

From PERC to Tunnel Oxide Passivated Contact (TOPCon) & Silicon Heterojunction (SHJ)

TOPCon

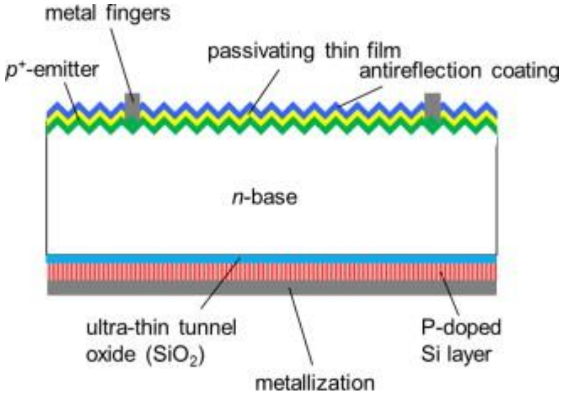

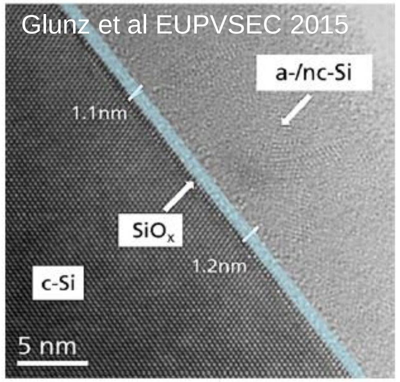

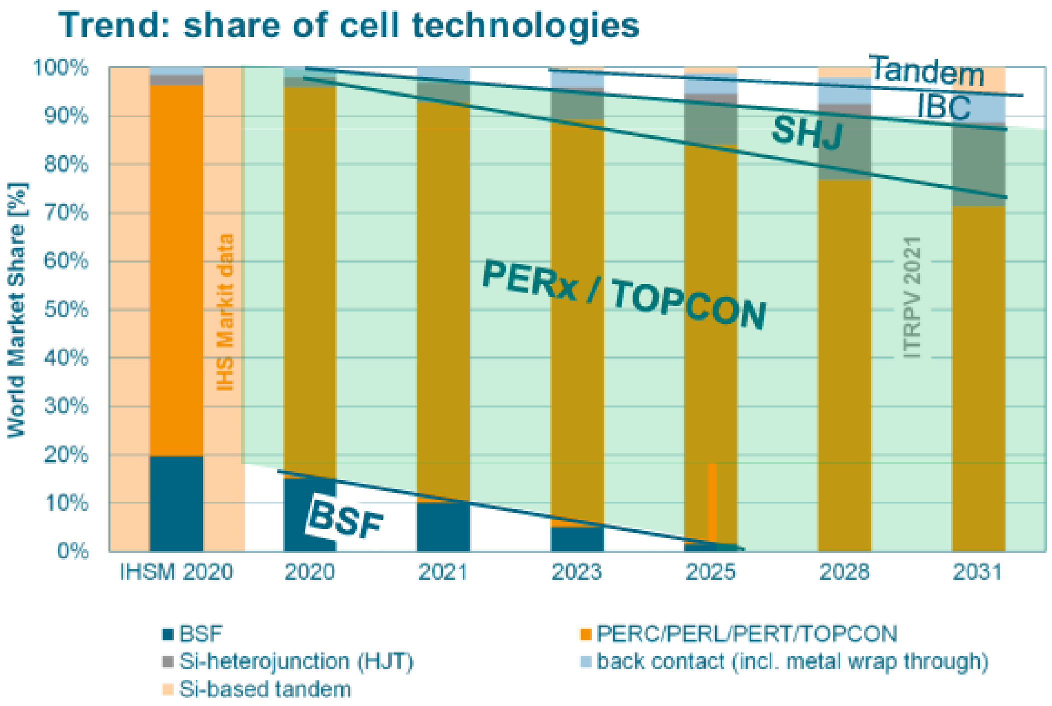

SHJ

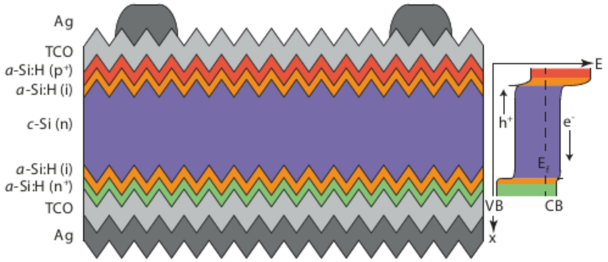

Green, Vol. **2** (2012), pp. 7–24

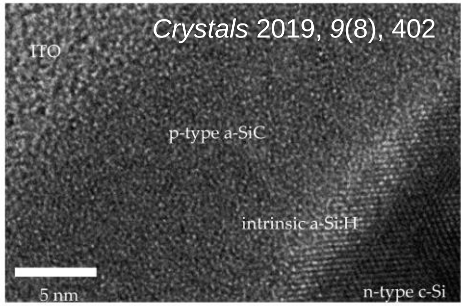

Photocarriers Collection & Extraction
Advanced Metallization & Interconnexion Processes

- **Wafer Size Increase**: from 156x156 mm² to 210x210 mm²
  - → I_{sc} increased from ~9.6 A for M0 to 17.6 A for M12
  - → Need to cut wafer to reduce current and resistive losses
  - → **M6 wafers cut in 2, M12 wafers cut in 3!**

- Historically **IR laser used for edge isolation and cutting** BUT material damage.
  - → With improving both material quality & surface passivation edge recombination = not negligeable loss!
  - → **Thermal Laser Separation** develop to reduce damage as much as possible
  - → **'mimick' cleaving = reduced damage/roughness**

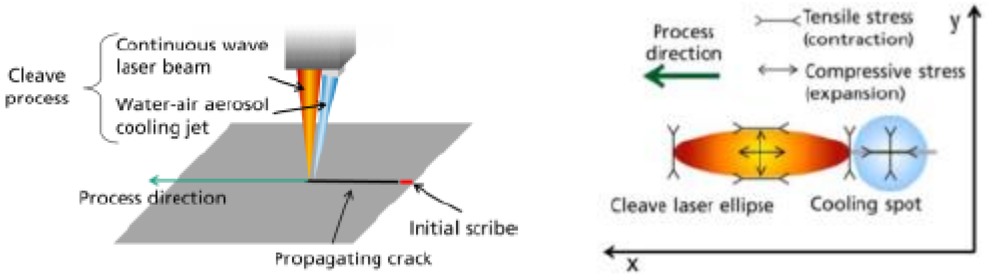

IEEE JOURNAL OF PHOTOVOLTAICS, VOL. 11, NO. 2, MARCH 2021

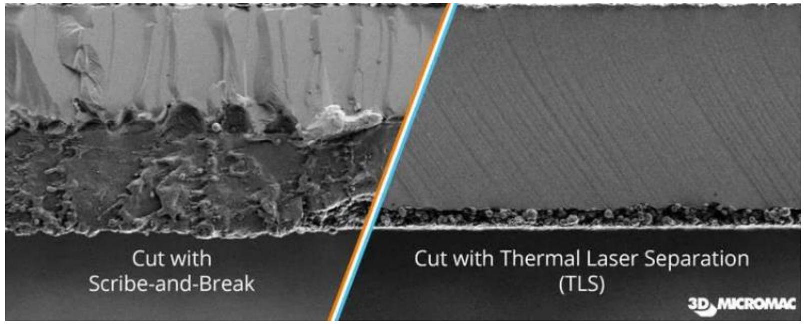

Photocarriers Collection & Extraction
Advanced Metallization & Interconnexion Processes

- **From standard tabbing to advanced interconnections**

Reduced Interconnexion shading

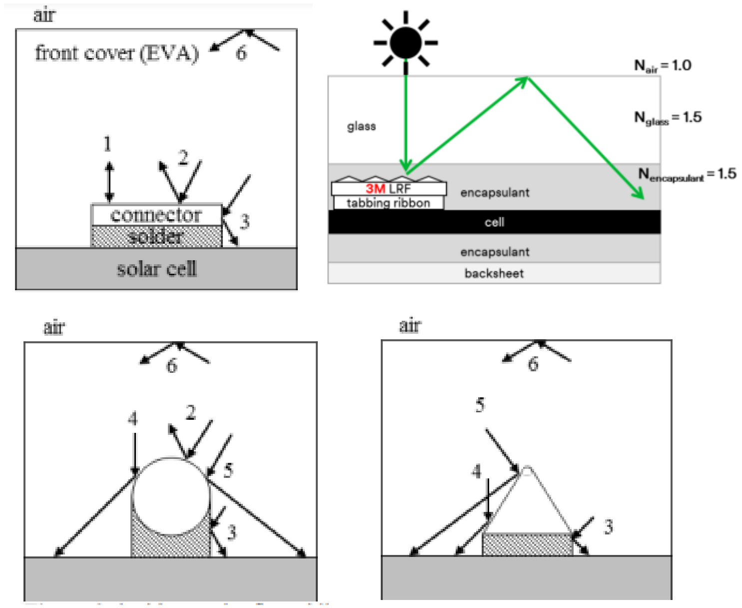

Mittag et al. EUPVSEC 2016

Higher Integration Density

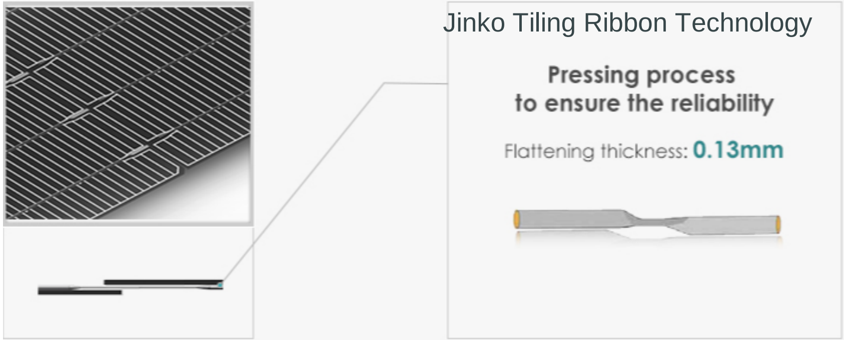

Longi Seamless Soldering

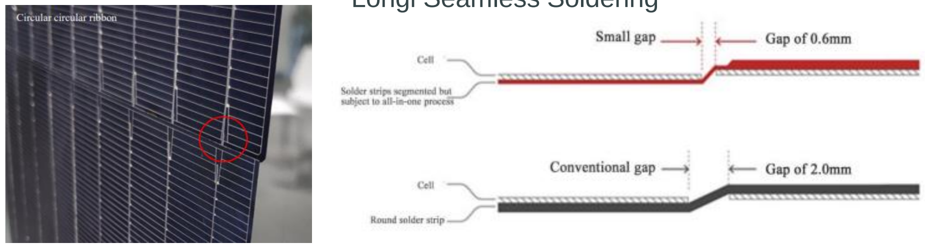

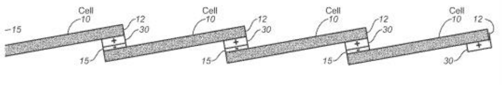

FIG. 3A

EP 2 917 940 B1

AgriPV installation in Channay – TotalEnergies Renewables France

Agenda

- **Introduction**
- **Improved Photon Conversion**
  - From Simple Absorption to Light Trapping
  - Bifaciality: The Future of PV Has Two Sides
- **Photocarriers Separation & Transport**
  - Bulk Material Quality Improvement
  - Wafer Thickness Reduction
- **Photocarriers Collection & Extraction**
  - From Passivated Contacts to Passivating Contacts
  - Advanced Metallization & Interconnexion Processes
- **Conclusions**

Conclusions

PV Learning Curve: Swanson's Law

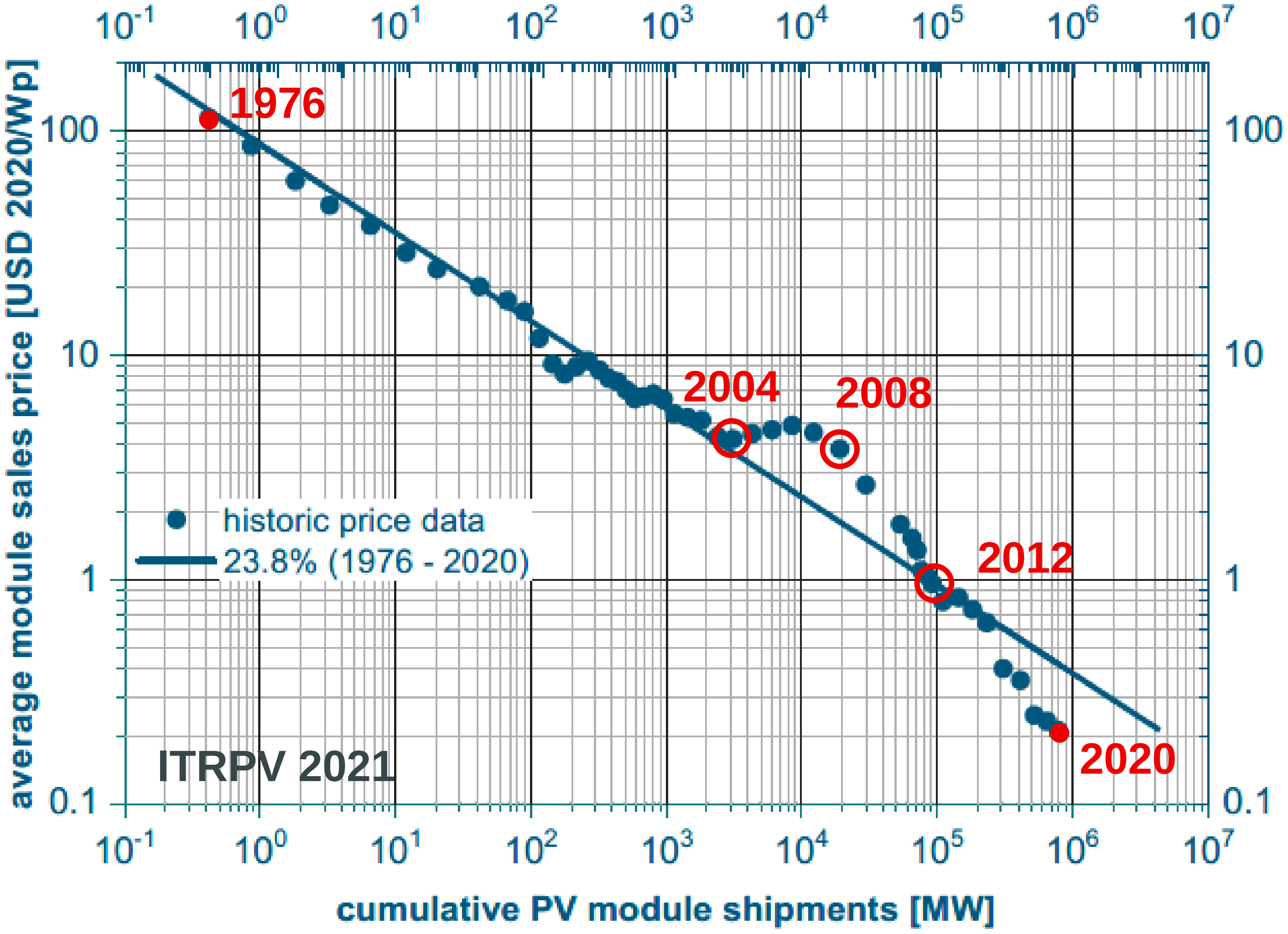

>40 years industrial history:

- **In 1976: 0.3 MW_p shipped capacity for 107 $/$W_p$**
- **In 2020: 789 GWp shipped capacity for 0.21 $/Wp**
- **756 GWp cumulative installed capacity**
- **135 GWp shipped in 2020**

Learning Rate = Swanson's Law

Each time the cumulative PV module production doubled; the price went down by 20-25% for the last 40 years

Conclusions
PV Learning Curve: Swanson's Law

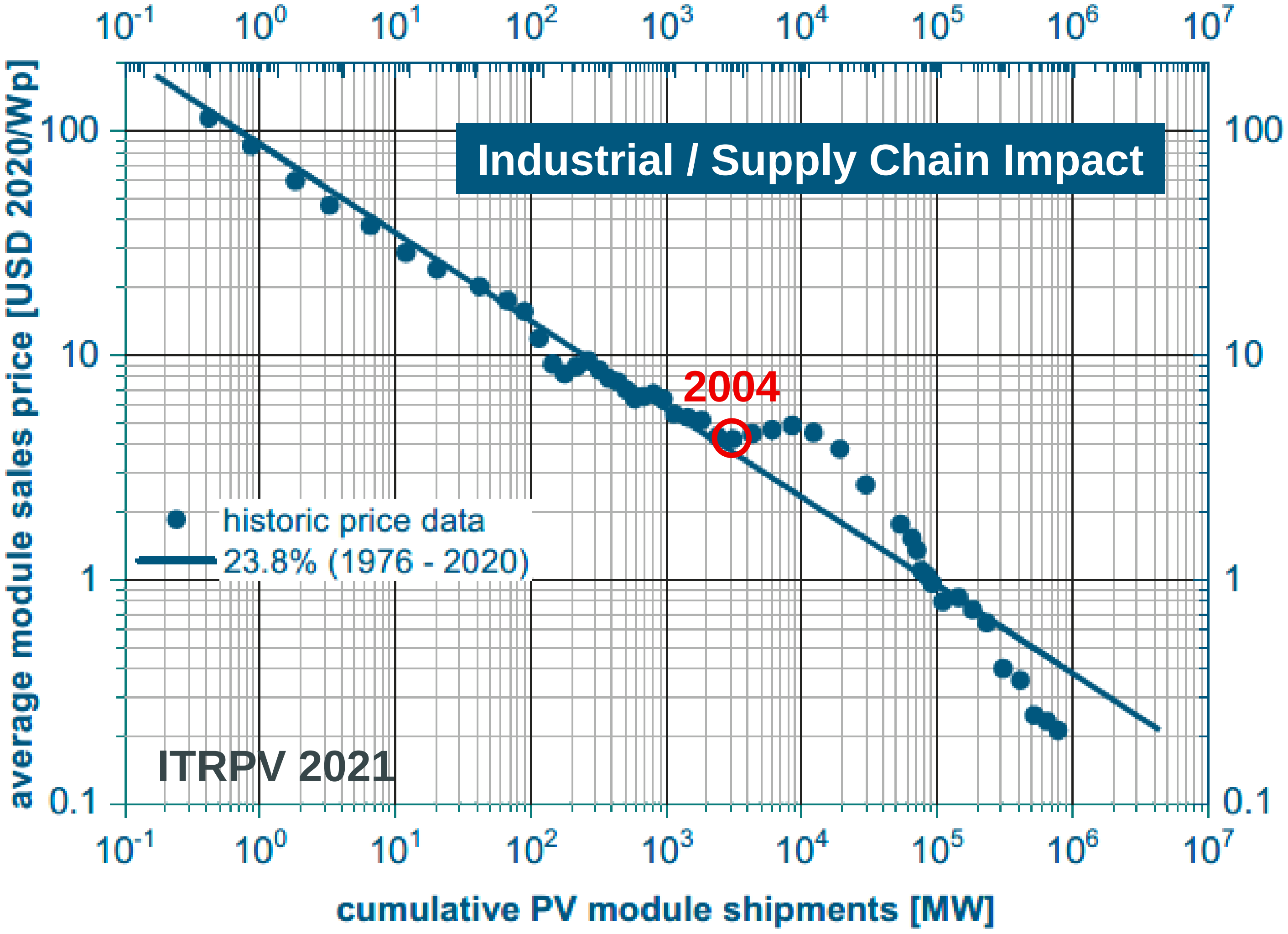

- Polysilicon price decreasing since 1975 due to **electronics/microelectronics boom**
- **Polysilicon shortage starting in 2004**
- **PV starting to be a driver for polysilicon industry** → specific products targeting PV needs

Figure 3.9 Share of PV in polysilicon demand (left) and polysilicon price (right), 1975-2010

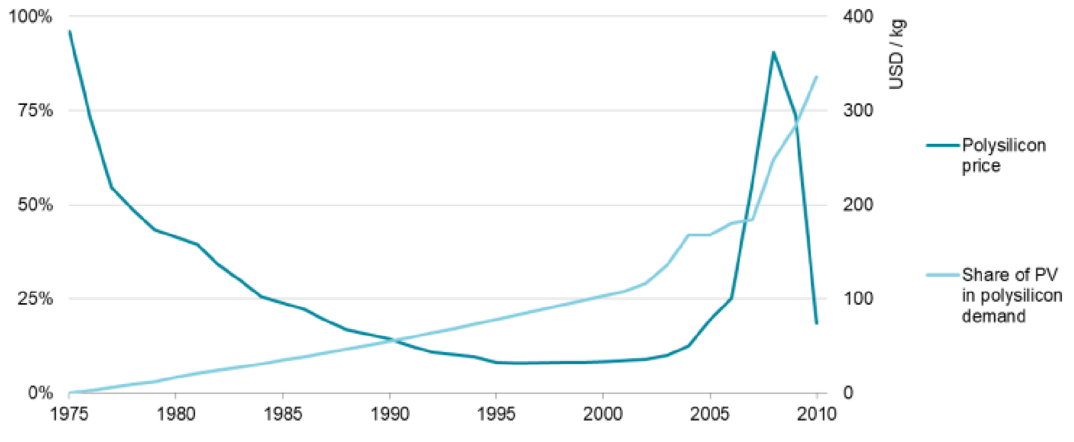

Note: The 2008 price spike was due to shortage of supply after spike in demand for PV panels that rebalanced after the global financial crisis.

Sources: Mehta (2014); Ferber, Costogue and Pellin (1982).

\+ Introduction of **M0 Wafer format by QCells in 2006**

Conclusions
PV Learning Curve: Swanson's Law

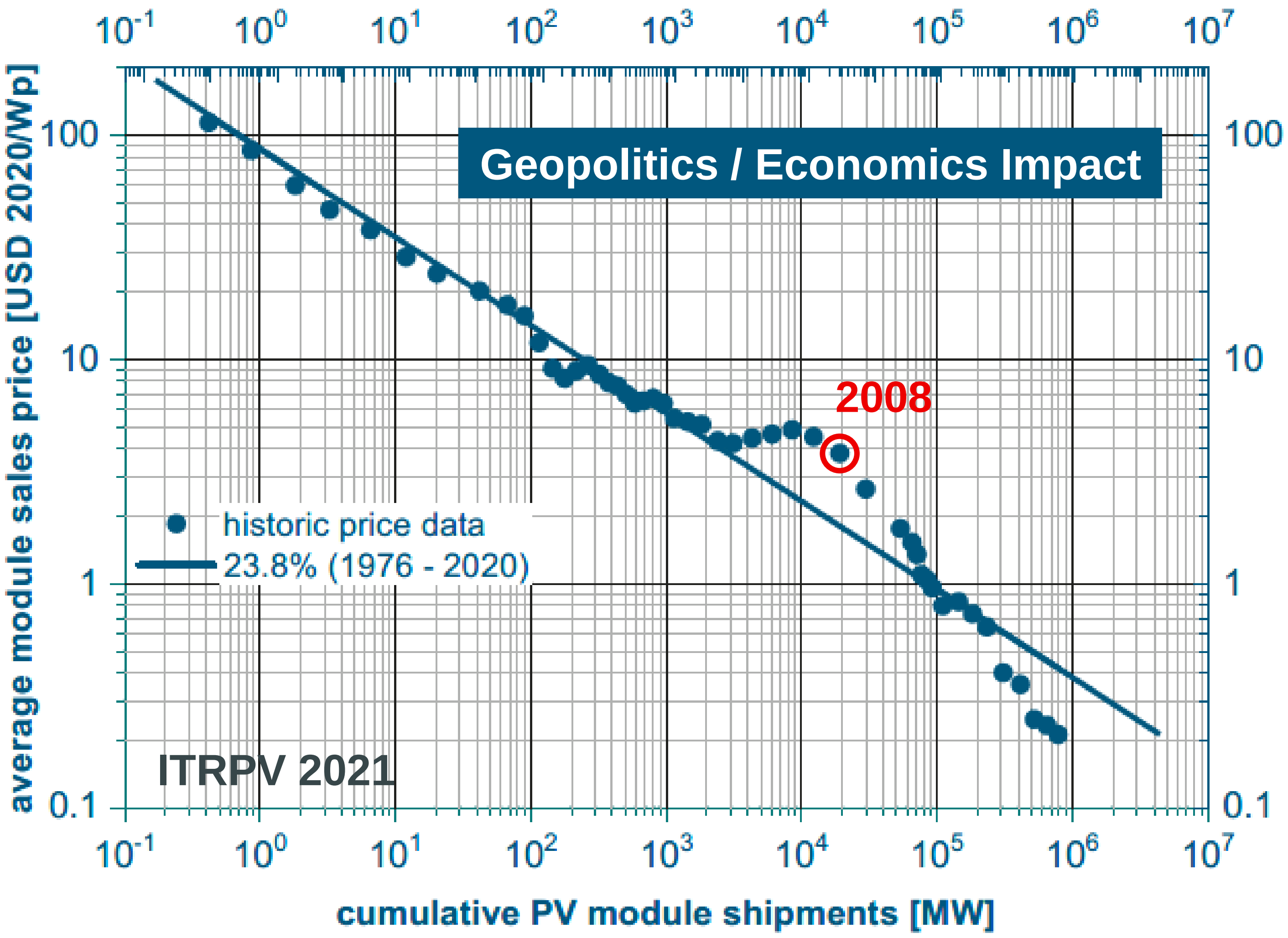

In 2007, the National Development and Reform Commission planned to **have China's solar capacity increase to 1.8 GW by 2020.**

"*The goal that we made originally is probably too low*" he said at a solar energy conference in Shanghai. "*By 2020, we can reach 10 GW or more*" Wang Zhongying, assistant director at the NDRC's Energy Research Institute

PV Module Production by Region 1990-2020 Percentage of Total MW_p Produced

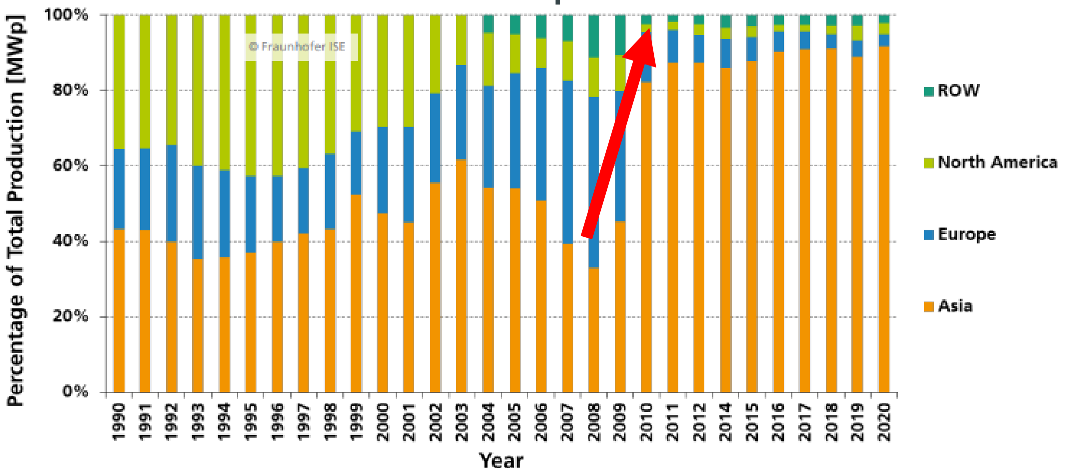

https://www.reuters.com/article/china-solar-idAFPEK12384620090505

Conclusions
PV Learning Curve: Swanson's Law

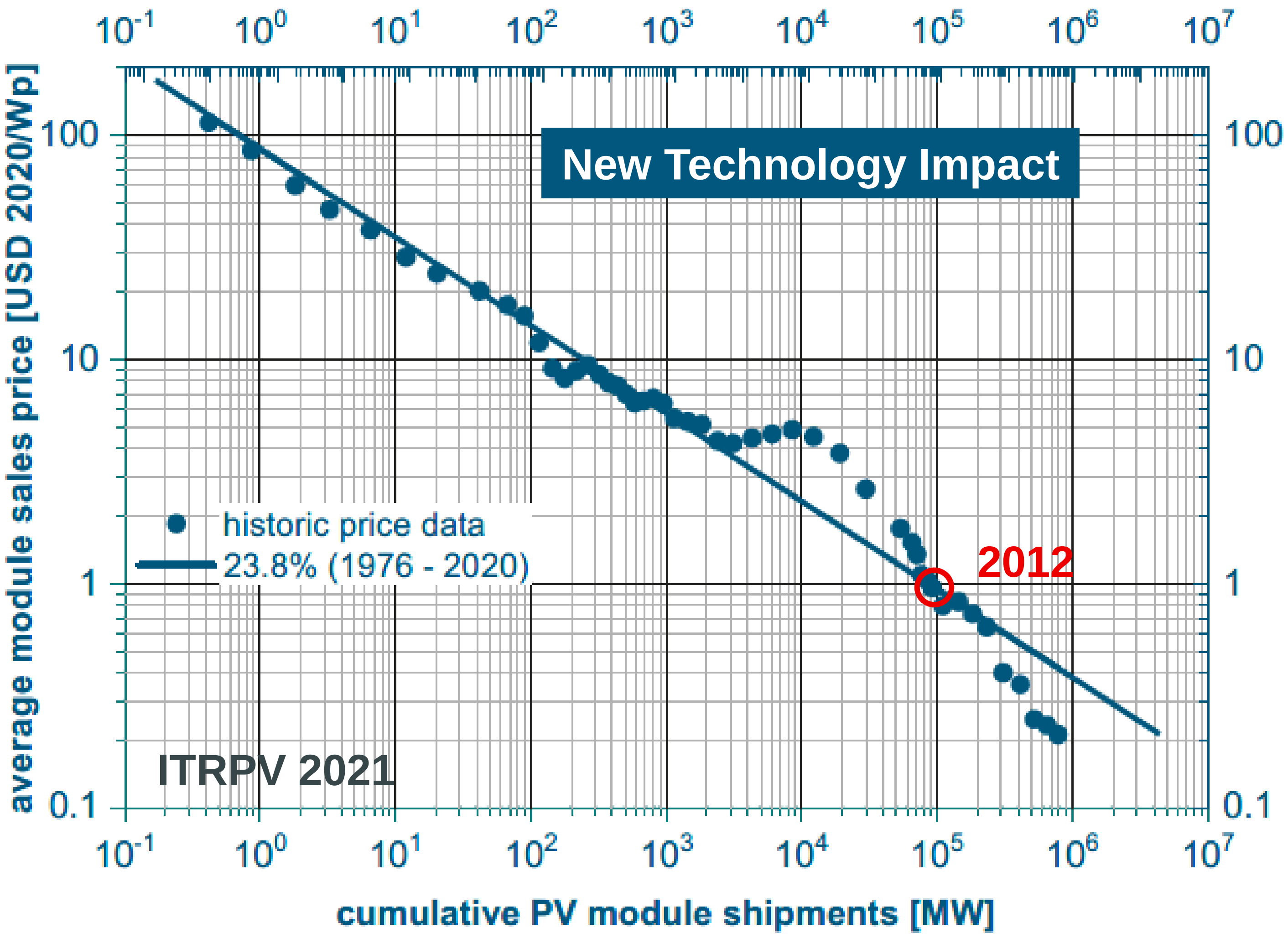

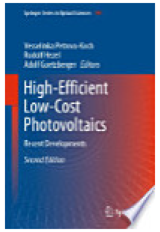

books.google.fr › books · Traduire cette page

High-Efficient Low-Cost Photovoltaics: Recent Developments - Page 96

Vesselinka Petrova-Koch, Rudolf Hezel, Adolf Goetzberger · 2019

TROUVÉ À L'INTÉRIEUR – PAGE 96

Hanwha **Q CELLS** was one of the first companies to **start** the **production** of Si **PERC**-like **cells** in 2012. From the first internal **PERC cell** samples in mid-2009 to the transfer of the Q.ANTUM [1] process sequence to our **production** facility in ...

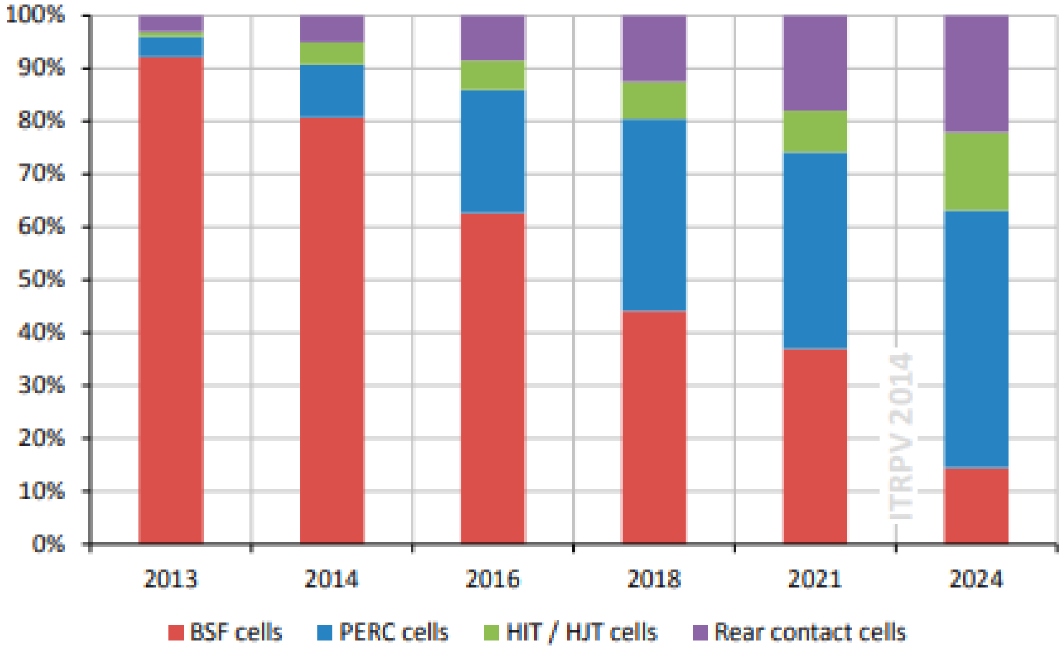

Conclusions
Key Messages

TotalEnergies

- **Historical Learning Rate divided in 3 zones:**
  - Small Scale Production = ~18%
  - Polysilicon Shortage = ~stagnation or price increase
  - Mass Production = ~41%

- PV and especially c-Si **PV development enabled by strong collaboration** between:
  - **Academics** on several fields such as materials science, chemistry, physics, electronics, optics… Research & Education
  - **Technologists/Industrials**: transfer of technologies from other industries and optimization for PV: Si crystallization & cutting, Laser processes, Screen-printing, vacuum deposition processes… + Supply Chain.
  - **Policy makers & Society**: incentive for early adoption and deployment, research support

🕵 Spoiler alert 🕵: This is just the beginning of PV!

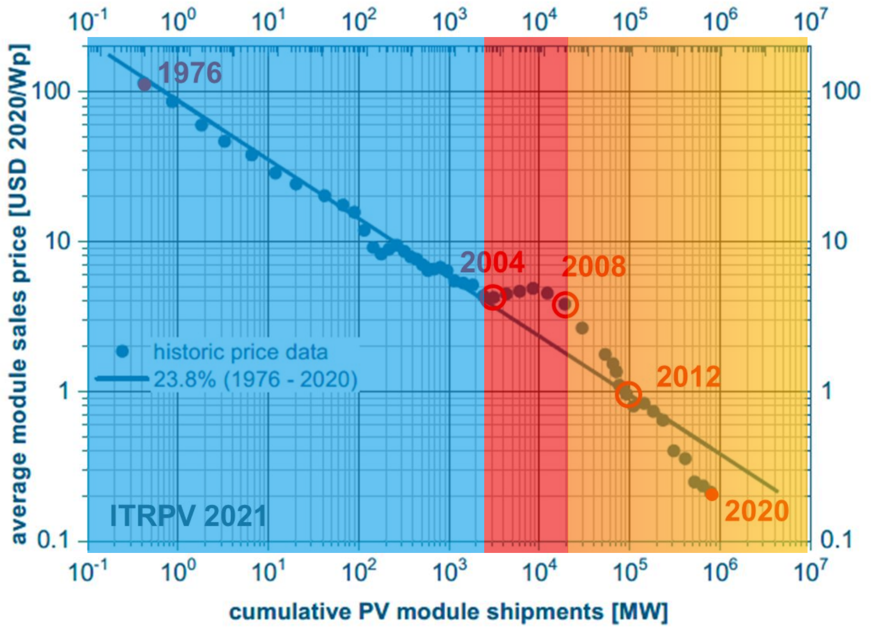

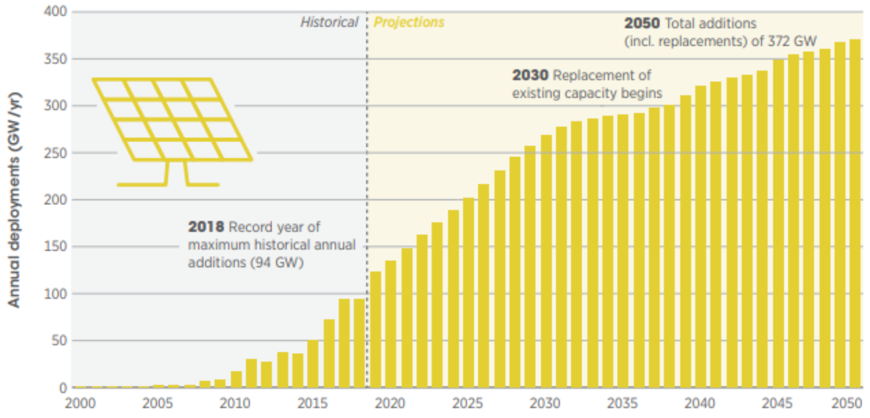

Source: Historical values based on IRENA (2019b) and future projections based on IRENA (2019a).

COLLÈGE DE FRANCE 1530
Fondation Bettencourt Schueller


Merci

Bibliography (1/)

TotalEnergies

- **General:**

  - T. Tiedje, E. Yablonovitch, G. D. Cody and B. G. Brooks, "Limiting efficiency of silicon solar cells," in IEEE Transactions on Electron Devices, vol. 31, no. 5, pp. 711-716, May 1984, doi: 10.1109/T-ED.1984.21594.
  - A. Richter, M. Hermle and S. W. Glunz, "Reassessment of the Limiting Efficiency for Crystalline Silicon Solar Cells," in IEEE Journal of Photovoltaics, vol. 3, no. 4, pp. 1184-1191, Oct. 2013, doi: 10.1109/JPHOTOV.2013.2270351.
  - Yoshikawa, K., Kawasaki, H., Yoshida, W. et al. Silicon heterojunction solar cell with interdigitated back contacts for a photoconversion efficiency over 26%. Nat Energy 2, 17032 (2017). https://doi.org/10.1038/nenergy.2017.32
  - https://doi.org/10.1016/j.solmat.2017.06.024
  - High-Efficient Low-Cost Photovoltaics: Recent Developments, Volume 140 de Springer Series in Optical Sciences Vesselinka Petrova-Koch, Rudolf Hezel, Adolf Goetzberger, https://doi.org/10.1007/978-3-540-79359-5
  - Silicon shortage hits solar power hopes Financial Times November 20th 2006
  - IEA, Share of PV in polysilicon demand (left) and polysilicon price (right), 1975-2010, IEA, Paris https://www.iea.org/data-and-statistics/charts/share-of-pv-in-polysilicon-demand-left-and-polysilicon-price-right-1975-2010
  - Photovoltaic Report 2021 Fraunhofer ISE
  - https://www.reuters.com/article/china-solar-idAFPEK12384620090505
  - https://doi.org/10.1016/j.solmat.2017.06.024
  -

Bibliography (2/)

- **Improved Photoconversion**
  - From Simple Absorption to Light Trapping

- Massiot, I., Cattoni, A. & Collin, S. Progress and prospects for ultrathin solar cells. Nat Energy 5, 959–972 (2020). https://doi.org/10.1038/s41560-020-00714-4
- Fischer, G. PhD Thesis 2018 Plasma Nanotexturing of Silicon for Photovoltaic Applications: Tailoring Plasma-Surface Interactions for Improved Light Management.
- Oliver Höhn, Nico Tucher, and Benedikt Bläsi, "Theoretical study of pyramid sizes and scattering effects in silicon photovoltaic module stacks," Opt. Express 26, A320-A330 (2018)
- K. Tokoro, D. Uchikawa, M. Shikida and K. Sato, "Anisotropic etching properties of silicon in KOH and TMAH solutions," MHA'98. Proceedings of the 1998 International Symposium on Micromechatronics and Human Science. - Creation of New Industry - (Cat. No.98TH8388), 1998, pp. 65-70, doi: 10.1109/MHS.1998.745752.
- K. Saliou et al., "Powerful topographic analyzing technique using Fast Fourier Transform for c-Si solar cells and emerging technologies," 2019 IEEE 46th Photovoltaic Specialists Conference (PVSC), 2019, pp. 0412-0417, doi: 10.1109/PVSC40753.2019.8980904.
- S A Campbell et al 1995 J. Micromech. Microeng. 5 209
- Langmuir 1998, 14, 2925-2928

Bibliography (3/)

- **Improved Photoconversion**
  - Bifaciality: The Future of Energy Has Two Sides
    - https://doi.org/10.1016/j.solmat.2020.110586
    - Dullweber nPV Workshop 2017: http://npv-workshop.com/fileadmin/layout/images/Konstanz-2017/2__T._Dullweber_ISFH_PERC_.pdf
    - US3278811A Hiroshi Mori 1966 Radiation energy transducing device
    - ITRPV roadmaps: https://itrpv.org/
    - Imec and Jolywood achieve a record of 23.2 percent with bifacial n-PERT solar cells
    - IEEE JOURNAL OF PHOTOVOLTAICS, VOL. 10, NO. 2, MARCH 2020
    - https://www.ise.fraunhofer.de/content/dam/ise/de/documents/publications/conference-paper/36-eupvsec-2019/Rauer_2CO121.pdf

Bibliography (4/)

- **Photocarriers Separation & Transport**
  - Material Quality Improvement:

    - Wenham & Green, Progress In Photovoltaics: Research And Applications, Vol 4, 3-33 (1996)
    - Hallam et al. RAPID PROCESSING OF BORON OXYGEN DEFECTS EUPVSEC 2015
    - IEEE JOURNAL OF PHOTOVOLTAICS, VOL. 10, NO. 1, JANUARY 2020
    - A. Richter et al. / Energy Procedia 27 (2012) 88 – 94
    - Gianluca Coletti PhD Thesis - Impurities in silicon and their impact on solar cell performance
    - J. R. Davis et al., "Impurities in silicon solar cells," in IEEE Transactions on Electron Devices, vol. 27, no. 4, pp. 677-687, April 1980, doi: 10.1109/T-ED.1980.19922.
    - J. Schmidt et al., "Impurity-related limitations of next-generation industrial silicon solar cells," 2012 IEEE 38th Photovoltaic Specialists Conference (PVSC) PART 2, 2012, pp. 1-5, doi: 10.1109/PVSC-Vol2.2012.6656779.
    - Meng Xiajie, LONGi Solar 2019, PV-Tech https://www.pv-tech.org/white-papers/the-complexity-of-lid-letid-and-hid

Bibliography (5/)

- **Photocarriers Separation & Transport**
  - Wafer Thickness Reduction:

- Applied Physics Letters 104, 113902 (2014); doi: 10.1063/1.4868880
- Xuegong Yu, Peng Wang, Xiaoqiang Li, Deren Yang, Thin Czochralski silicon solar cells based on diamond wire sawing technology, Solar Energy Materials and Solar Cells, Volume 98, 2012, Pages 337-342, https://doi.org/10.1016/j.solmat.2011.11.028
- EU PVSEC Proceedings - Diamond Wire-Sawn Silicon Wafers – from the Lab to the Cell Production (eupvsec-proceedings.com)
- Post | Feed | LinkedIn
- AIP Conference Proceedings 2147, 150001 (2019); https://doi.org/10.1063/1.5123902
- Arkadeep Kumar et al. / Procedia Manufacturing 21 (2018) 549–566
- https://doi.org/10.1016/j.precisioneng.2015.08.008

Bibliography (6/)

- **Photocarriers Collection & Extraction**
  - From passivated contacts to Passivating Contacts

- A. W. Blakers and M. A. Green Appl. Phys. Lett. 48, 215 (1986); https://doi.org/10.1063/1.96799
- A. W. Blakers et al., "18-percent efficient terrestrial silicon solar cells," in IEEE Electron Device Letters, vol. 5, no. 1, pp. 12-13, Jan. 1984, doi: 10.1109/EDL.1984.25813.
- E. S. Rittner, A. Meulenberg, and J. F. Allison, J. Energy 5, 9 (1981).
- M. A. Green, A. W. Blakers, Jiqun Shi, E. M. Keller and S. R. Wenham, "High-efficiency silicon solar cells," in IEEE Transactions on Electron Devices, vol. 31, no. 5, pp. 679-683, May 1984, doi: 10.1109/T-ED.1984.21589.
- Murray, J.L., McAlister, A.J. The Al-Si (Aluminum-Silicon) system. Bulletin of Alloy Phase Diagrams 5, 74 (1984). https://doi.org/10.1007/BF02868729
- V.A. Popovich et al. / Solar Energy Materials & Solar Cells 95 (2011) 93–9696
- Y. Chen et al. / Solar Energy Materials & Solar Cells 120 (2014) 356–362
- Wan et al. 5th SiliconPV 2015
- https://doi.org/10.1016/j.solmat.2013.09.017
- Glunz et al EUPVSEC 2015
- Crystals 2019, 9(8), 402; https://doi.org/10.3390/cryst9080402
- Green, Vol. 2 (2012), pp. 7–24

Bibliography (7/)

TotalEnergies

- **Photocarriers Collection & Extraction**
  - Advanced Metallization & Interconnexion Processes
    - https://multimedia.3m.com/mws/media/1595429O/3m-light-redirecting-film-white-paper-august-2018.pdf
    - https://www.ise.fraunhofer.de/content/dam/ise/de/documents/publications/conference-paper/32-eupvsec-2016/Mittag_1BV532.pdf
    - https://energy.economictimes.indiatimes.com/files/cp/755/cdoc-1626266000-Technical%20whitepaper%20on%20LONGi%E2%80%99s%20proprietary%20Smart%20Soldering%20technology.pdf
    - HIGH EFFICIENCY CONFIGURATION FOR SOLAR CELL STRING EP 2 917 940 B1
    - https://www.ise.fraunhofer.de/content/dam/ise/de/documents/publications/conference-paper/36-eupvsec-2019/Schiller_4AV18.pdf

COLLÈGE DE FRANCE 1530 Fondation Bettencourt Schueller Reconnue d'utilité publique depuis 1987

Other useful resources

- Ecole de physique des Houches 2020 Courses: https://www.youtube.com/watch?v=s43cwPWLvUE&list=PLo9ufcrEqwWHtA_R5Sf8PBD16FMOB37gE&ab_channel=EcoledePhysiquedesHouches

- Pveducation: https://www.pveducation.org/

- PVlighthouse website: https://www.pvlighthouse.com.au/

Annexes

Improved Photons Conversion

Bifaciality: The Future of PV Has Two Sides

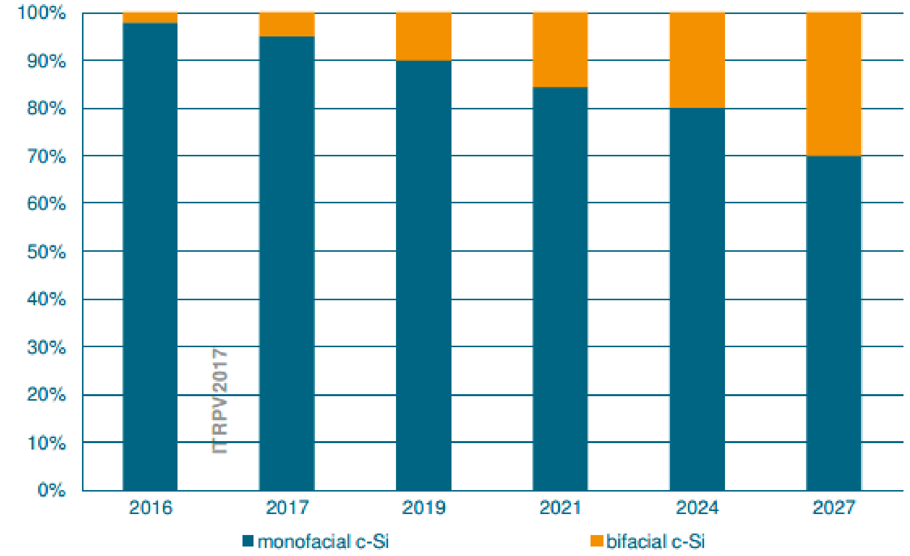

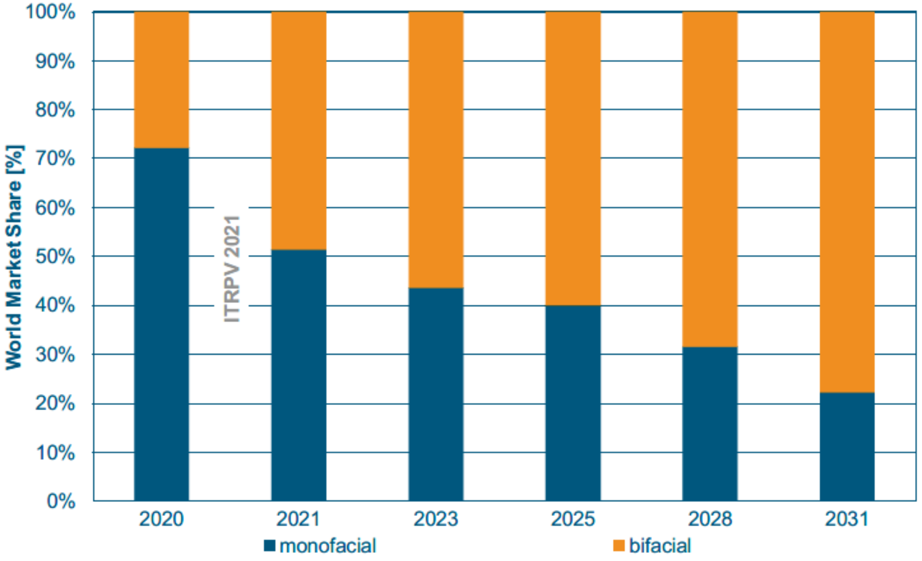

The first round of tendering saw 27 companies qualify for a 300-MW solar PV project at Sakaka in the Al Jouf region and 24 companies for a 400-MW wind farm in Dumat Al Jandal, in the same region, in April 2017. When bids for the Sakaka plant were opened in early October 2017, they saw the lowest prices ever pitched for a solar PV plant. Abu Dhabi's Masdar and Electricité de France (EDF) offered to supply power for as little as $0.0179 per KWh, which was $0.0063 less than the previous all-time low, and broke the $0.02-per-KWh barrier for the first time.

Prices for solar PV hardware have been on a downward trend for some time now. China is likely leading the downward charge in prices and costs, with large-scale projects and major production there spurring competition on the global market. According to the International Energy Agency of France, this has made solar PV projects comparable to or even lower in cost than similar fossil fuel plants, boosting global solar PV capacity by around 50% in 2016 alone.

Nonetheless, the Masdar/EDF offer is an exceptionally low figure, with the prices potentially

The solar energy segment has seen a number of businesses, alongside academic and governmental bodies, brought together under the mantle of the Saudi Arabia Solar Industry Association.

Rear Surface Passivation: and the Winner is…

- **UNSW papers using thick thermal oxide, BUT:**
  - high sensitivity of the silicon bulk charge carrier lifetime to high-temperature processes.
  - Especially detrimental for mc-Si wafers

- **PECVD SiN_x which is a standard material for front passivation/ARC has been tested:**
  - SRV<10 cm/s achieved
  - BUT reduced J_{sc} due to positive fixed charges in SiNx creating an inversion layer at p-type c-Si/SiNx interface → parasitic shunting
  - NEED FOR: low D_{it} and No or negative Q_{eff} (the higher the better)

- **PECVD SiO_2/SiN_x or SiO_xN_y/SiN_z stacks have been tested:**
  - ~10 nm SiO_2 reduces parasitic shunting due to much lower $+Q_{eff}$.
  - SRV <10 cm/s
  - High temperature process + SiN_x capping improves interface through H release
  - still implemented industrially (mostly for users of Centrotherm tools)

- **Even (i) a-Si:H has been tested with success due to its top class chemical passivation and almost no charges:**
  - Low thermal stability (up to 300°C) → not compatible with firing

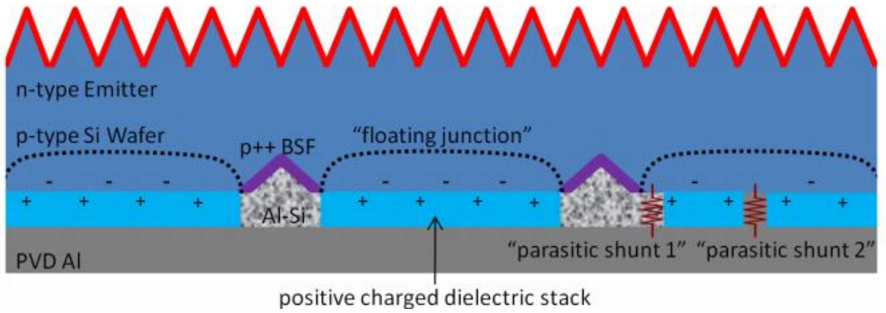

https://doi.org/10.1002/pssr.201206154

Wan et al. 5th SiliconPV 2015

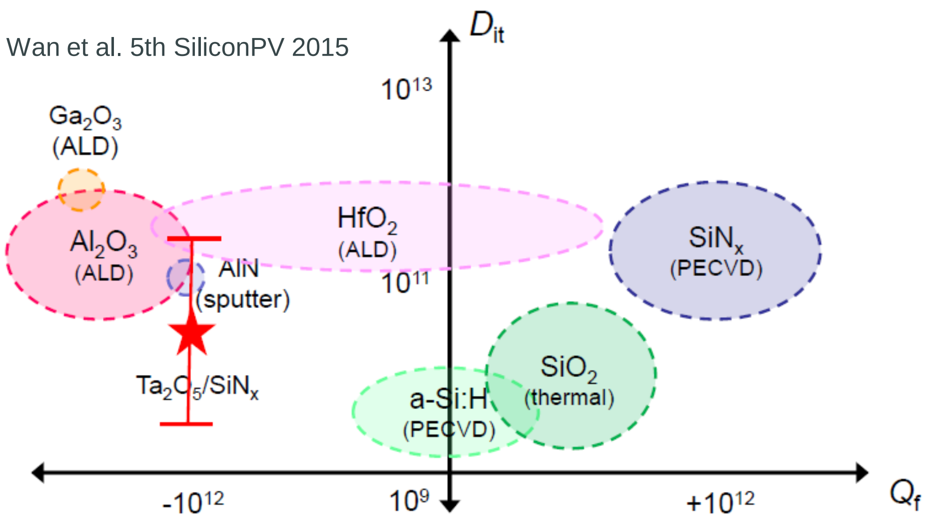

Rear Surface Passivation: Aluminum Oxide

- **And we are back in 1989:**
  - First demonstration by Hezel & Jaeger of Al_2O_3 dielectric layer in a solar cell.
  - SRV around 200-300 cm/s

- Roughly two decades later Agostinelli et al. reached SRV <10 cm/s on p-type c-Si

- **Al_2O_3 can be deposited by various techniques:**
  - PECVD
  - ALD ans spatial ALD
  - ICP
  - APCVD
  - Reactive sputtering

- **Low SRV with reduced dependence to injection level**

- **Al_2O_3 requires a capping layer usually PECVD SiN_x:**
  - Improves passivation: hydrogen pool → need to tbe careful of blistering issue
  - Protect thin Alox for high firing temperature
  - Protect Alox from Al paste

Low-Temperature Surface Passivation of Silicon for Solar Cells

R. Hezel and K. Jaeger*[1]

Institut für Werkstoffwissenschaften VI, Universität Erlangen-Nürnberg, D-8520 Erlangen, Germany

Table I. Fixed charge density Q_f/q, interface state density D_{it} at midgap, and recombination velocity S_0 at the depleted surface for MIS-capacitors with aluminum oxide as insulator

Al_2O_3-deposition temperature	Annealing	Q_f/q (cm^{-2})	D_{it} ($cm^{-2}\,eV^{-1}$)	S_0 (cm/s)
290°C	—	$(0.5 \pm 5) \cdot 10^{11}$	$(1.5 \pm 0.5) \cdot 10^{12}$	$(3.2 \pm 0.5) \cdot 10^{3}$
460°C	510°C, 15 min	$(-3.2 \pm 0.60) \cdot 10^{12}$	$(8.0 \pm 1.5) \cdot 10^{10}$	$(2.1 \pm 0.4) \cdot 10^{2}$

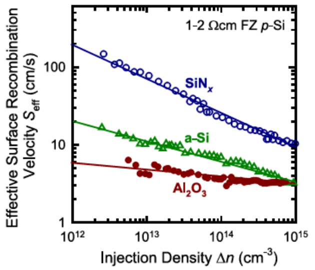

Fig. 5. Comparison of the injection-dependent effective SRVs $S_{eff}(\Delta n)$ measured on 1–2 Ω · cm p-type FZ silicon wafers passivated by 1) SiN_x deposited by remote-PECVD, 2) intrinsic a-Si deposited in a parallel-plate PECVD reactor, and 3) Al_2O_3 deposited by means of plasma-assisted ALD (taken from [64]).

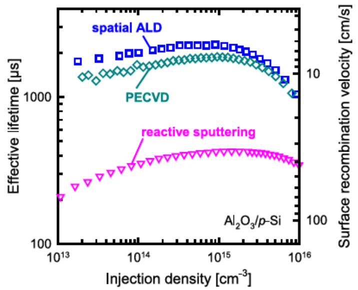

Fig. 6. Effective lifetime (left scale) and corresponding SRV (right scale) as a function of the injection density, measured on 1.3 Ω · cm p-type FZ-Si passivated by Al_2O_3 deposited by spatial ALD, PECVD, and reactive sputtering (taken from [63]).

Dullweber 2016

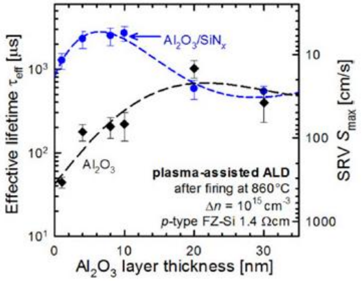

Fig. 7. Measured effective lifetime as a function of Al_2O_3 layer thickness after firing. Shown are the results for single Al_2O_3 layers and Al_2O_3 layers with SiN_x capping layer (taken from [69]).

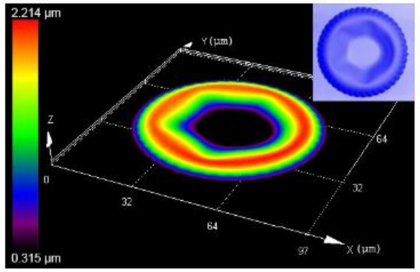

Fig. 1. Topography of a non-uniformly delaminated blister obtained by confocal microscopy. The colored scale indicates the height in the Z direction. Inset: Top view of the blister.

Lebreton 2017

Fondation Bettencourt Schueller

Rear parasitic emitter etch back process

- Diffusion process for emitter leads to a **P-doped layer wrapping completely the wafer**.

- Diffusion furnace suppliers developped a **back to back process** in order to have only on side diffusion

- Most implemented process is an **inline etch back** process consisting of **HF/HNO$_3$** (+ additive such as H_2SO_4) leading to:
  - Throughput >5000 wfr/hr
  - Single side removal of n$^+$ emitter
  - Etching of up to some microns of c-Si

  → Rounding of polishing of the c-Si pyramid is a result

Saw Damage Removal - KOH

Wet texturing – KOH + additive

Wet cleaning – DIW/O$_3$/HF

P diffusion – 800-1000 °C

Laser doping – selective emitter

PSG removal + Etch back process + rear polishing – HF/HNO$_3$(/H_2SO_4)

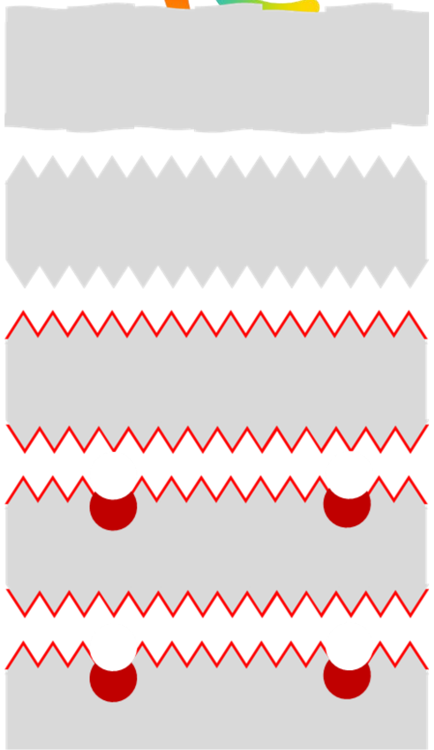

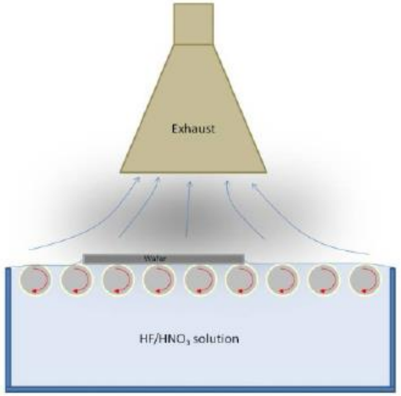

Rear parasitic emitter etch back process

- **Need to control etching:**
  - <u>**Thickness**</u>: emitter removal
  - <u>**Roughness**</u>: isotropic vs anisotropic etching?

- Concerning **light trapping**, what is the best rugosity?
  - A bit of polishing tends to be a bit better to increase Z and therefore J_{sc}.
  - Polishing also has an impact on V_{oc} (passivation quality) & contact quality (R_s & FF)

E. Cornagliotti 2012

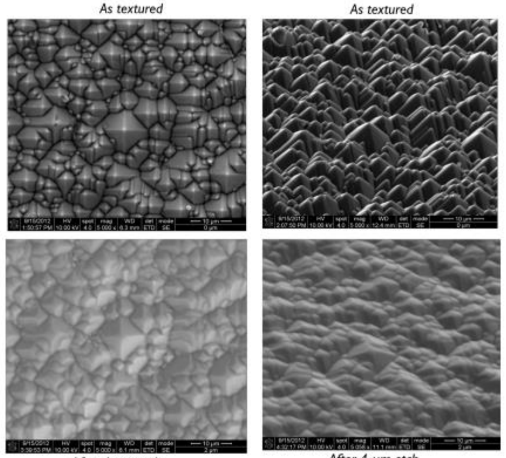

Figure 3: Top view SEM image (left) and with 45° tilt (right) after random pyramid texturing and after a 4 μm polishing etch.

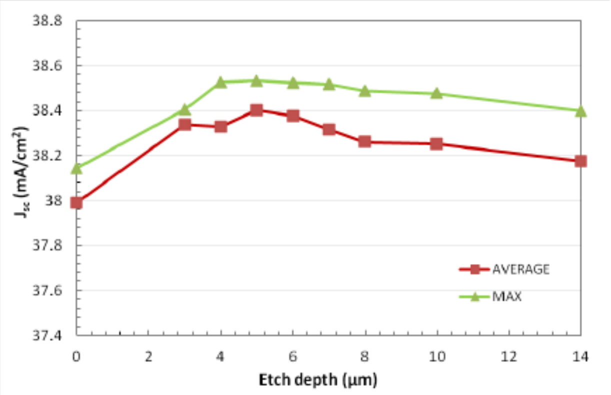

Figure 7: J_{sc} vs. polishing etch depth. Better light trapping is responsible for the increased current improvement between 0 and 6 μm. The decrease in J_{sc} after 6 μm is a combined effect of lowest light trapping performance and reducing thickness.

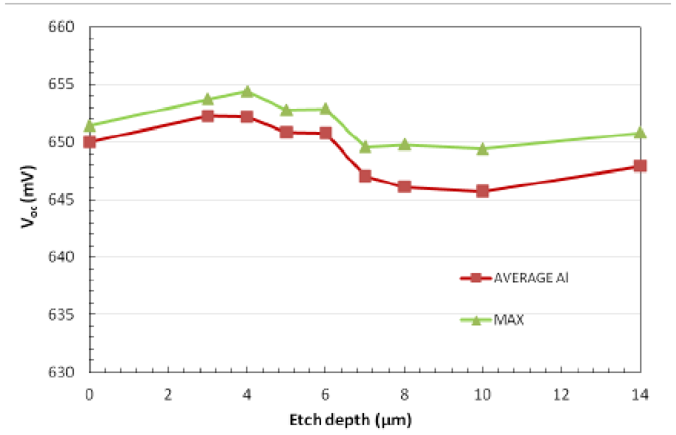

Figure 9: V_{oc} vs. etch depth. A decrease in V_{oc} is reported for etch depth higher than 5 μm. This does not follow the S_{eff} trend.

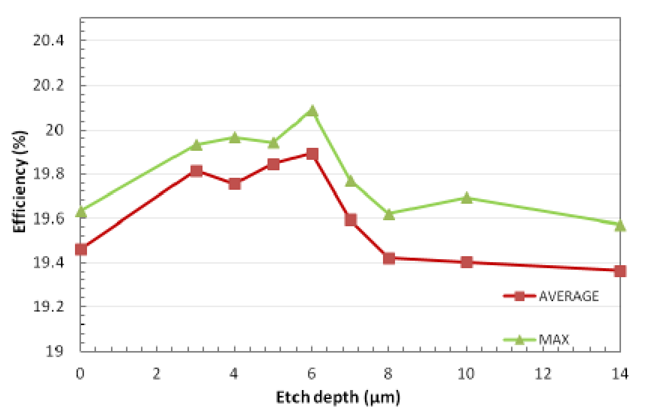

Figure 13: Solar cell efficiency vs. etch depth. The combined results of J_{sc} and V_{oc} variation causes the average efficiency to be the highest for etch depths comprised between 4-6 μm.

Rear contact opening

- Initially done in labs by photolithography → not compatible at industrial level with low cost and high throughput

→ **Development of laser processes allowed PERC industriallization**

- <u>**Main industrial process**</u>: **Laser Contact Opening (LCO) using ns or ps laser** (usually green)
  - Spot around 30 µm
  - Pulsed laser with high frequency 100 – 800 kHz
  - ns or ps to avoid damaging of silicon
  - UV or green for better selectivity between passivation layer and c-Si substrate
  - Usage of scanning heads (mirrors with very quick movement)
  - Very high throughput: between 3600-6000 wfr/hr

- **Possibility to do line, dash or point openings** → impact on the metallized fraction → $J_{0,met}$

→Impact on local BSF formation

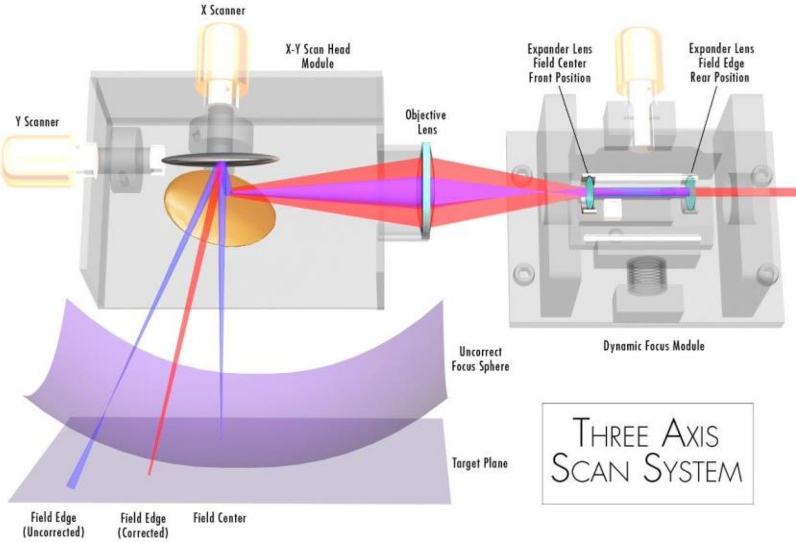

Some alternative metallization which still didn't make it industrially

P. Ortega 2012

- **Laser firing Contact (LFC)** has been studied as an alternative:
  - Evaporation, sputtering or screen printing of Al thin film on rear side
  - Pulsed laser through Al and passivation stack (SiO_2 or AlO_x + SiN_x)
  - <u>Cons</u>: Local BSF not as deep compared to LCO + metallization

- **Foil metalization (FolMet) using a laser pulse:**
  - >21% cell efficiency obtained with no *FF*, R_s or J_{sc} loss observed.
  - Even SiN_x capping can be reduced since an air gap is present
  - High reflection of nIR at the rear side of the cell = less parasitic absorption of at the metal surface.

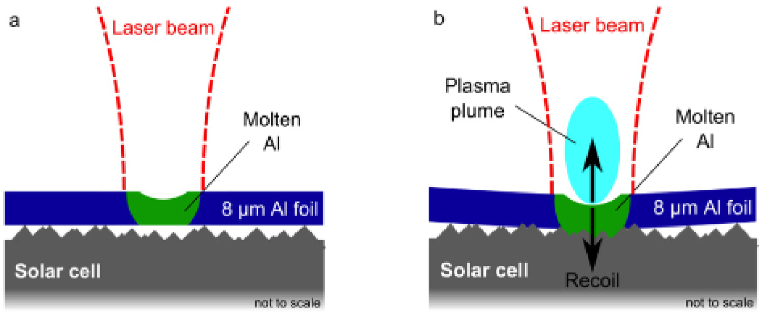

Figure 1: Model shown at schematic cross sections of a solar cell rear side during the laser contacting process; (a) Penetration depth of the melting front (green) through the solid aluminum foil (blue) with a total thickness of 8 µm; (b) Plasma plume (cyan) of the evaporated material leads to a recoil downwards to close the air gap between foil and solar cell (grey) under irradiated area.

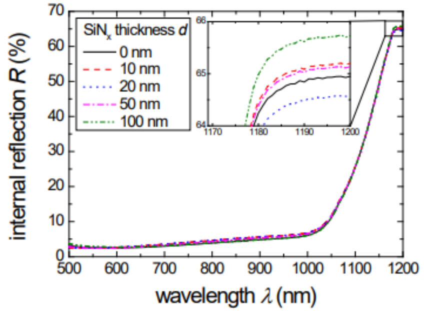

Figure 3: Measurement of the internal reflection R at the rear side, after foil attachment and laser fired contacts dependent on the SiN_x capping layer thickness. The reflection varies by < 0.5 % in the IR regime.

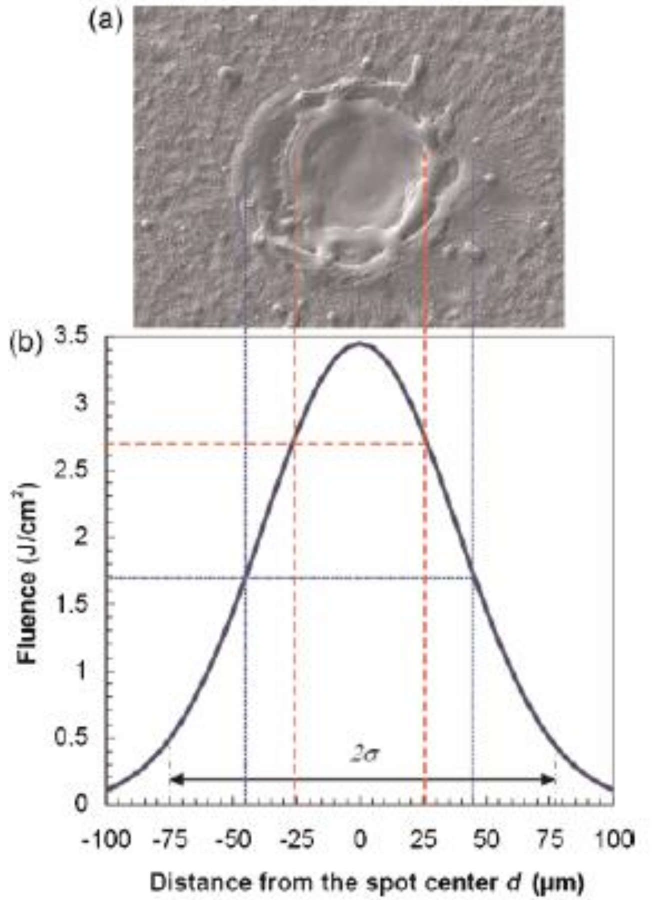

Figure 3. (a) SEM image of the footprint in the silicon once LFC is performed through a 110 nm SiO_2 layer (P=2.5 W, 125 pulses). (b) Theoretical laser spot fluence F.

M. Graf 2015

Front optimization: let’s go local

- **Front emitter high doping needed to ensure ohmic contact with Ag paste:**
  - **Standard surface doping for full emitter 5.10^{19} cm^{-3}**
  - Depth ~300 nm
  - **$J_{0,emet}$~900-1000 fA/cm²**

  → Strong recombination & loss

- **Laser selective emitter is usually performed using PSG glass as P-source**
  - Enables much higher R_{sheet} emitters ~300 Ohm
  - **~ 5.10^{19} cm^{-3} surface doping**
  - Depth of doping 500 nm to 1 µm
  - « rectangular »-like doping profile
  - **$J_{0,emet}$~200-500 fA/cm²**

- **Standard process using ns green laser with long pulse (10-50 ns) = high energy/fluence**

Saw Damage Removal - KOH

Wet texturing – KOH + additive

Wet cleaning – DIW/O_3/HF

P diffusion – 800-1000 °C

Laser doping – selective emitter

PSG removal + Etch back process + rear polishing – HF/HNO_3(/H_2SO_4)

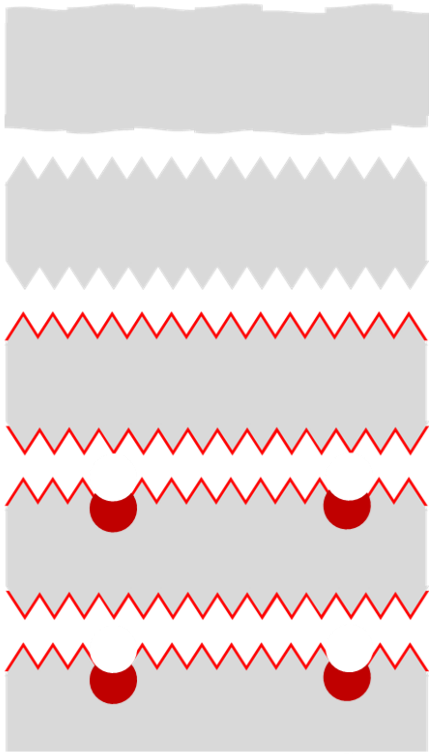

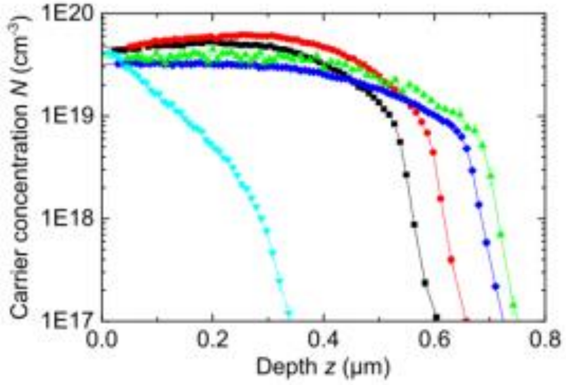

Bulk quality improvement

- As early as 1973 **degradation of p-type c-Si solar cell under illumination (strong J_{sc} loss)** has been observed by Fischer and Pschunder. They observed that **J_{sc} was recovered after annealing @200°C in the dark**. This phenomenon has later been called **LID – Light Induced Degradation**

- Later this phenomenon has been intensively studied by several authors:
  - It was quite early attributed to the **creation of B-O pairs reducing the bulk lifetime**.
  - By **replacing (part of) B by Ga**, this bulk lifetime reduction can be strongly mitigated.
  - **PERC are more sensitive than Al-BSF to LID** due to their better nIR absorption and creation of e-/h+ pairs at the rear of the cell which need to travel the whole thickness

- **B-O defects can be permanently deactivated** after the firing of the cell by:
  - Illuminating and annealing (~200 °C) the cell at the same time
  - This can be done in seconds even using LEDs or lasers
  - Cooling rate is crucial

- **Now LeTID (Light enhanced Temperature Induced Degradation) is kicking in!**
  - It's degradation like LID but appearing under illumination at temperature around 75°C
  - This a temperature which can be observed in real life condition in PV cells.

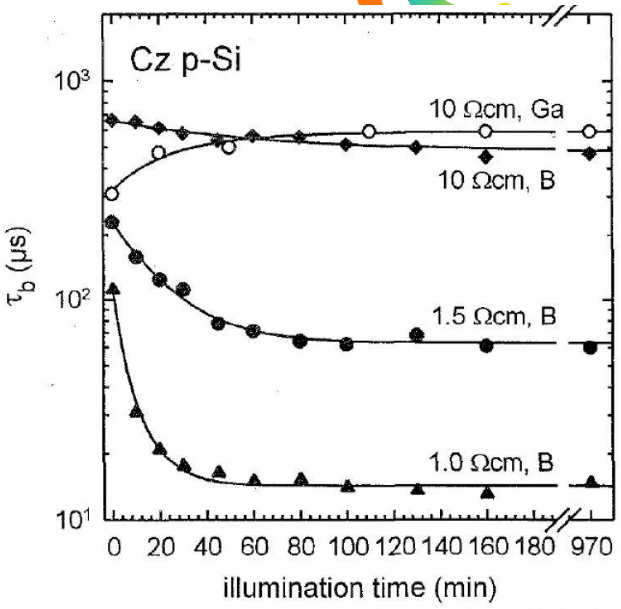

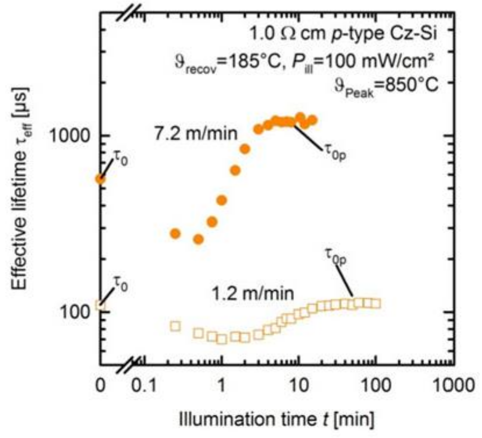

Fig. 11. Lifetime evolution of a 1 –Ω · cm boron-doped Cz-Si wafer during the permanent deactivation process performed at 185 °C and 1 sun for two different belt speeds, corresponding to different cooling rates after firing (taken from [112]).

Bulk quality improvement

- **Through B-O deactivation LeTID can be reduced but not fully avoided**
  - ~1-3% degradation to be expected
  - The higher the temperature the higher the degradation

- **Some recent studies tend to incriminates the passivation layers** ar especially the **hydrogen** contained within:
  - Especially SiNx
  - But probably also Alox
  - And what about poly-Si?

- **Mitigation routes:**
  - Use Phosphorus gettering → what will happen with p-type passivating contacts architecture?
  - Replacing part of B by Ga
  - Reduce wafer thickness
  - Controlling H content in passivation layers?
  - Temperature management of module to avoid high temperatures

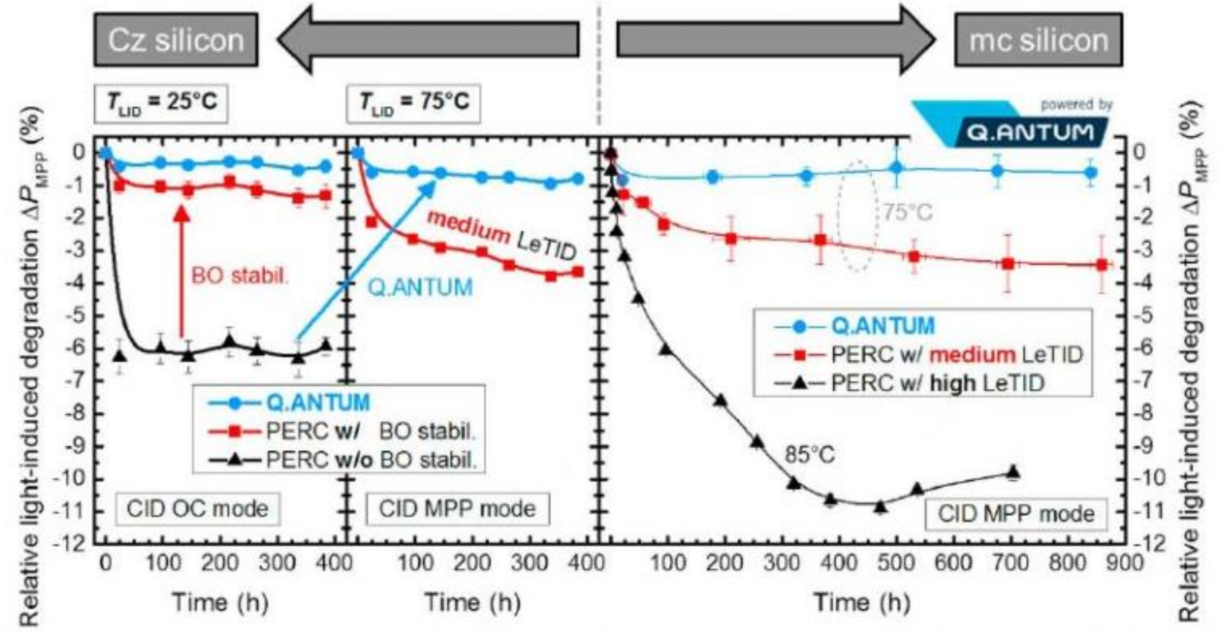

Meng Xiajie 2019, PV-Tech

Figure. 4 LeTID in mono-SI and multi-Si PERC cell [8]

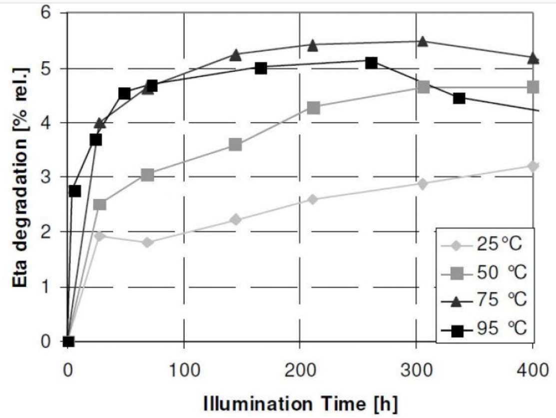

Figure 7 （1）LID evolution of cells made from Cz-BSF，Cz-PERC，mc-BSF, mc-PERC and cast-mono measured at 75°C，400W/m2（2）Multi PERC LID curve measured at temperature 25°C, 50°C, 75°C and 95°C(All the cells was made without LIR process）[13]

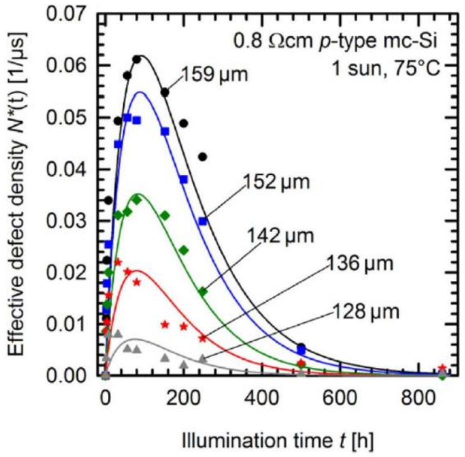

Figure 9 （1）LeTID curves of different wafer thicknesses normalized by effective defect density （2）Maximum defect density fitted from LeTID curve (3） Comparison of the fitted diffusion coefficient range with the common defect category [15]

Current industrial PERC process flow

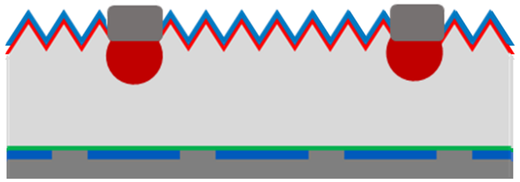

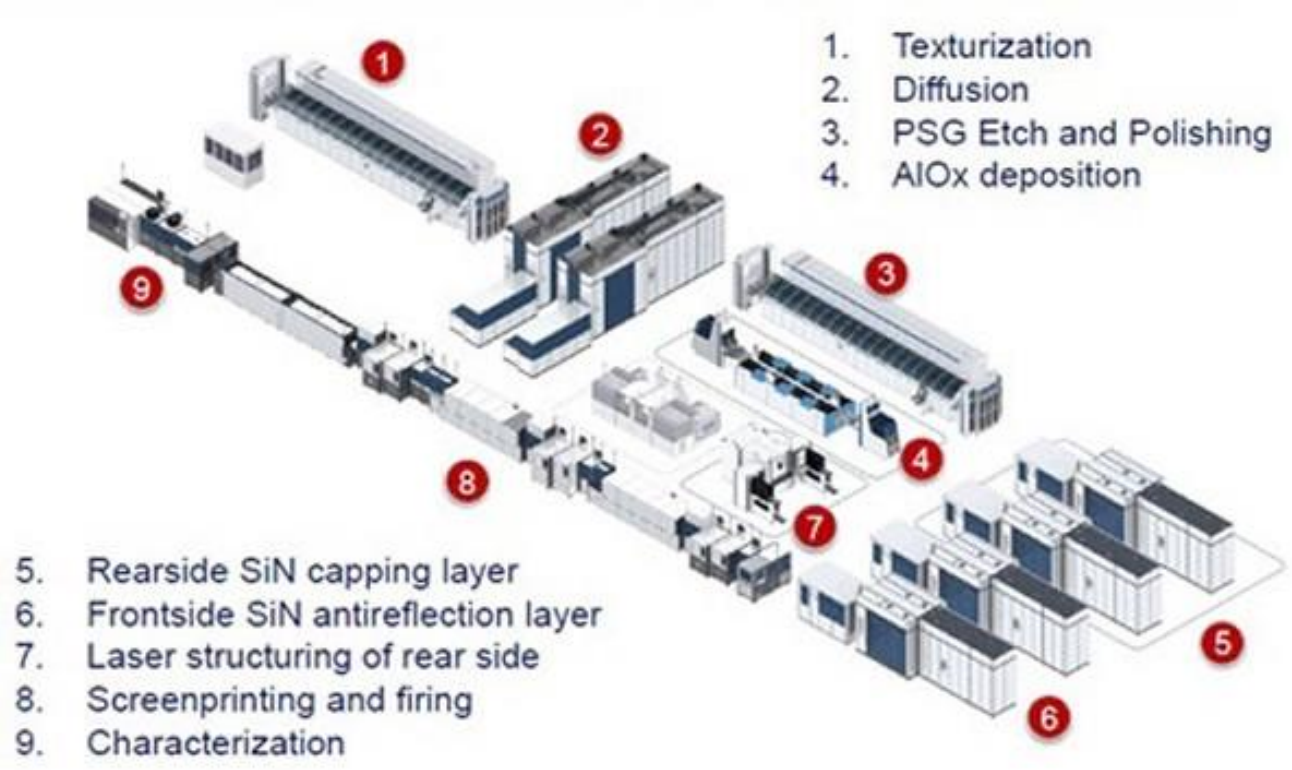

http://cetcsolarenergy.com/products/solar_pv_production_equipments.html

- Saw Damage Removal - KOH
- Wet texturing – KOH + additive
- Wet cleaning – DIW/O_3/HF
- P diffusion – 800-1000 °C
- Laser doping – selective emitter
- PSG removal + Etch back process + rear polishing – HF/HNO_3(/H_2SO_4)
- Wet cleaning – DIW/O_3/HF
- PECVD Front SiN_x passivation
- ALD or PECVD rear Al_2O_3
- PECVD SiNx
- Laser contact opening (rear)
- Screen-printing Al (rear) & Ag (front) + firing

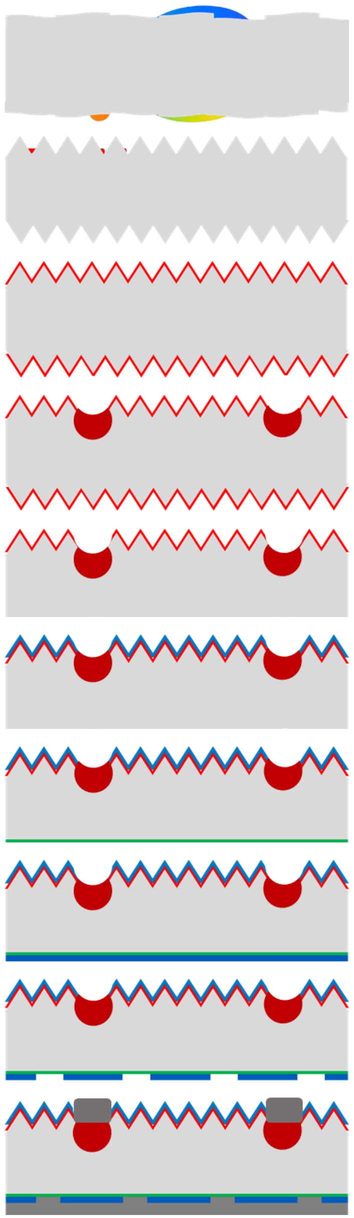

PERC device loss analysis

10.1109/JPHOTOV.2016.2571627

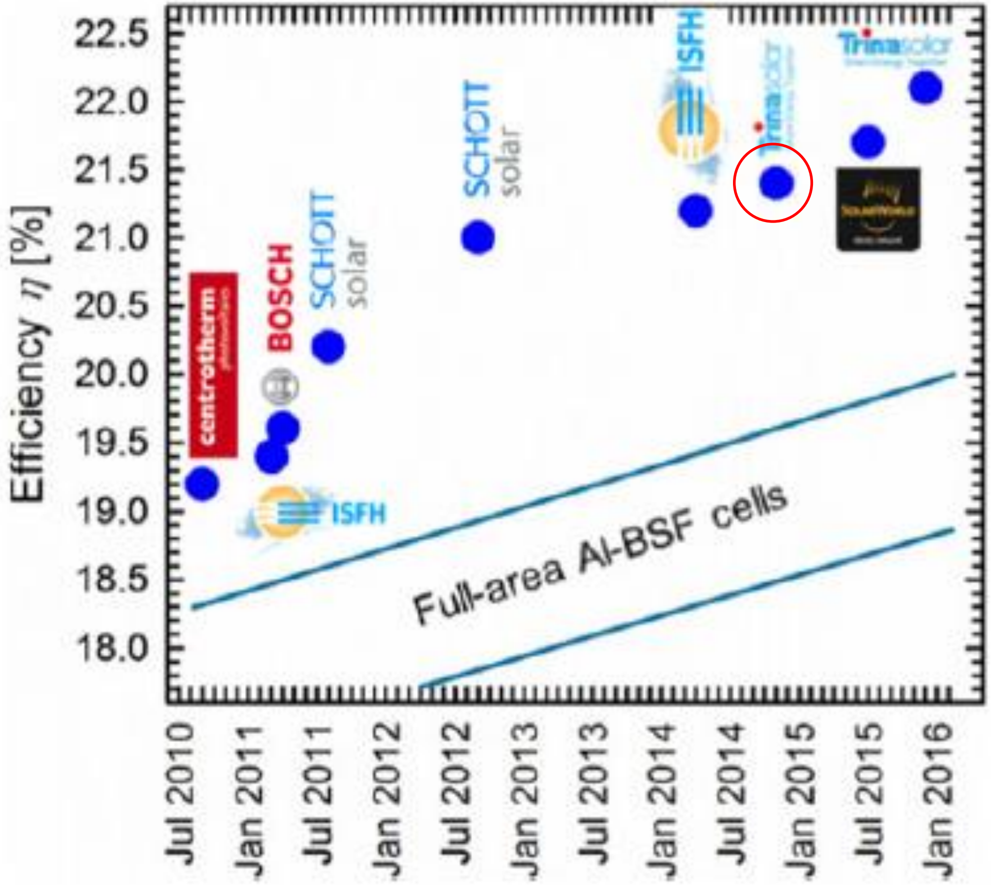

Fig. 4. Independently confirmed record conversion efficiencies of industrial-type PERC solar cells with printed metal contacts using monocrystalline large area p-type Cz silicon wafers. Typical efficiencies of full-area Al-BSF solar cells are indicated as well. Graph updated from [42].

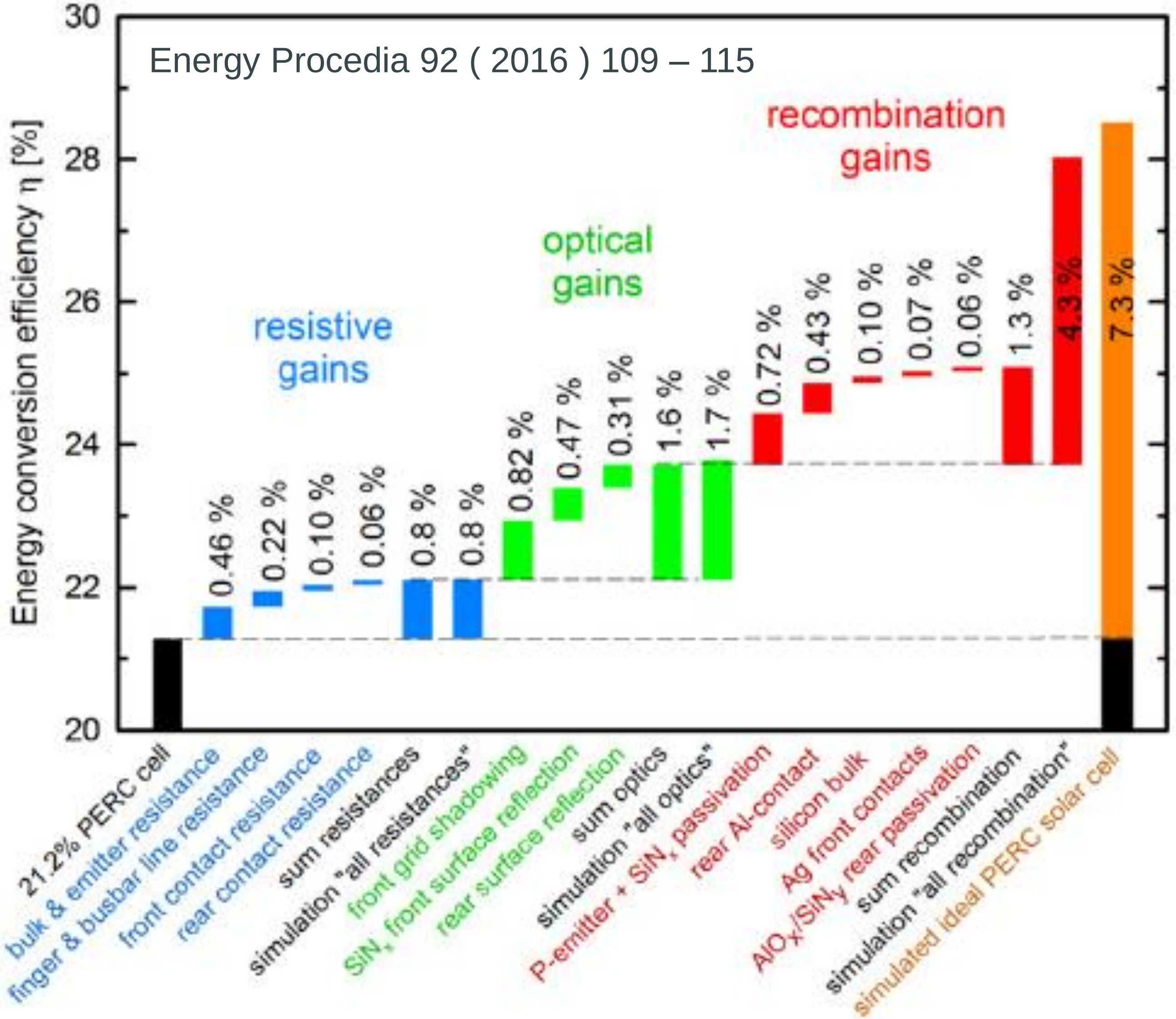

PERC technological roadmap

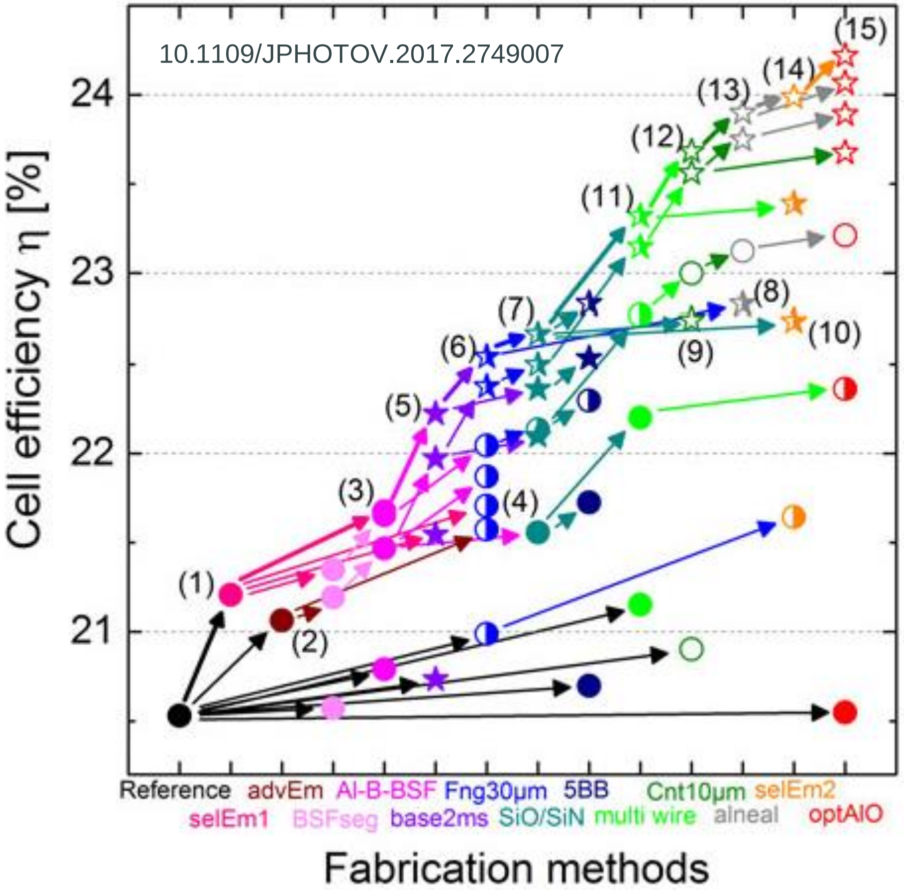

Fig. 4. Simulated impact of different technologies on PERC cell efficiency. The stars indicate the efficiencies obtained with improved wafer materials, and the filling of symbols indicates the following front metal finger designs: 91 fingers/60 μm wide (filled), 155/30 (half-filled), 155/20.82 (empty). The numbers in brackets refer to the text.

1. **Improved emitter structure**
   - Selective emitter implementation + higher R_{sh} emitter

2. **Improved BSF structure**
   - Dashed local BSF → recombination reduction
   - Higher local BSF doping using B-based pastes

3. **High quality bulk material**
   - Long lifetime bulk + no BO pairs (t=2 ms)

4. **Advanced metallization technologies**
   - 30 µm width fingers + 5-6 BB
   - + Multiwire or SmartWire approach
   - 20 µm width Ni(/Cu) fingers

5. **Advanced surface passivation**
   - SiO_x/SiN_x front passivation stack
   - Reduced D_{it} and increased Qeff for AlO_x/SiN_x rear passivation stack

PERC Efficiency Records

LONGi 24.06% Efficiency PERC Cell World Record

CPVT Confirms LONGi Produced First Bifacial Monocrystalline Silicon PERC Solar Cell Exceeding 24% On Commercial Wafer Size

08:10 PM (Beijing Time) - 18. January 2019

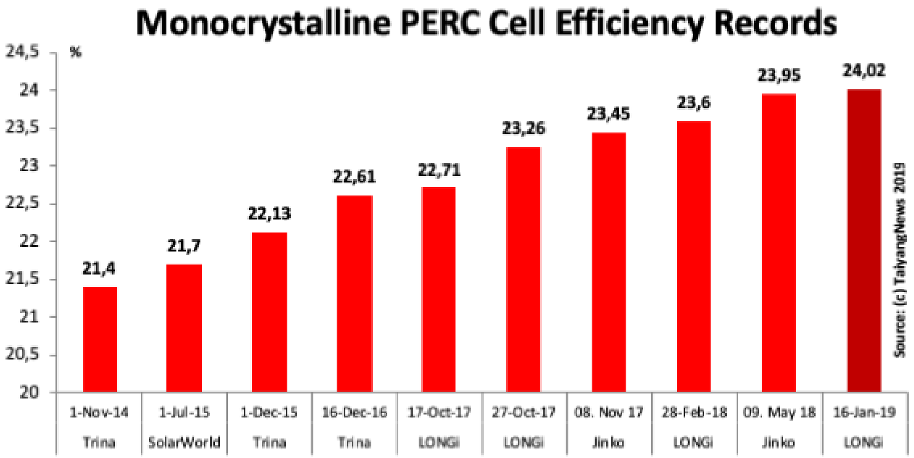

In achieving a 24.06% conversion efficiency for its bifacial mono PERC solar cell, LONGi Solar took over the helm from JinkoSolar, which had announced a 23.95% advanced PERC cell in May 2018. (Source: LONGi Solar)

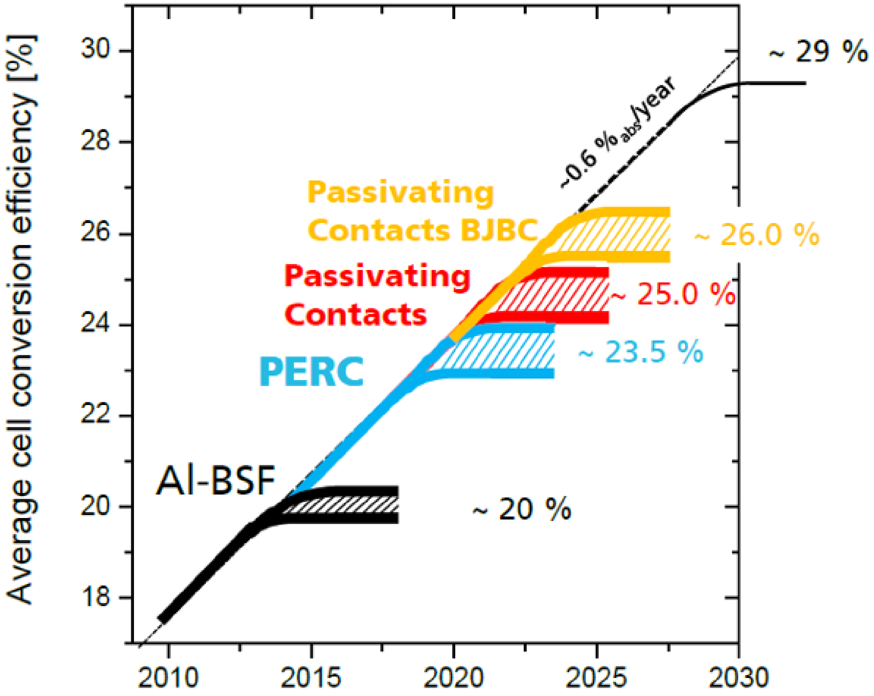

- We are already there in industry R&D pilot lines
- But complex process flow (↑ $\$/W_p$) and not standard processes

The next step: reducing $J_{0,met}$ at the rear side

- Al_2O_3/SiNx is providing an **excellent passivation with SRV<10 cm/s**.
- What has to be gained now is **reduced $J_{0,met}$** on the rear. The use of passivating contact is allowing that and therefore boost in **V_{oc}>700 mV**

- **Main challenges for passivating contacts:**
  - Being compatible with screen-printing, especially for p-type layers. Al alloying is provoking some spiking through the passivation stack
  - Reduce UV parasitic absorption to enable both side passivating contact cells
  - Demonstrate potential implementation on p-type?
  - If usage of p-type wafers, demonstrate impact of H, LeTID on performance & reliability.
  - Demonstrate bifaciality improved compared to PERC and on par with n-PERT?

- **Main challenges for the heterojunction:**
  - Demonstrate LCOE cost advantage even with increased CAPEX compared to a PERC line enhanced for poly-silicon passivating contact
  - Improve Jsc → reduce parasitic absorption on the front side
  - Demonstrate stable process control in fab >3600-6000 wfr/hr and same yield than PERC.

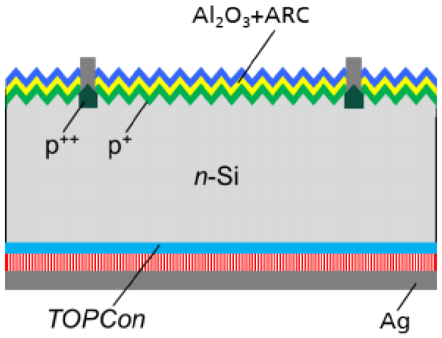

Fig. 8: Sketch of *n*-type solar cell with diffused front boron emitter and full-area rear passivated contact (TOPCon).

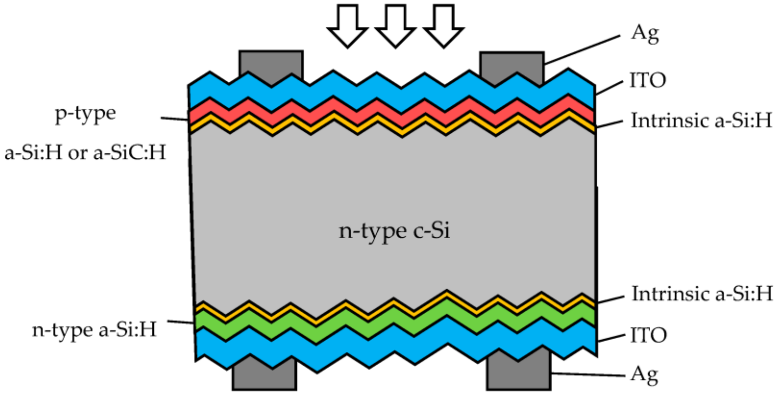

PV market and current c-Si technologies:
Standard and high c-Si technologies: where are we headed?

Source Valerick Cassagne Master REST course

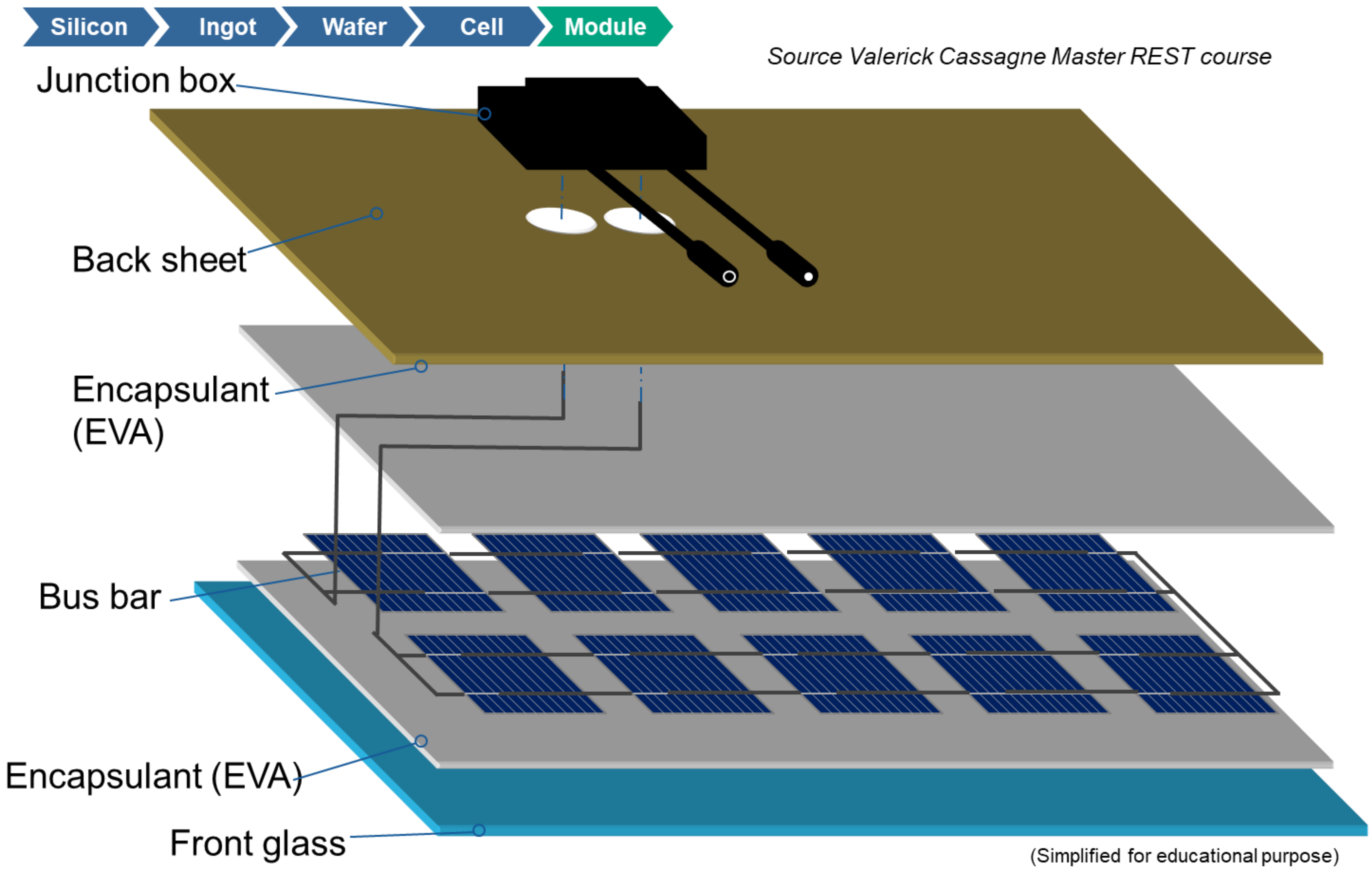

https://www.youtube.com/watch?v=_KTrq63Q2u4&ab_channel=MondragonAssembly

PV modules: technologies and specifications

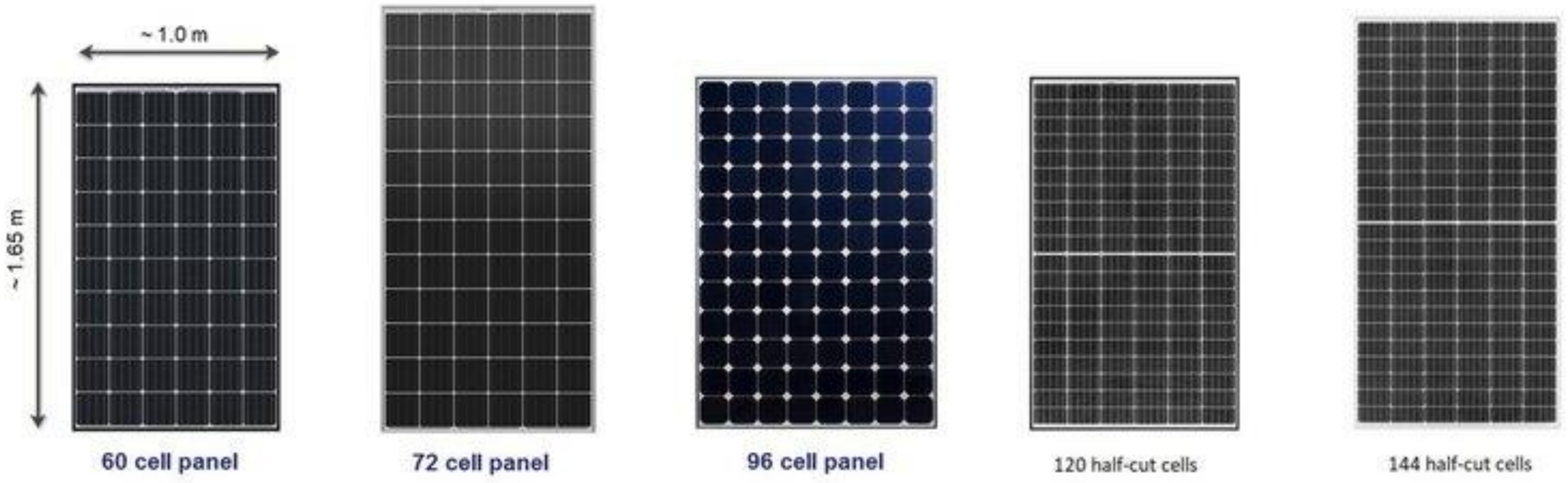

- Module size depends on:
  - Wafer size
  - Number of wafers
  - If cells are cut or full

https://www.cleanenergyreviews.info/blog/most-efficient-solar-panels

PV modules and PV systems
PV modules: technologies and specifications

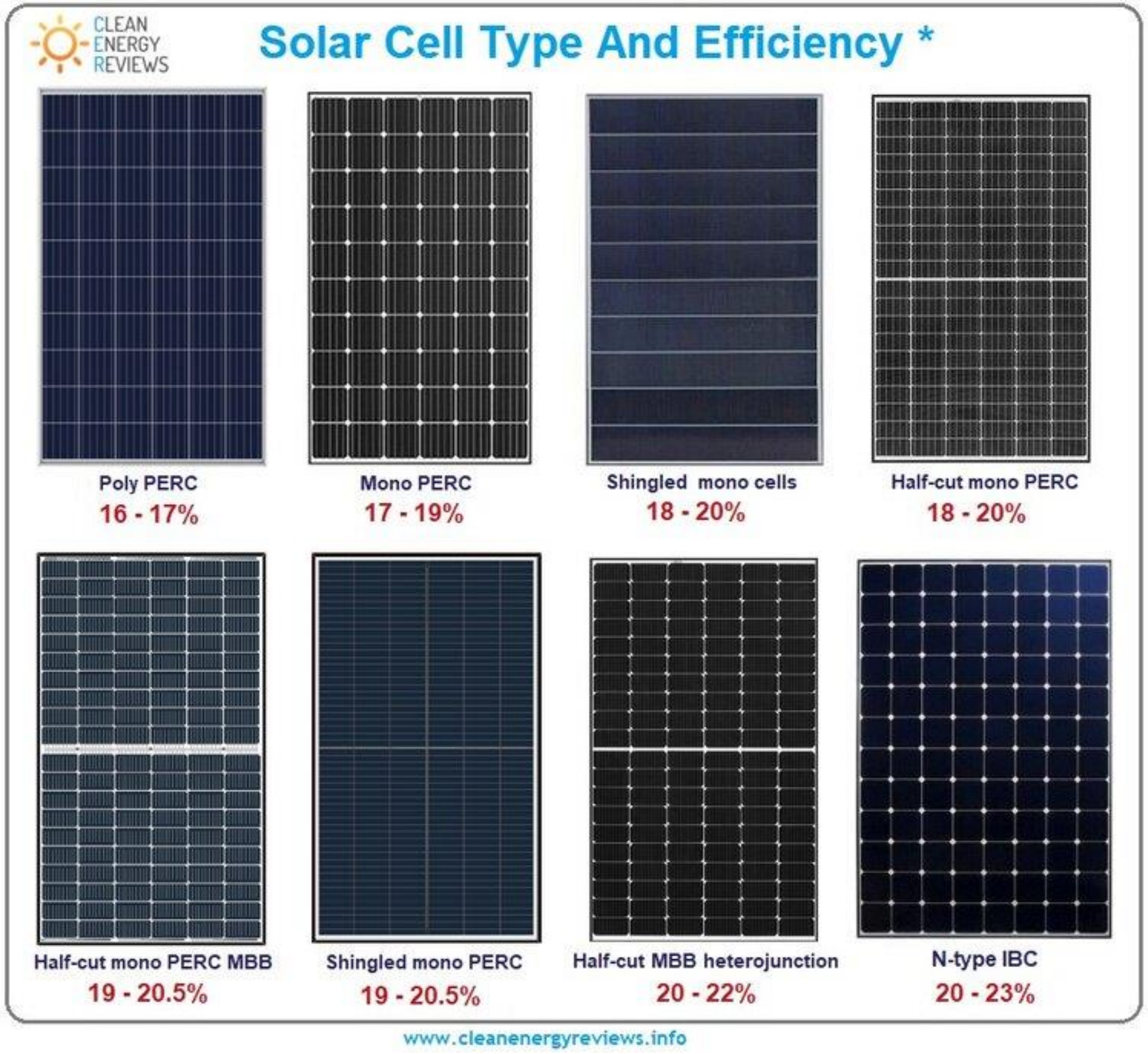

CLEAN ENERGY REVIEWS — **Most Efficient Solar Panels 2022 *** — V3.0 - Jan 2022

Manufacturer	Model	Max power (W)	Cell Type	Efficiency
SUNPOWER	Maxeon 3	400W	N-type **IBC**	22.6 %
LG	Neon R	405W	N-type **IBC**	22.3 %
Panasonic	EverVolt H	410W	N-type **HJT** Half-cut	22.2 %
REC Solar	Alpha Pure	405W	N-type **HJT** Half-cut	21.9 %
Silfab Solar	Elite BK	405W	P-type **IBC**	21.4 %
Jinko Solar	Tiger N-type 66TR	410W	N-Type Mono Half-cut	21.4 %
FuturaSun	FU 360 M Zebra	360W	N-type **IBC** Half-cut	21.3 %
HYUNDAI	HiE-S400UF	400W	P-Type Mono Shingled	21.3 %
risen	Titan S	410W	P-Type Mono Half-cut	21.3 %
SUMEC Phono Solar	TwinPlus Pro	415W	P-Type Mono Half-cut	21.2 %
AXITEC	AXIpremium HC	415W	P-Type Mono Half-cut	21.2 %
Trinasolar	Vertex S	405W	P-Type Mono Half-cut	21.1 %
LONGi Solar	Hi-MO 4m	385W	P-Type Mono Half-cut	21.1 %
SPIC Solar	Andromeda	355W	N-type **IBC** Half-cut	21.0 %
ASTRONERGY	Astro 4 Semi	380W	P-Type Mono Half-cut	20.9 %
Q CELLS	Q.PEAK DUO ML-G9	390W	P-Type Mono Half-cut	20.8 %
YINGLI SOLAR	YLM 120	380W	P-Type Mono Half-cut	20.8 %
WINAICO	WST-375MG	375W	P-Type Mono Half-cut	20.6 %
SOLARIA	Power XT	370W	P-Type Mono Half-cut	20.5 %
CanadianSolar	HiDM CS1H-MS	345W	P-Type Mono Shingled	20.4 %

* **Residential panels** - 60 or 66 cells (120 or 132HC), or 96 & 104 cell. Does not include large (>2m) commercial panels

PV modules and PV systems
PV modules: technologies and specifications

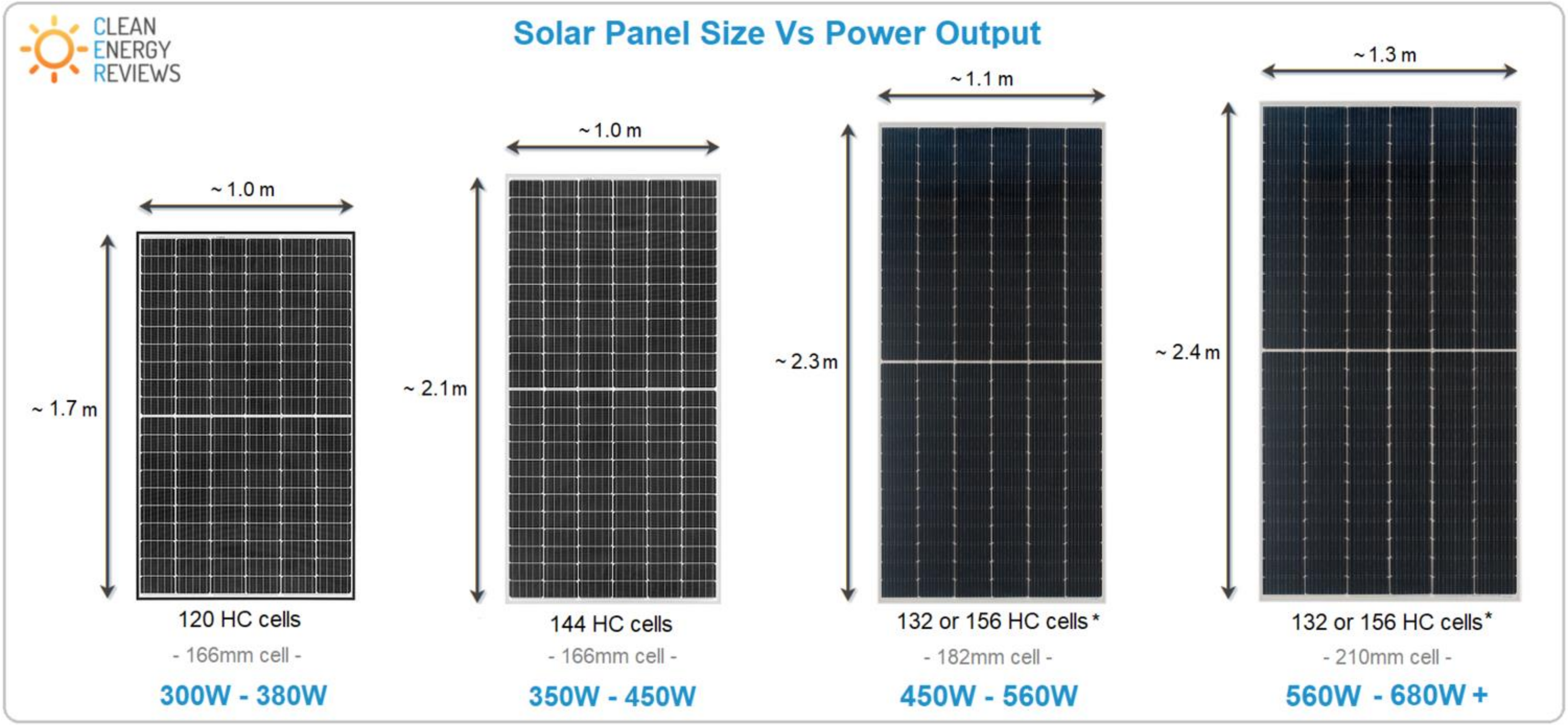

HC = Half-Cut cells HC* = Half-Cut or 1/3 Cut cells

www.cleanenergyreviews.info

The impact of silicon solar cell architecture and cell interconnection on energy yield in hot & sunny climates

TotalEnergies

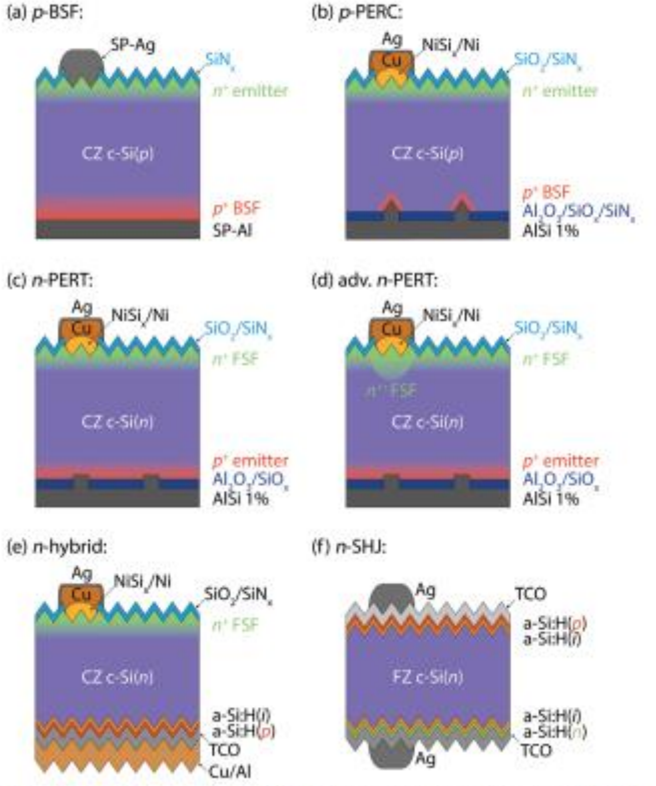

Fig. 1 Schematic sketches of the different device architectures investigated in this study.

Table 2 Relative TCs at AM 1.5G irradiance of 1000 W m^{-2} of the devices shown in Fig. 1, derived from linear fitting between 25 °C and 75 °C of the temperature-dependant *J*(*V*) parameters shown in Fig. 3. For the TCs marked with an asterisk, the fitting was limited to the range between 50 °C and 75 °C, as the data are only linear in this range. To obtain the relative TCs in these cases, $P_{MPP}^{25°C}$, $FF^{25°C}$ and $R_{MPP}^{25°C}$ were obtained by linear extrapolation. Fitting between 25 °C and 75 °C would lead to a TC_{FF} of −0.05% K^{-1} and thus $TC_{P_{MPP}}$ of −0.26% K^{-1} for the *n*-SHJ solar cell. Additionally, the temperature coefficient of the characteristic load resistance, $TC_{R_{MPP}}$, is included

Architecture	$TC_{V_{OC}}$ (%/K)	$TC_{J_{SC}}$ (%/K)	TC_{FF} (%/K)	$TC_{P_{MPP}}$ (%/K)	$TC_{R_{MPP}}$ (%/K)
p-BSF	−0.31	0.05	−0.14	−0.39	−0.39
p-PERC	−0.29	0.04	−0.12	−0.36	−0.37
n-PERT	−0.28	0.04	−0.11	−0.33	−0.34
adv. *n*-PERT	−0.27	0.04	−0.11	−0.33	−0.33
n-hybrid	−0.28	0.04	−0.12*	−0.35*	−0.33*
n-SHJ	−0.25	0.04	−0.08*	−0.29*	−0.30*

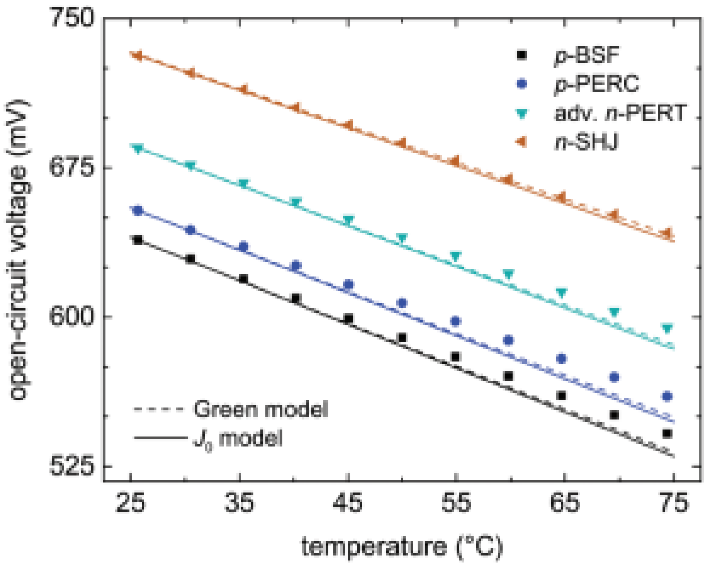

Fig. 4 V_{OC} values of four of the investigated solar cells *versus* temperature compared with two different modelled characteristics: a formula for the $TC_{V_{OC}}$ as proposed by Green *et al.*[20,55] and $V_{OC}(T)$ calculated from the temperature dependency of J_0 due to SRH recombination at low injection.[57]

Energy Environ. Sci., 2017,**10**, 1196-1206

Conclusions
PV Learning Curve: Swanson's Law

Global Cumulative PV Installation From 2010 to 2020

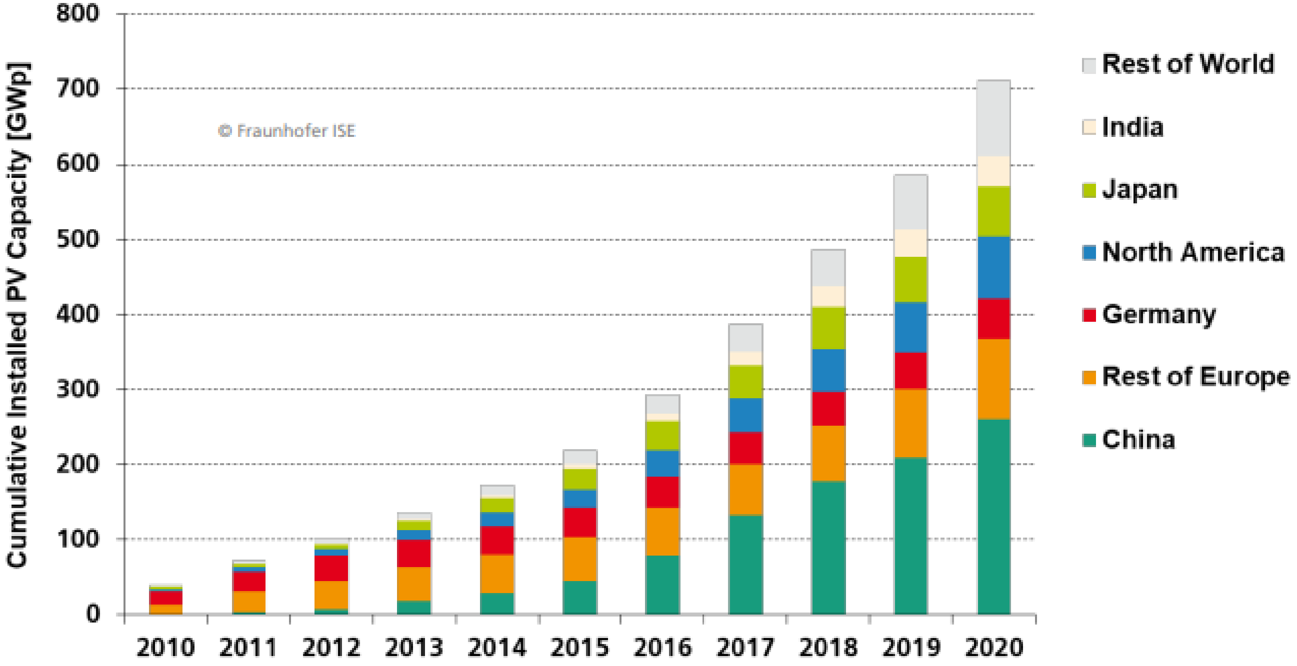

PV Module Production by Region Global Annual Production

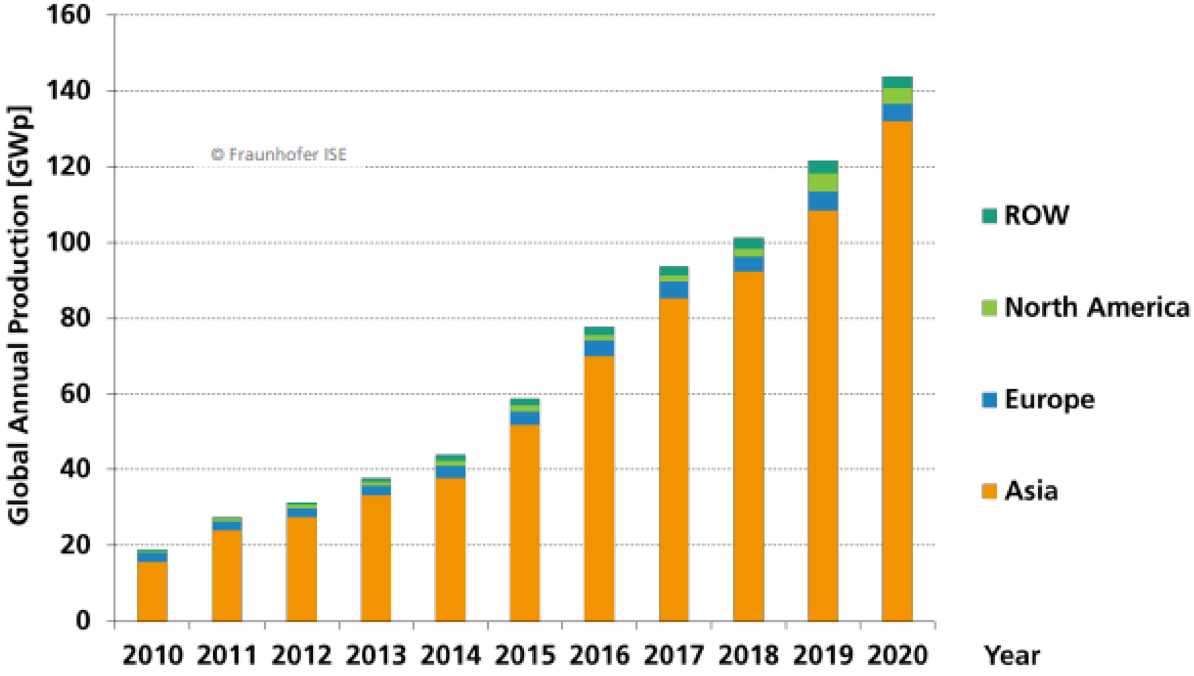

Conclusions
PV Learning Curve: Swanson’s Law

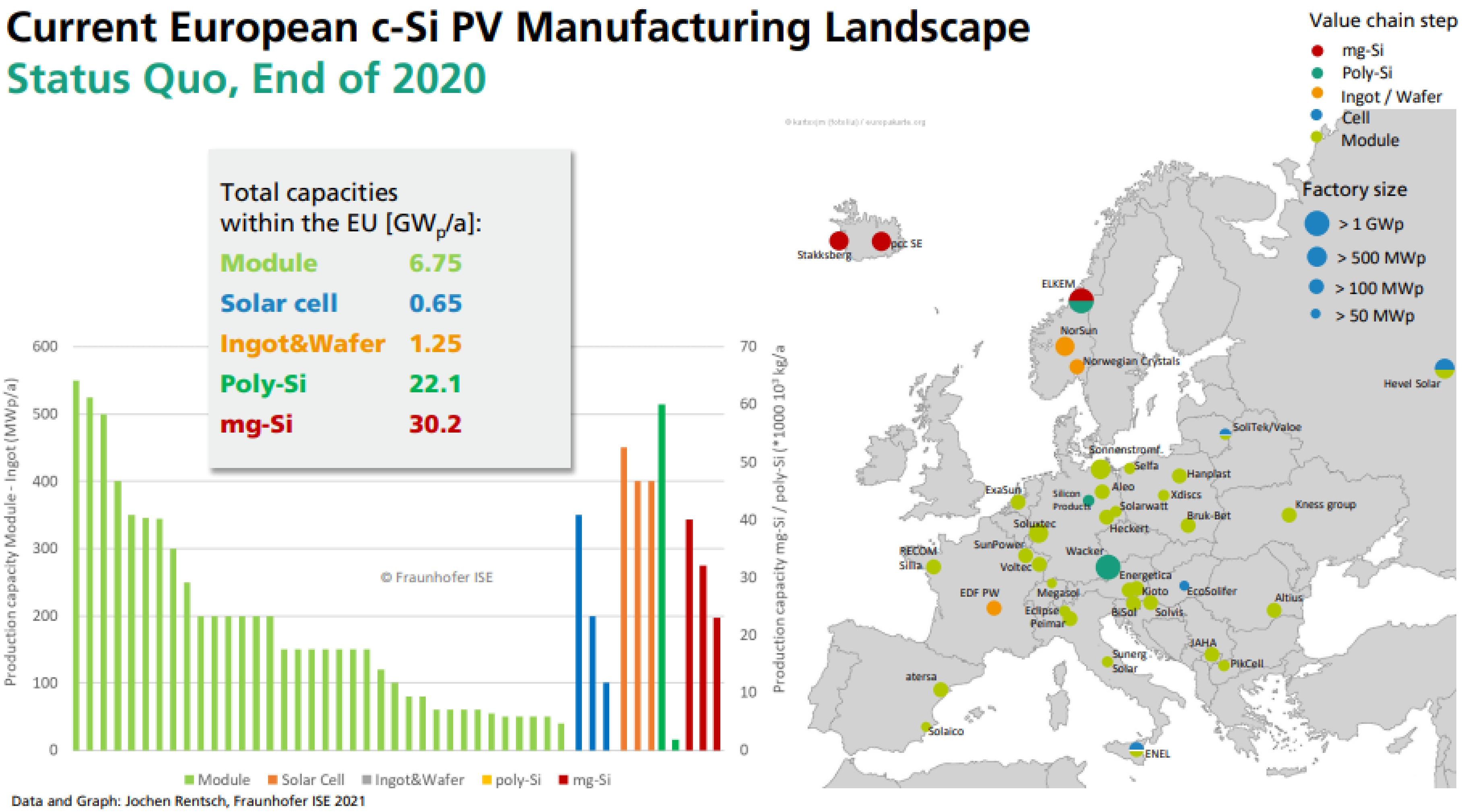

Cost Evolution

Figure 1.8 The global weighted-average total installed cost learning curve trends for solar PV, CSP, onshore and offshore wind, 2010-2020

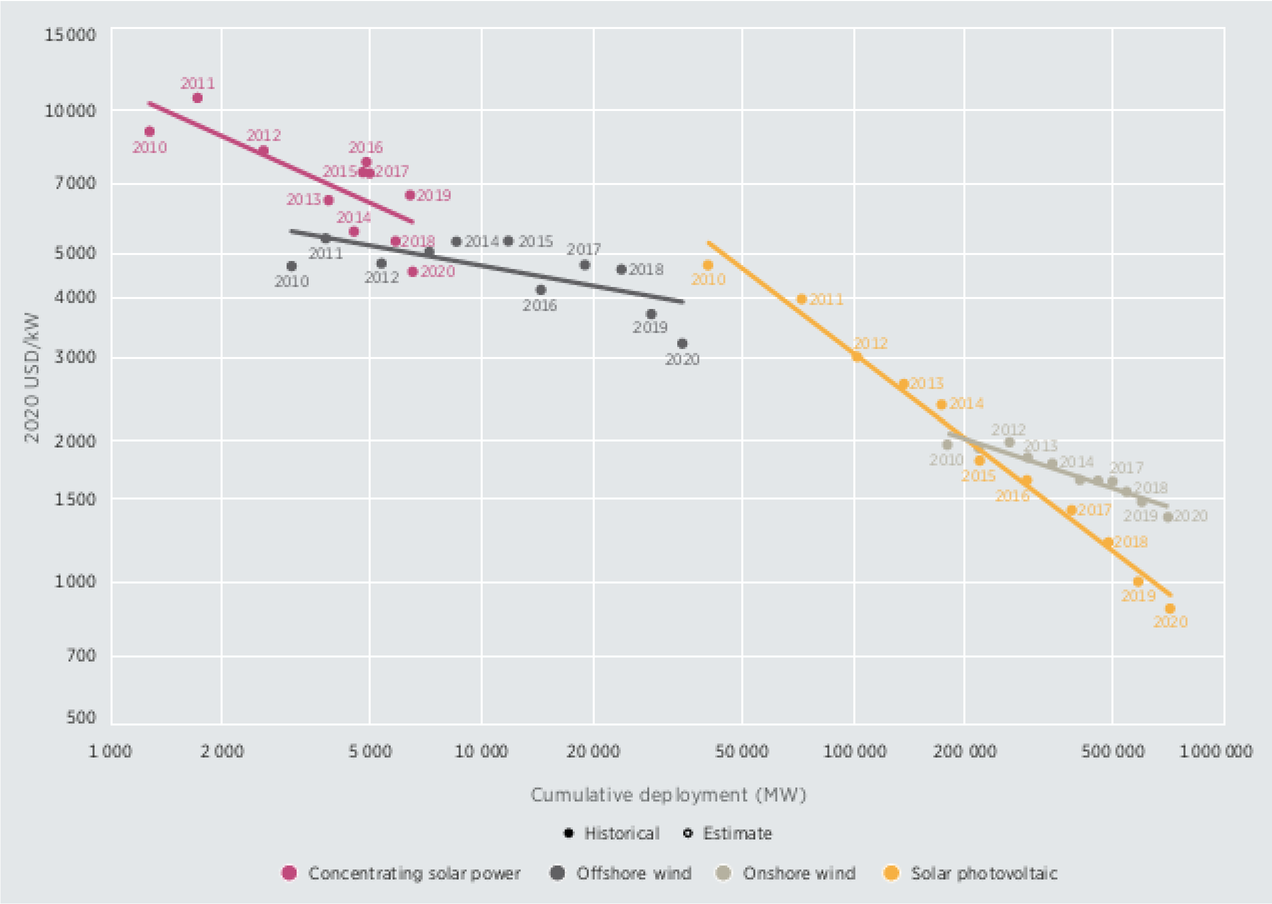

Source: IRENA Renewable Cost Database

Figure 1.9 The global weighted-average LCOE learning curve trends for solar PV, CSP, onshore and offshore wind, 2010-2021/23

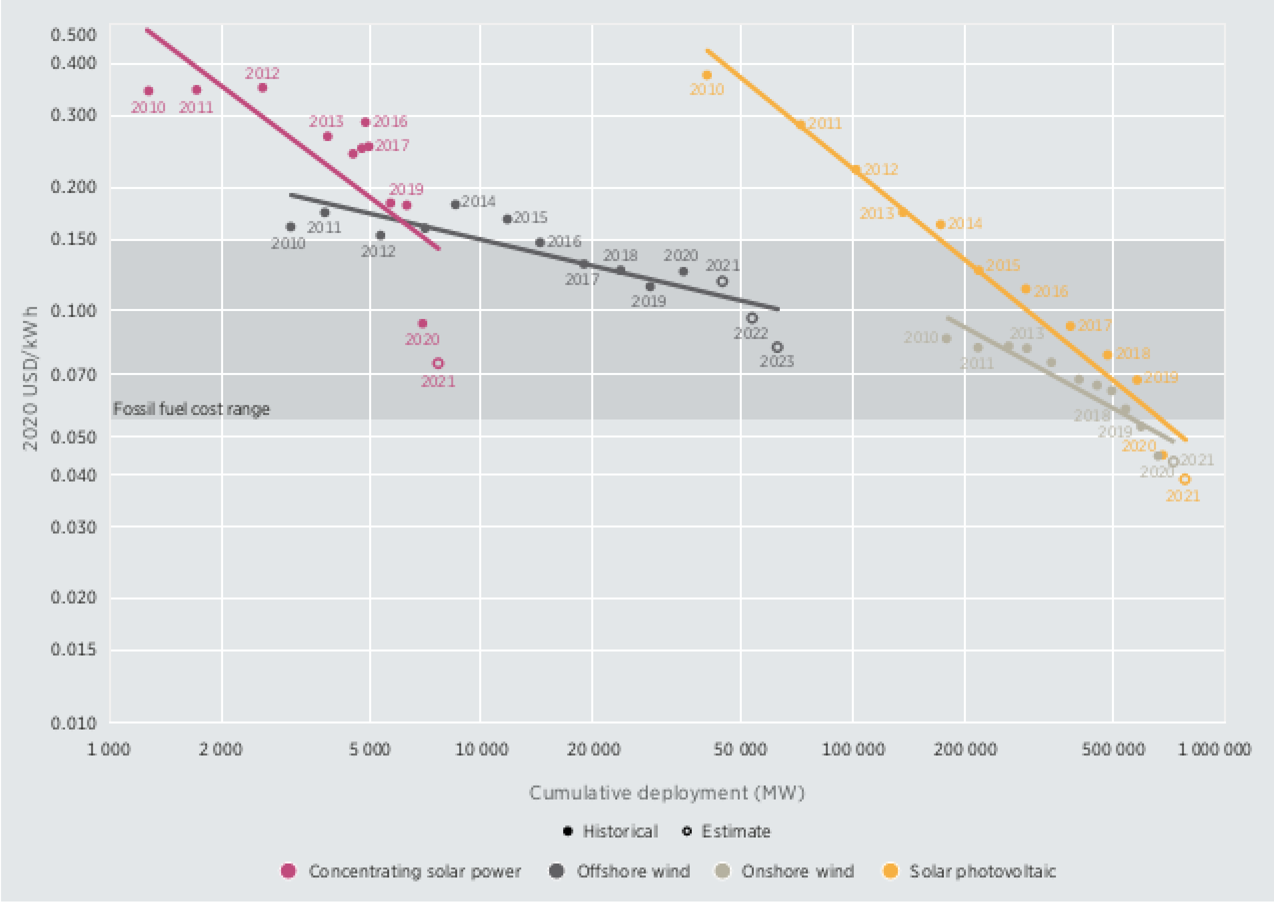

Source: IRENA Renewable Cost Database

Cost Evolution Drivers

Figure B3.2 Drivers of the decline of LCOE of utility-scale solar PV (2010-2020)

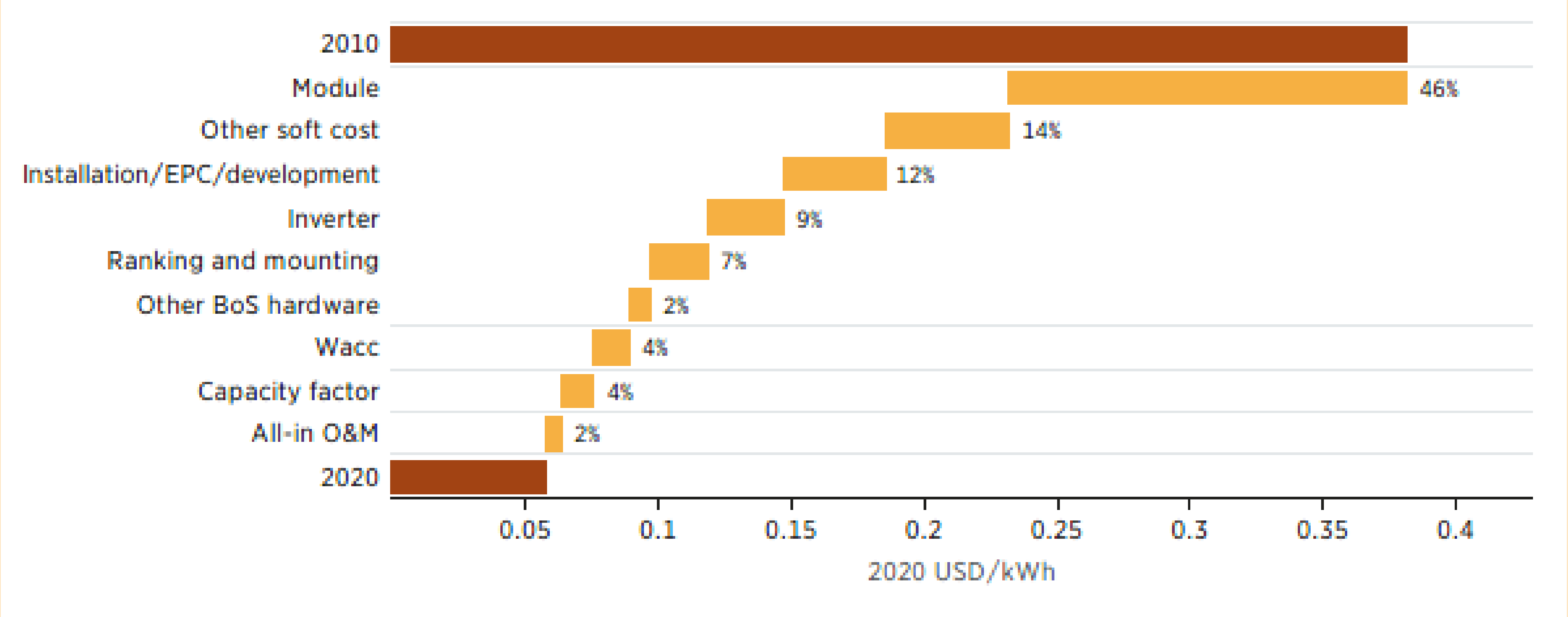

Source: IRENA Renewable Cost Database

Norsun diamond wire sawing introduction

TotalEnergies

NorSun

NorSun

2,851 followers

View full profile

NorSun

NorSun
2,851 followers
1w • Edited •

In 2012, after four years of R&D, NorSun was the first company in the world to fully convert production to use diamond coated steel wires for slicing silicon wafers. At that time, the steel core had a diameter of 0.12 mm. Since then, the technological development in the industry has been amazing and steel cores of 0.04 to 0.05 mm are now mainstream. This has lead to a drastic reduction in the amount of expensive silicon raw material lost as sawdust, which has helped significantly in reducing the cost and CO_2 footprint of solar modules. And the story continues: NorSun is now testing steel cores of 0.038 mm, about half the diameter of a human hair. It's hard to predict the future when we are doing today what we only five years ago believed would never be possible.
This work has been co-financed by The Research Council of Norway through the project Ultra-Sustainable semiconductor Substrates for tomorrow's solar cells.
#solar #wafers #technology #development #innovation

COLLÈGE DE FRANCE 1530

Fondation Bettencourt Schueller

c-Si Solar Cell Development Wafer Thickness [µm] & Silicon Usage [g/Wp]

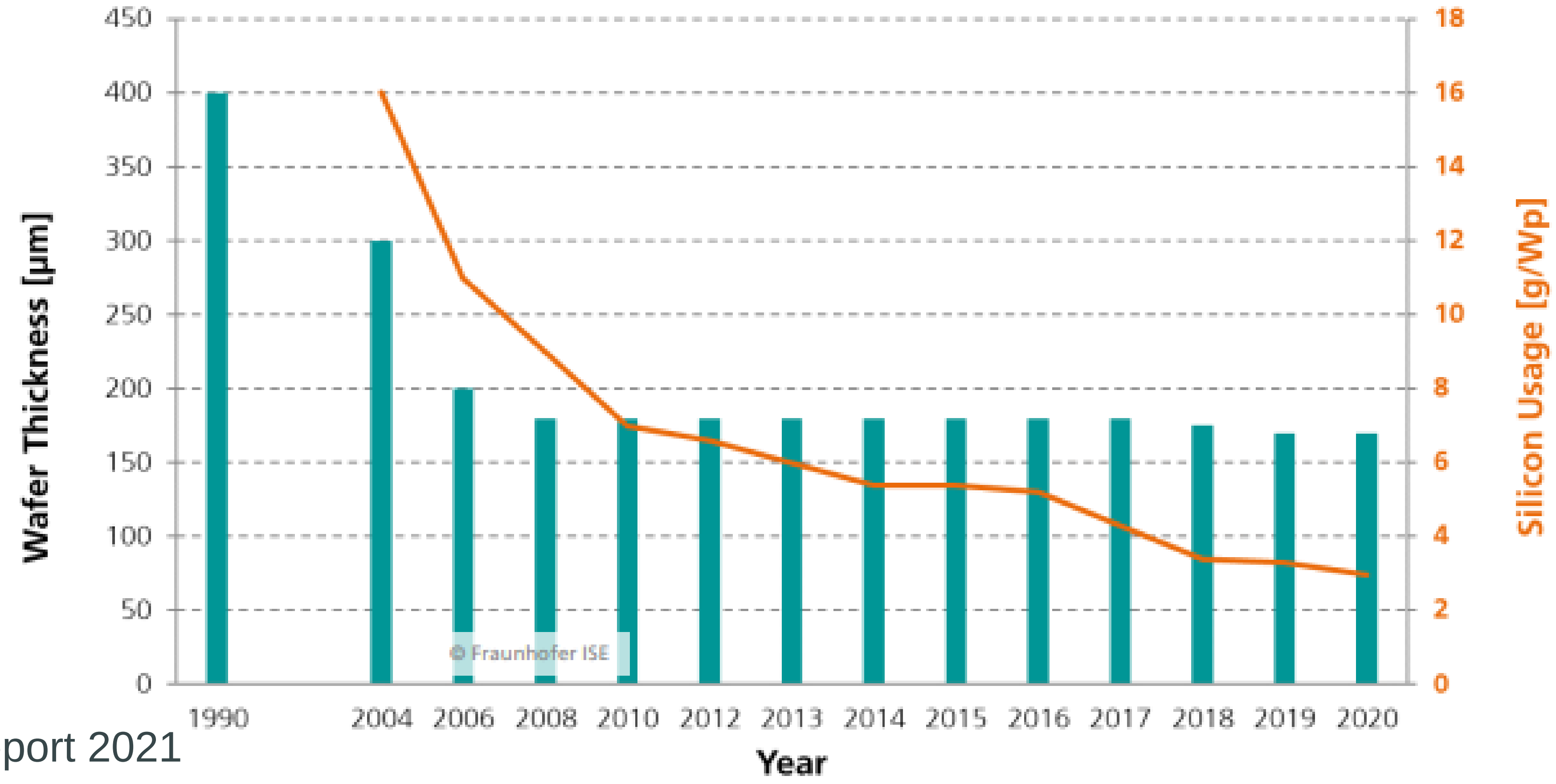

Fraunhofer PV report 2021

Data: until 2012: EU PV Technology Platform Strategic Research Agenda, from 2012: ITRPV 2015; ISE 2016 without; 2017 to 2020 with recycling of Si. Graph: PSE Projects GmbH 2021

Energy Pay-Back Time of Silicon PV Rooftop European comparison

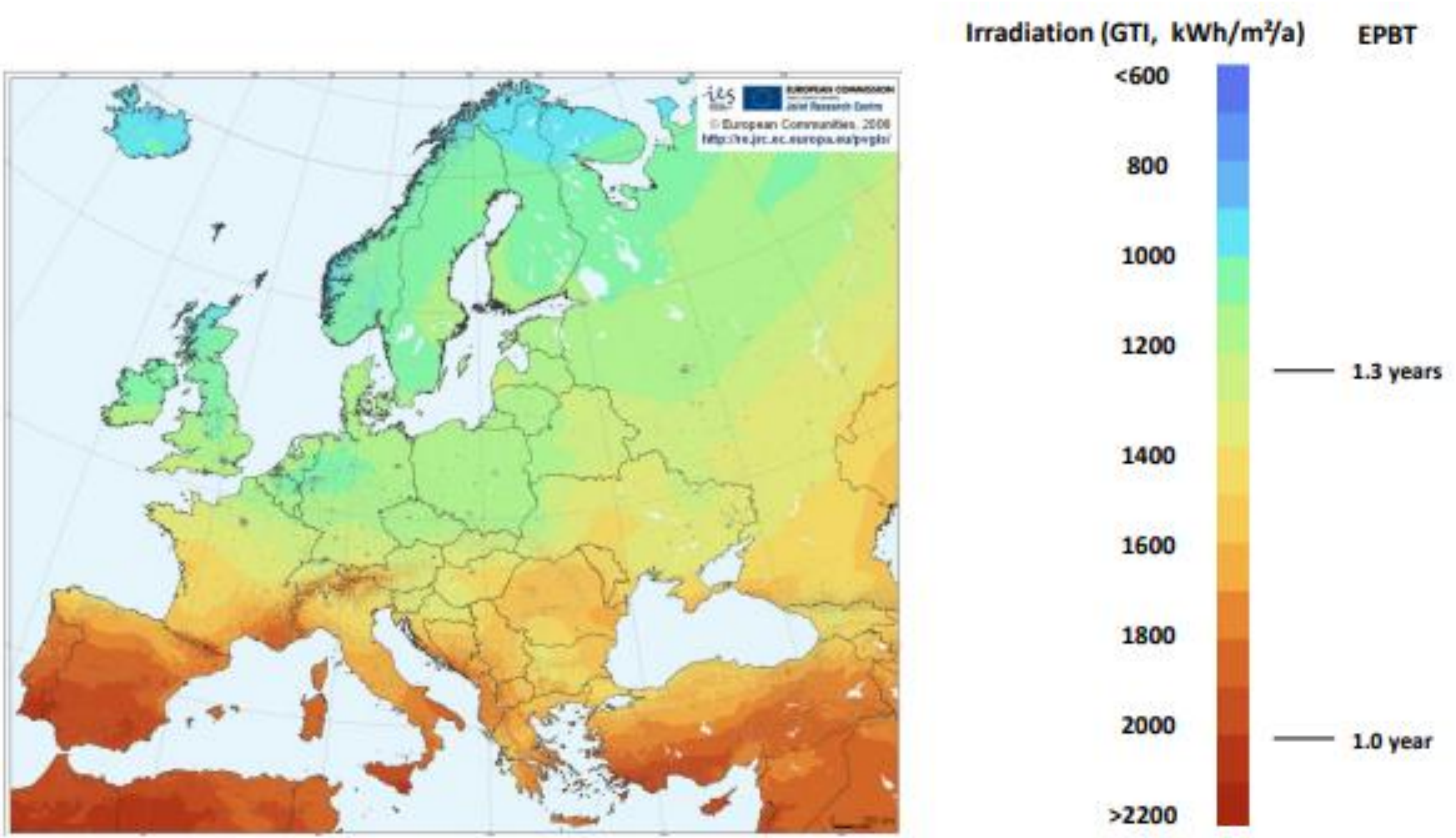

Fraunhofer PV report 2021

World Map EPBT of Silicon PV Rooftop Systems

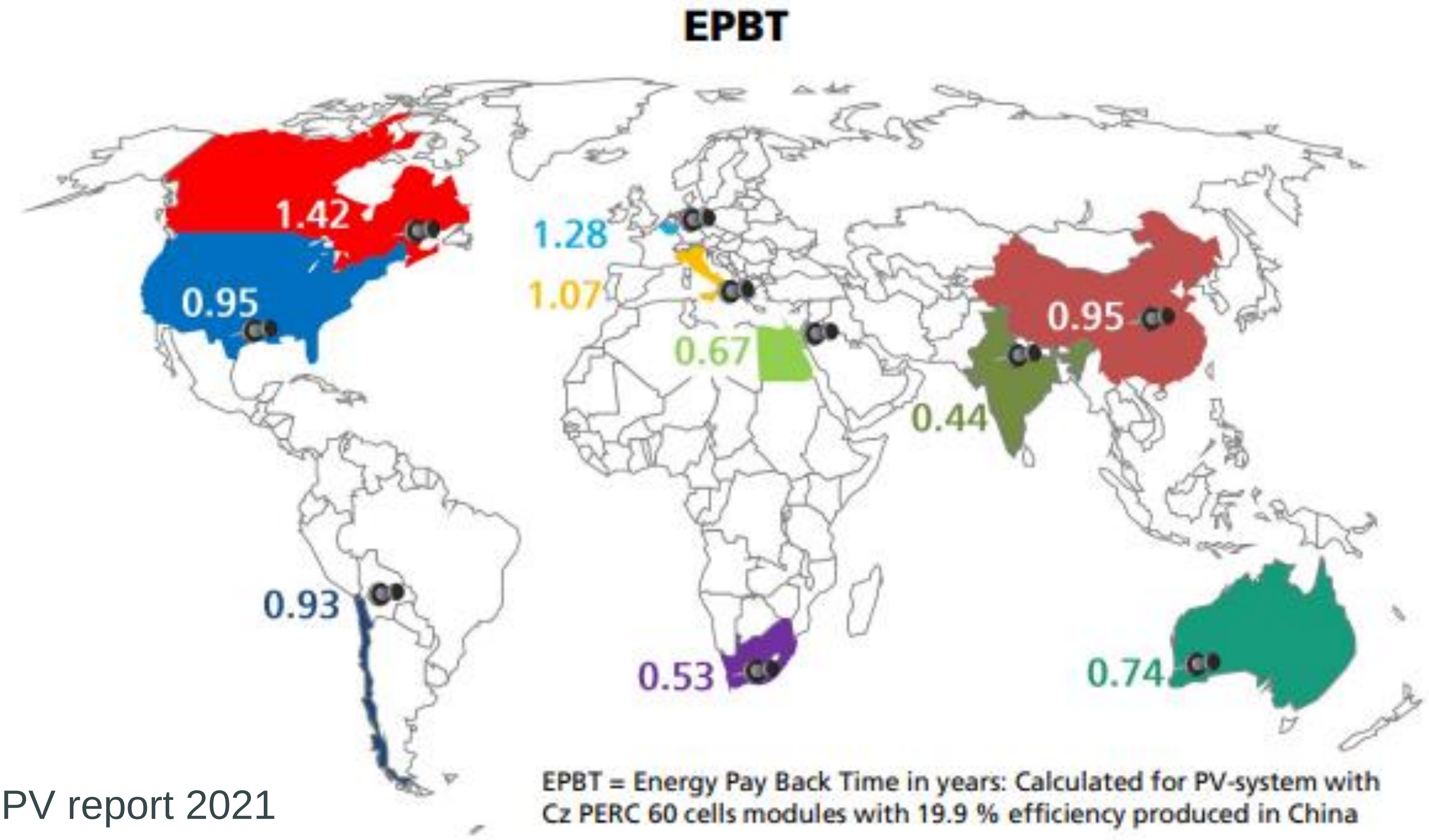

Fraunhofer PV report 2021

Energy Pay-Back Time of Silicon PV Rooftop Systems – Impact of production in EU vs China

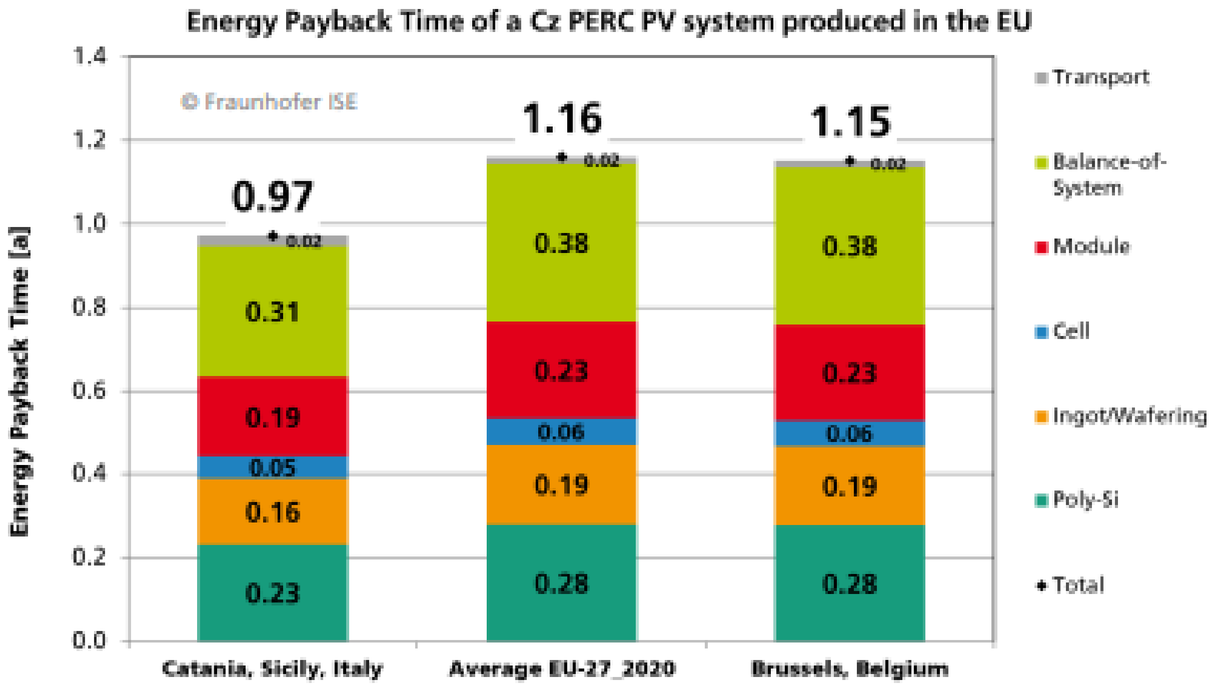

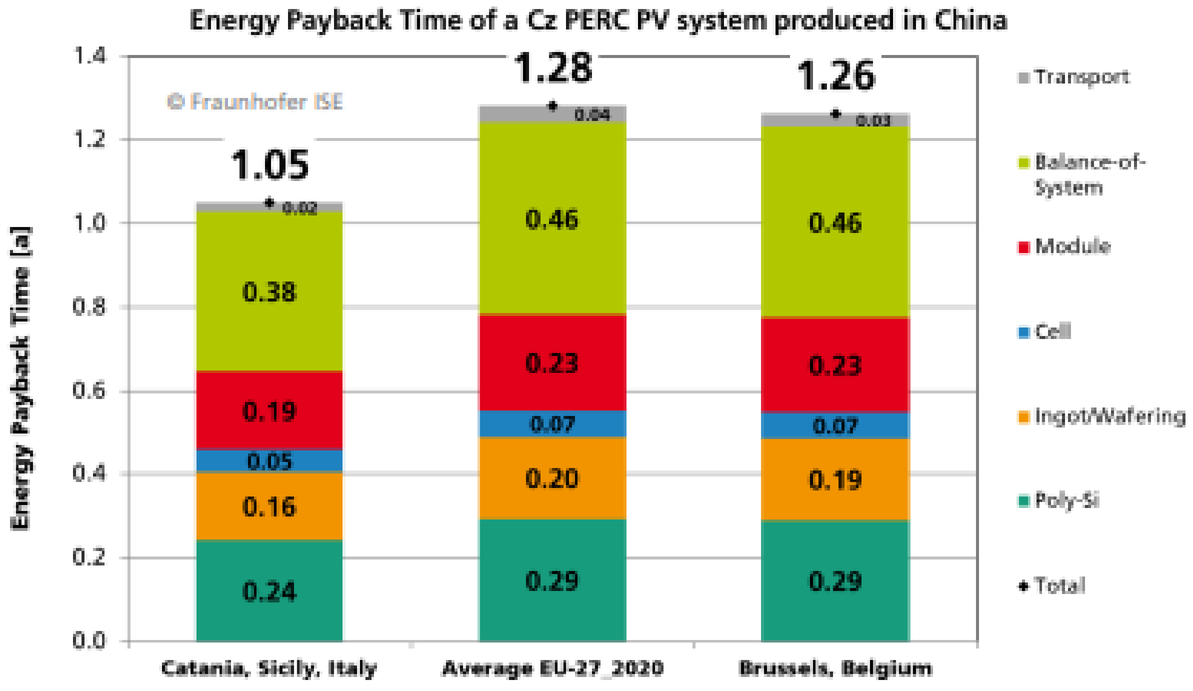

Fraunhofer PV report 2021